A SIMPLE NUMERICAL MODEL

OF THE DYNAMICS OF THE THERMOSPHERE

by

Cirilo Pablo Lagos
S. B. Universidad de San Marcos, Lima
(1964)

SUBMITTED IN PARTIAL FULFILLMENT
OF THE REQUIREMENTS FOR THE
DEGREE OF MASTER OF
SCIENCE

at the

MASSACHUSETTS INSTITUTE OF TECHNOLOGY

June, 1967

Signature of Author .....
Department of Meteorology, May 19, 1967

Certified by.....
Thesis Supervisor

Accepted by .....
Chairman, Departmental Committee
on Graduate Students

A Simple Numerical Model of the Dynamics Of the Thermosphere

by Cirilo Pablo Lagos

Submitted to the Department of Meteorology on May 19, 1967 in partial fulfillment of the requirement for the degree of Master of Science.

ABSTRACT

A dynamically consistent set of simplified equations applicable to large-scale motion in the thermosphere is rigorously developed from the Navier-Stokes equations. The simplifications are justified by means of a scale analysis. These equations form a basis of the dynamics of the thermosphere. Sources and sinks of energy are discussed and analytic solutions of the heat conduction equation are obtained, using a Green's function technique.

The diurnal pattern of heating and the accompanying structural changes in the thermosphere is first studied in a numerical model depending only upon altitude and time. The energy sources are taken to be solar heating, radiation cooling and conduction. No explicit account is taken of horizontal variation and horizontal motion in the model. Comparison of model structure with the observed structure of the thermosphere points to the existence of large-scale poleward transport of heat by horizontal motion in the thermosphere. The transport is required in middle and high latitudes at equinox and at all latitudes in the winter hemisphere near the solstice.

When explicit account is taken of the horizontal variation and the equations of motion are included, a dynamical model of the thermosphere is obtained. The full set of equations are discussed. A two dimensional model, allowing no latitudinal variation, is used to study the effect of horizontal motion on the phase and amplitude of the diurnal temperature oscillation. Under these conditions the computations indicate: 1) Horizontal energy transport by advective processes can not modify the phase of the diurnal temperature oscillation; 2) Adiabatic heating and cooling by vertical motion provide a heat source in the thermosphere. With vertical motions included, the calculated maximum temperature shifts from about 1800 local time, as calculated from the one dimensional model, to about 1400 local time, as is observed.

Thesis Supervisor: Reginald E. Newell
Title: Associate Professor of Meteorology

ACKNOWLEDGMENTS

The author wishes to express his appreciation to his thesis supervisor, Professor Reginald E. Newell for his enthusiasm, guidance, and for many helpful discussions. He has also benefited from valuable discussions with Drs. R. E. Dickinson and J. R. Mahoney.

Dr. J. E. Geisler read the manuscript and made many useful comments, for which the author is most grateful. The computational work was done on the IBM 7094 at the M. I. T. Computation Center. Part of the program was done by Miss Judy Roxborough. Miss Isabel Kole drafted all of the diagrams. Mrs. Susan Nemeti helped with the data reduction. Thanks are also due to Mrs. Cynthia Webster for typing the manuscript.

Finally the author wishes to thank the Organization of American States for Fellowship Support and to the Instituto Geofisico del Peru for generous support during the course of this work.

TABLE OF CONTENTS

LIST OF FIGURES

LIST OF TABLES

1. INTRODUCTION

1.1 Problem Background

1.1.1 The thermosphere

Physical considerations: The region of the atmosphere above the mesopause, where the temperature increases with altitude, is called the thermosphere. In contrast with the region below, it is characterized by a large diurnal variation of temperature and by atomic and molecular processes giving rise to such interesting phenomena as the airglow, aurorae and the ionosphere. Solar radiation of wavelengths less then 1750 A^{o} is absorbed in the thermosphere and in the region above about 100 km., the heat generated by the absorption of radiation is distributed in the vertical by molecular conduction. The vertical distribution of atmospheric constituents above about 100 km. is governed by molecular diffusion.

Dynamical considerations: As a result of the large diurnal variation in the heating of the thermosphere, a horizontal pressure gradient is created. This external forcing excites the thermosphere into motion . When motion is so brought about, transport of heat, momentum and mass becomes important. Generation, conversion and dissipation of potential and kinetic energy then take place, and we no longer can isolate the thermodynamics from the dynamics of the region.

It is now our task to combine physical and dynamical principles into a consistent mathematical theory capable of describing the over-all behavior of the thermosphere.

1.1.2 Observed physical state of the thermosphere

The thermospheric quantities usually considered are temperature, density, pressure and composition. Investigations have concentrated on determining the space and time variations of these observable parameters, the properties of the incoming solar radiation and the interaction thereof. Several techniques, the latest being rockets and satellites, have been used for measuring the composition and structure of the thermosphere.

Rocket flights have been used for measurement of the vertical distribution of molecular oxygen (see e. g. Jursa et al., 1965), vertical distribution of molecular weight and ratio of $n(O)/n(O_2)$ (see e. g. Schaefer, 1963; Pokhunkov, 1963a, b, c), and density distribution (see e. g. Faire and Champion, 1966).

Most of the information concerning the properties of the thermosphere above 200 km. has been derived from the determination of density from satellite observations (Jacchia, 1965; Jacchia and Slowey, 1966; King-Hele, 1966; Anderson and Francis, 1966; Reber, 1967; Jacobs, 1967). The analysis of the density data obtained from several satellites have revealed the existence of four major types of variation in the physical properties of the thermosphere, they are:

a) Diurnal variation: the diurnal variation in density reaches its maximum around 14 hours local time and minimum around 4 a. m. local time.

b) Variation with geomagnetic activity: Variation in geomagnetic activity is correlated with density fluctuations. The correlation of the density

or temperature variation with the planetary index K_p, or with the planetary geomagnetic index a_p is non linear. The perturbations in the thermosphere,ie. density lag behind the geomagnetic disturbance by about 6.7 hours (Jacchia et .al., 1967), depending on latitude.

c) Semi-annual variation: A semi-annual effect in satellite orbital decay data has been found by Paetzold and Zschorner (1961). They interpreted this effect to be a world-wide semi-annual density variation in the thermosphere. The origin of this behavior is still unknown, Anderson (1966) has indicated that this effect is correlated with the difference in latitude between satellite perigee and the subsolar point, and that this behavior might be due only to the existence of the seasonal and latitudinal variation in density.

d) Variation with solar cycle: two types of density fluctuations have been found, namely, the 27 day variation and the 11 year sun-spot cycle. A good correlation exists between density fluctuations and the solar flux in the 10.7 cm. radio emission. The solar decimeter radiation is an indication of the changes in the EUV radiation which in turn is the cause of the thermospheric variation.

Spatial and temporal variations of other parameters in the upper-atmosphere have been obtained from the density measurements by means of atmospheric models.

1.1.3 Previous investigations

A time dependent model of the thermosphere has been developed by

Harris and Priester (1962, 1965) by solving numerically the one dimensional heat conduction equation. In addition to the heat source provided by the absorption of the extreme ultraviolet solar radiation, they included an ad hoc variable heat source in order to obtain agreement between the calculated and observed densities. This model has been incorporated in the Cospar International Reference Atmosphere (CIRA 1965) and is often referred to as the quasi-static model. A further discussion of this model will be given in section 4.2.

Another numerical model for the thermosphere has been constructed by Mahoney (1966). The model is similar in many respects to that of Harris and Priester. Mahoney has also considered latitudinal effects . We leave further discussion to section 4.2.

The need for considering possible dynamical effects in the general behaviour of the thermosphere has been realized only quite recently. A few attempts to estimate the magnitude of the horizontal motion in the thermosphere have appeared within the last year or so (Geisler, 1966; Lindzen, 1966, 1967). More recently Volland (1966) has considered qualitatively the effect of the zonal wind system in the thermodynamic equation. He has used a simple two-dimensional dynamical model for this purpose. Following Mahoney (1966) and Lindzen (1966), he has also suggested that a zonal wind of the order 200 m sec^{-1} can behave like a "second heat source" needed in the model of Harris and Priester, thus shifting the phase and the amplitude of the calculated temperature and density in agreement with observations.

1.2 Statement of Purpose

The object of this investigation is to formulate a model describing the dynamics of large-scale motion in the thermosphere which results from the thermally-driven diurnal oscillation. We shall also examine various sources of energy in the system (e. g. vertical and horizontal advection) which may account for the second heat source proposed by Harris and Priester.

A qualitative analysis of the relative importance of each term in the hydrodynamic and thermodynamic equations will be presented. A simple mathematically consistent system of equations involving the most important terms will be derived. The set of equations are capable of describing the principal features of interest.

For two special cases the system of equations are solved numerically. The first case describes a thermospheric model which depends on height and time only. The characteristics of this model have been reported in full by Mahoney (1966). Here we extend the calculations to investigate the seasonal and latitudinal variations of the heating rates and the thermospheric structure. In the second case we explicitly allow horizontal variability. The solutions are referred to as a two-dimensional dynamical model. Vertical and longitudinal wind profiles are obtained. Special attention is given to the diurnal temperature variation and the role played by the vertical and horizontal motion in the energy balance of the thermosphere.

For many practical purposes the temperature behavior in the thermosphere can be described quite well with a simple time-dependent heat conduction equation with sources and sinks. Under certain assumptions about the

temperature dependence of the thermal conductivity, it is possible to obtain an expression for the temperature in closed form, in terms of a Green's function.

The Green's function for the heat conduction equation is derived for several cases, each characterized by an assumed form of the ratio of thermal conductivity to scale height.

It is shown how these results may be used for guidance in the solutions of the simple hydrodynamic and thermodynamic equations.

1.3 Outline of Thesis Content

In chapter 2 we present the mathematical formulation for the dynamics of the thermosphere. The Navier-Stokes equations, extended to take into account the coriolis force and the ion drag are reduced to a simpler set of equations by means of scale analysis. Scale analysis of the ion drag, viscous stresses, heat conduction and radiational heating rates are explicitly considered. The solutions are assumed to be represented by a power series in the Rossby number and zero order equations describing large-scale wave disturbances in the thermosphere, are derived. The expansion can easily be used to obtain higher order approximations.

In chapter 3, approximate analytical solutions of the time dependent heat conduction equation are obtained and discussed.

In chapter 4, the one dimensional numerical model is described and the variability of the thermospheric parameters with season and latitude are considered.

In chapter 5 a two-dimensional numerical model is developed using a highly truncated Fourier expansion. Solutions for the motion and temperature fields are presented.

In chapter 6, the main results obtained from the present study are summarized. Suggestions for further research are also presented.

2. FORMULATION OF THE EQUATIONS GOVERNING PLANETARY TIDAL MOTION IN THE THERMOSPHERE

2.1 The Hydrodynamic and Thermodynamic Equations

The purpose of this chapter is to derive systematically a consistent set of hydrodynamic and thermodynamic equations applicable to the thermosphere. Starting with the complete Navier-Stokes equations, several approximations and assumptions will be needed to obtain the final system capable of describing the features of principal interest. Some of these approximations are quite realistic, while others eliminate some physical effects which may be important to the complete understanding of the dynamical processes, but do not appear to change the physical picture.

2.1.1 Physical and scaling assumptions

The governing system of equations is obtained by allowing the following assumptions:

a) Hydrostatic balance occurs. The large scale atmospheric motions of the thermosphere exist in hydrostatic balance and a simple scale analysis suffices to show that this is so.

b) The spherical geometry of the earth's atmosphere may be approximated by a tangential plane, that is, the problem can be formulated in a cartesian coordinate system.

c) the gravity force g is constant.

d) No interactions between the ionospheric plasma and the neutral atmosphere are considered; however the force experienced by the neutral air in moving through the ionized constituent, the so-called ion-drag, is taken into

account.

The method of scale analysis described below is based on the existence of well defined space and time scale of the thermospheric disturbance to be described by the equations. Consequently it is assumed that all dependent variables, the temperature for example, are confined to a known range of variation.

One of the most striking features of the observed large scale atmospheric motion in the lower atmosphere is its geostrophic nature. Geostrophic motion occurs when the pressure gradient force is nearly balanced by the component of the coriolis force in a horizontal plane. Both inertial and viscous forces are generally assumed to be of higher order in the perturbation equations. Furthermore diabatic heating is neglected to a first approximation. These approximations are consistent with the observed dynamical behaviour of the lower atmosphere. In the case of the upper atmosphere these approximations no longer hold. Above the mesopause inertial forces, ion drag, heat conduction and viscous dissipation become very important for describing the expected motions. Heating rates due to the absorption of EUV solar radiation and cooling rates due to atomic oxygen radiation are of basic importance. The order of magnitude of all of these terms is as large as the other terms in the hydrodynamic and thermodynamic equations, and the resultant motions must reflect the consequence of these additional physical processes.

When viscocity, heat conduction, energy sources, and ion drag are considered -- and they must be taken into account together if we are interested in

the general circulation of the thermosphere--the problem becomes much more complicated. Several approaches are available for solving the problem stated above, and the course we are going to take is as follows: starting with the Navier-Stokes equations, we define characteristic space and time scales and transform the dimensional equations to their equivalent non-dimensional system. . Next, we assume that the solution can be expanded in a power series of a small parameter and then obtain a sequence of equations for the various order terms.

The present nondimensional analysis is an extension of similar studies used in dynamical meteorology (Charney, 1947; Burger, 1958; Charney and Stern, 1962; Phillips, 1963 and Pedlosky, 1964), and in the theory of rotating fluids (Greenspan, 1964).

2.1.2 Unscaled equations

Based upon the physical assumptions made above, the general equations of momentum and energy conservation relative to a rotating system in an x_1, x_2, x_3 cartesian co-ordinate system are obtained from the Navier-Stokes equations (cf. Schlichting, 1962) extended to take into account the coriolis force and the ion drag. This system may be written

$$\rho \frac{d\vec{u}}{dt} + 2\rho\Omega\vec{k}\times\vec{u} = -\operatorname{grad} p - \rho\vec{g} + \vec{D} + \operatorname{div}\vec{\tau} \tag{2.1}$$

$$\frac{\partial \rho}{\partial t} + \operatorname{div}(\rho\vec{u}) = 0 \tag{2.2}$$

$$\rho C_p \frac{dT}{dt} + p \operatorname{div}\vec{u} = \operatorname{div}(K \operatorname{grad} T) + \Phi + \rho Q \tag{2.3}$$

(2.4) $$p = R\rho T$$

where

$$\mathrm{div}\,\vec{\tau} = \mu\left(\tfrac{1}{3}\nabla\chi + \nabla^2\vec{u}\right)$$

$$\chi = \nabla\cdot\vec{u}$$

$$\Phi = (\vec{\tau}\cdot\nabla)\cdot\vec{u}$$

$$\vec{D} = \rho_i \nu_i (\vec{v}_i - \vec{u})$$

$$Q = \dot{q}_{sR} + \dot{q}_{IR}$$

$$\frac{d}{dt} = \frac{\partial}{\partial t} + \vec{u}\cdot\nabla$$

In these equations and definitions, equation (2.1) is the equation of momentum, (2.2) is the equation of continuity, (2.3) is the equation of thermal energy and (2.4) is the equation of state;

$\vec{u} = u\hat{i} + v\hat{j} + w\hat{k}$ ($\hat{i}$, $\hat{j}$ and $\hat{k}$ are in east, north and upward directions respectively)

t = time

p = thermodynamic pressure

T = Kelvin temperature

g = acceleration of gravity

ρ = density

c_p = specific heat at constant pressure

Φ = viscous dissipation function

$\vec{\tau}$ = viscous stress tensor under the Stokes hypothesis

χ = velocity divergency

$\vec{k}$ = vector having components (0, 0, 1)

K = thermal conductivity ($K = B(z)T^{1/2}$; $B(O) = 3.6 \times 10^2$, $B\ (O_2,\ N_2) = 1.8 \times 10^2$)

μ = dynamic viscocity coefficient ($\mu = A(z)\ T^{1/2}$)

$\vec{D}$ = ion drag

ρ_i = ion density

ν_i = ion-neutral collision frequency

V_i = x_i component of ion velocity

Q = non-adiabatic heating rate per unit mass

$\dot{q}_{SR}$ = heating rate due to solar absorption

$\dot{q}_{IR}$ = cooling rate due to infrared radiation

R = gas constant ($R = R^*/M$, where R^* is the Universal gas constant and M is the mean molecular weight.)

Ω = the rate of rotation of the earth

$B = \frac{5}{2} AC_v$

C_v = specific heat at constant volume

2.2 Scale Analysis

2.2.1 General remarks

The basic plan of this section is as follows: given a set of dimensional equations that characterize a general class of large scale thermospheric motions, we construct a set of nondimensional parameters, i.e. the Rossby number, R_o, Taylor number, γ, etc. We assume an asymptotic solution to the system, expand each dependent variable in a power series in R_o and then insert

these expansions into the nondimensional governing equations. We require the equations to be satisfied for all sufficiently small but finite values of R_o. This leads to an ordered set of equations. The simplest system is obtained from the zero order in Rossby number. Higher order systems, which may be of interest in some specific problems, can be easily written down following the same procedure.

Since we are interested in the thermospheric disturbance associated with the diurnal oscillation of the temperature and density, the global horizontal length scale will be characterized by the wave length of the disturbance. Let us take this scale, denoted by L, to be 10^7 meters. The wave disturbance is characterized by its periodicity in time and we shall choose for the time scale this oscillation time Ω^{-1}, where Ω is the rate of rotation of the earth.

Let U represent a typical horizontal velocity scale, and let H_s, the horizontal and time average scale height, represent the characteristic vertical scale. Define the nondimensional parameter R_o, the Rossby number, by $R_o = U/\Omega L$. This parameter will be a measure of the magnitude of the non linear terms. With the assumption of hydrostatic balance the third component of the momentum equation (2.1) reduces to

$$-\frac{\partial p}{\partial x_3} - \rho = 0 \tag{2.5}$$

2.2.2 Scaled equations

The scale arguments can be presented in a most convenient form if we introduce a special coordinate system. In place of x_3, let us use the logarithm

of pressure as the vertical coordinate (Eliassen, 1949)

$$(2.6) \qquad Z = -\ln P \;, \qquad P = p/p_0$$

where $p_0 = 1 \times 10^{-2}$ mb. at 80 km., is the reference level. Z is related to the actual height h($h \equiv x_3$) and the geopotential height $\phi = gh$, by the ideal gas law and the hydrostatic relation (2.5)

$$(2.7) \qquad RT = \frac{p}{\rho} = -p g \frac{\partial h}{\partial p} = \frac{\partial \phi}{\partial Z}$$

It must be noticed that the above definition of Z is equivalent to

$$(2.8) \qquad Z = \int \frac{dh}{H}$$

that is, Z is approximately equal to the ratio of the actual height to the scale height $H = \frac{RT}{g}$.

The advantage of using Z is that further simplications are possible when the motion is hydrostatic (cf. Phillips, 1963): If ξ represents x, y, or t, then

$$(2.9) \qquad \frac{1}{\rho}\left(\frac{\partial p}{\partial \xi}\right)_h = \left(\frac{\partial \phi}{\partial \xi}\right)_Z$$

$$\left(\frac{\partial}{\partial Z}\right)_\xi = \frac{RT}{g}\left(\frac{\partial}{\partial h}\right)_\xi$$

where the subscripts indicate differentiation at constant h, Z or ξ .

The Z-velocity, denoted by $\dot{Z}$ is related to the vertical velocity w by

$$(2.10) \qquad \dot{Z} = -\frac{\dot{p}}{p} = -\frac{1}{RT}\left(\frac{\partial \phi}{\partial t} + u\frac{\partial \phi}{\partial x} + v\frac{\partial \phi}{\partial y} - gw\right)_Z$$

Using equations (2.7), (2.9), and (2.10), the continuity equation (2.2) can be rewritten in a simple and convenient form,

$$(2.11) \qquad \left(\frac{\partial u}{\partial x} + \frac{\partial v}{\partial y}\right)_Z + \frac{\partial \dot{Z}}{\partial Z} - \dot{Z} = 0$$

Similarly, the thermal energy equation (2.3) can be rewritten

$$(2.12)\quad \left(\frac{\partial}{\partial t} + u\frac{\partial}{\partial x} + v\frac{\partial}{\partial Y}\right)\frac{\partial \phi}{\partial Z} + \dot{Z}\frac{\partial}{\partial Z}\left(\frac{\partial \phi}{\partial Z} + \varkappa \phi\right) = \frac{1}{c_p}\,\mathrm{div}\left(K\,\rho\,\mathrm{grad}\,\frac{\partial \phi}{\partial Z}\right) + \frac{\varkappa}{\rho}\Phi + \varkappa Q$$

where $\varkappa = R/c_p$.

2.2.2.1 The nondimensional Navier-Stokes equations

Using the scaling parameter defined above and with the notation used by Charney and Stern (1962) and Phillips (1963), the variables in equations (2.1), (2.11) and (2.12) will be made nondimensional in the following manner:

Introduce nondimensional (primed) quantities by assuming

$$(x, y) = L\,(x', y')$$

$$(u, v) = U\,(u', v')$$

$$\dot{Z} = \frac{U}{L} W'$$

$$w = U\,\delta\,W'$$

$$(2.13)$$

$$H = H_s\,(1 + R_o f H'(x', y', Z, t'))$$

$$\rho = \rho_s\,(1 + R_o f \rho'(x', y', Z, t'))$$

$$t = \Omega^{-1} t'$$

where

$$(2.14)\quad \delta = \frac{H_s}{L}\,, \qquad R_o = \frac{U}{\Omega L}\,, \qquad f = \frac{\Omega^2 L^2}{g H_s}$$

The geopotential may be expressed in the convenient form:

$$(2.15)\quad \phi = \phi_s + \Omega U L\,\Phi'(x', Y', Z, t')$$

In the definitions given here a subscript s denotes quantities which depend only on Z and which define a basic state, e. g. a standard atmosphere, while the prime quantities are the deviation from this mean.

We define the nondimensional static stability S by

$$S = \frac{g}{(\Omega L)^2}\left(\kappa H_s + \frac{dH_s}{dZ}\right) \tag{2.16}$$

When the equations (2.1), (2.11), and (2.12) are made nondimensional the following set of equations result:

$$\frac{\partial u}{\partial t} + R_o\left(u\frac{\partial u}{\partial x} + v\frac{\partial u}{\partial y} + W\frac{\partial u}{\partial Z}\right) - 2v\sin\varphi = -\frac{\partial \Phi}{\partial x} + \frac{D_x}{\Omega U} + \frac{F_x}{\Omega U} \tag{2.17}$$

$$\frac{\partial v}{\partial t} + R_o\left(u\frac{\partial v}{\partial x} + v\frac{\partial v}{\partial y} + W\frac{\partial v}{\partial Z}\right) + 2u\sin\varphi = -\frac{\partial \Phi}{\partial y} + \frac{D_y}{\Omega U} + \frac{F_y}{\Omega U} \tag{2.18}$$

$$\frac{\partial u}{\partial x} + \frac{\partial v}{\partial y} + \frac{\partial W}{\partial Z} - W = 0 \tag{2.19}$$

$$\frac{\partial^2 \Phi}{\partial t\,\partial Z} + R_o\left(u\frac{\partial}{\partial x} + v\frac{\partial}{\partial y}\right)\frac{\partial \Phi}{\partial Z} + WS + R_o W\frac{\partial}{\partial Z}\left(\frac{\partial \Phi}{\partial Z} + \kappa\Phi\right) = R_o\frac{\kappa Q_{NET}}{\Omega U^2} \tag{2.20}$$

The primes have here been dropped from the nondimensional variables. Here $\frac{\partial}{\partial x}$, $\frac{\partial}{\partial y}$ and $\frac{\partial}{\partial t}$ are at constant Z. In equation (2.20) the dissipation function Φ has been neglected for simplicity. φ is the latitude. The terms D_x and D_y are the x and y components of the ion drag. Similarly, F_x and F_y are the x and y components of the viscous stresses. The term Q_{NET} stands for

$$Q_{NET} = \dot{q}_{COND} + \dot{q}_{SR} + \dot{q}_{IR} \tag{2.21}$$

where $\dot{q}_{COND}$ is the conductivity heating rate. All these quantities remain to be expressed in convenient nondimensional form.

2.2.2.2 Scale analysis of the ion drag

A simplified analysis of the ion drag term may be given as follows: the

equation of motion for the ions is approximately given by (Fejer, 1965).

$$(2.22) \quad \rho_i \frac{d\vec{V}_i}{dt} = \rho_i \vec{A} + \rho_i \nu_i (\vec{u} - \vec{V}_i) - \rho \, \mathrm{grad} \, p_i$$

where

$$(2.23) \quad \vec{A}_i = \frac{q_i}{m_i} \left(\vec{E} + \vec{V}_i \times \vec{B} \right) + \vec{g}$$

and

$\vec{V}_i$ = Velocity of ions

ρ_i = ion density

ν_i = ion-neutral collision frequency

P_i = ion partial pressure

q_i = ion charge

m_i = ion mass

$\vec{E}$ = electric field

$\vec{B}$ = magnetic field

$\vec{g}$ = acceleration of gravity

Several terms can be neglected in (2.22) and (2.23) for the region of interest, such as $\rho_i \vec{g}$, grad P_i and $\vec{E}$. Further simplication is made by neglecting the nonlinear terms and considering all other quantities as constant. Under these assumptions equation (2.22) may be solved for $\vec{V}_i$. A time scale of O(1) is assumed. Noticing that the relation $1 \ll \nu_i \ll \sigma_i$ holds over the range of altitude where ion drag makes an appreciable contribution, the expression for V_i (Geisler, 1966; Lindzen, 1967) is

$$(2.24) \quad \vec{V}_i = (u_i, v_i, w_i)$$

$$(2.25) \quad u_i = u \left(1 - \frac{1}{1 + \frac{\nu_i^2}{\sigma_i^2}} \right)$$

(2.26) $$v_i = v\left(1 - \frac{1}{1 + \frac{\nu_i^2}{\sigma_i^2}}\right)\sin^2 I$$

(2.27) $$w_i = \frac{u}{\frac{\sigma_i}{\nu_i} + \frac{\nu_i}{\sigma_i}}$$

where

$$\sigma_i = \frac{N_i q_i B}{\rho_i}$$

N_i = ion number density

I = dip angle

In the F-region where the ion-drag may have its largest effect, the ratio of the ion to neutral particle mass is of order unity. As a result, ρ_i / ρ may be replaced by N_i/N where N is the neutral number density.

The term $\vec{D}$ in (2.1) can now be rewritten as

(2.28) $$\vec{D} = -\frac{N_i}{N}\nu_i \frac{\vec{u}}{1 + \frac{\nu_i^2}{\sigma_i^2}}$$

Define the nondimensional parameters

(2.29) $$\alpha_1 = \frac{\nu_i}{\sigma_i}$$

$$\alpha_2 = \frac{N_i}{N}\frac{\nu_i}{\Omega}$$

$$\beta = -\frac{\alpha_2}{1 + \alpha_1^2}$$

Hence the ion drag term becomes

(2.30) $$\frac{D_x}{\Omega U} = \beta u'$$

(2.31) $$\frac{D_y}{\Omega U} = \beta v' \sin^2 I$$

2.2.2.3 Scale analysis of the viscous stresses

The x-component of the viscous stress F_x can be written in the (x, y, Z) co-ordinate system as

$$(2.32)\quad F_x = \frac{1}{\rho}\left\{\frac{\partial}{\partial x}\left[\mu\left(2\frac{\partial u}{\partial x} - \frac{2}{3}\,\mathrm{div}_z\,\vec{u}\right)\right] + \frac{\partial}{\partial Y}\left[\mu\left(\frac{\partial u}{\partial Y} + \frac{\partial v}{\partial x}\right)\right] + \frac{1}{H}\,\frac{\partial}{\partial Z}\left[\mu\left(\frac{\partial w}{\partial x} + \frac{1}{H}\,\frac{\partial u}{\partial Z}\right)\right]\right\}$$

where

$$(2.33)\quad \mathrm{div}_z\,\vec{u} = \frac{\partial u}{\partial x} + \frac{\partial v}{\partial Y} + \frac{1}{H}\,\frac{\partial w}{\partial Z}$$

and the relation

$$\frac{\partial}{\partial h} = \frac{1}{H}\,\frac{\partial}{\partial Z}$$

has been used.

Let $\bar{\mu}$ be a characteristic dynamic viscosity, and $\bar{\nu} = \frac{\bar{\mu}}{\rho_s}$ a characteristic kinematic viscocity.

Define the nondimensional parameter Υ by $\Upsilon = \frac{\Omega L^2}{\bar{\nu}}$, which may be identified as the Taylor number,

When the variables in (2.32) are made nondimensional, the resultant expression for F_x and hence the last term in the R.H.S. of (2.17) is

$$(2.34)\quad \frac{F_x}{\Omega U} = \frac{\Upsilon^{-1}}{(1+R_o f\rho)}\left\{\frac{\partial}{\partial x}\left[2\frac{\partial u}{\partial x} - \frac{2}{3}\left(\frac{\partial u}{\partial x} + \frac{\partial v}{\partial Y} + \frac{H_s}{H}\,\frac{\partial w}{\partial Z}\right)\right] + \frac{\partial}{\partial Y}\left(\frac{\partial u}{\partial Y} + \frac{\partial v}{\partial x}\right) + \frac{L}{H}\,\frac{\partial}{\partial Z}\left(\frac{H_s}{L}\,\frac{\partial w}{\partial x} + \frac{L}{H}\,\frac{\partial u}{\partial Z}\right)\right\}$$

Similarly the last term in the R.H.S. of (2.18) is

$$(2.35)\quad \frac{F_Y}{\Omega U} = \frac{\Upsilon^{-1}}{(1+R_o f\rho)}\left\{\frac{\partial}{\partial Y}\left[2\frac{\partial v}{\partial Y} - \frac{2}{3}\left(\frac{\partial u}{\partial x} + \frac{\partial v}{\partial Y} + \frac{H_s}{H}\,\frac{\partial w}{\partial Z}\right)\right] + \frac{L}{H}\,\frac{\partial}{\partial Z}\left(\frac{L}{H}\,\frac{\partial v}{\partial Z} + \frac{H_s}{L}\,\frac{\partial w}{\partial Y}\right) + \frac{\partial}{\partial x}\left(\frac{\partial u}{\partial Y} + \frac{\partial v}{\partial x}\right)\right\}$$

The primes have here been dropped from the nondimensional variables.

2.2.2.4 Scale analysis of the heat conduction

The net rate of heating is expressed by

(2.36) $$\dot{Q}_{NET} = \dot{q}_{COND} + \dot{q}_{SR} + \dot{q}_{IR}$$

and hence the R.H.S. of (2.20) becomes

(2.37) $$\frac{R_o \kappa \dot{Q}_{NET}}{\Omega U^2} = \frac{R_o \kappa \dot{q}_{COND}}{\Omega U^2} + \frac{R_o \kappa (\dot{q}_{SR} + \dot{q}_{IR})}{\Omega U^2}$$

where

(2.38) $$\dot{q}_{COND} = \frac{1}{\rho R}\left(\frac{\partial}{\partial x} K \frac{\partial}{\partial x} + \frac{\partial}{\partial Y} K \frac{\partial}{\partial Y} + \frac{1}{H}\frac{\partial}{\partial Z}\frac{K}{H}\frac{\partial}{\partial Z}\right)\frac{\partial \phi}{\partial Z}$$

use of (2.7) has been made to express T in terms of ϕ (x, y, Z, t). Since

$\phi = \phi_s(Z) + \Omega U L \tilde{\phi}(x, Y, Z, t)$, (2.38) is transformed to

(2.39) $$\dot{q}_{COND} = \frac{1}{\rho R}\left(\frac{1}{H}\frac{d}{dZ}\frac{K}{H}\frac{d}{dZ}\right)\frac{d\phi_s}{dZ} + \frac{\Omega U L}{\rho R}\left(\frac{\partial}{\partial x} K \frac{\partial}{\partial x} + \frac{\partial}{\partial Y} K \frac{\partial}{\partial Y} + \frac{1}{H}\frac{\partial}{\partial Z}\frac{K}{H}\frac{\partial}{\partial Z}\right)\frac{\partial \tilde{\phi}}{\partial Z}$$

We introduce a characteristic thermal conductivity $\bar{K}$, a characteristic thermal diffusivity Θ, given by $\Theta = \frac{\bar{K}}{c_p \rho_s}$ and the nondimensional parameters ϵ_1 and ϵ_2 by

(2.40) $$\epsilon_1 = \frac{\Theta}{\Omega L^2}, \qquad \epsilon_2 = \epsilon_1 \delta^{-2}$$

We shall find convenient, below, to define the nondimensional parameter Π by

(2.41) $$\Pi = \frac{\kappa \bar{K}}{\Omega^2 U L \rho_s R}\left(\frac{1}{H_s^2}\frac{d^2}{dZ^2}\right)\frac{d\phi_s}{dZ}$$

When equation (2.39) is made nondimensional, the first term in the R.H.S. of (2.37) becomes

(2.42) $$\frac{R_o \kappa \dot{q}_{COND}}{\Omega U^2} = \frac{\kappa \bar{K}}{\Omega^2 U L \rho R}\left(\frac{1}{H}\frac{d}{dZ}\frac{1}{H}\frac{d}{dZ}\right)\frac{d\phi_s}{dZ} + \frac{\epsilon_1}{(1+R_o f \beta)}\left\{\left(\frac{\partial^2}{\partial X^2}+\frac{\partial^2}{\partial Y^2}\right)\frac{\partial \Phi}{\partial Z} + \left(\frac{L}{H}\frac{\partial}{\partial Z}\frac{L}{H}\frac{\partial}{\partial Z}\right)\frac{\partial \phi}{\partial Z}\right\}$$

where again we have dropped the primes from the nondimensional variables.

2.2.2.5 Scale analysis of the radiational heating rate

The second term in the R.H.S. of (2.37) is made nondimensional by letting

$$\dot{q}_R = \dot{q}_{SR} + \dot{q}_{IR}$$

and defining

(2.43) $$\dot{q}_R = \frac{\Omega^2 L U}{\kappa}\dot{q}_R'$$

where

$$\dot{q}_R' = \dot{q}_{SR}' + \dot{q}_{IR}$$

is the nondimensional radiational heating variable. Hence $\frac{R_o \kappa \dot{q}_R}{\Omega U^2} = \dot{q}_R'$

2.2.3 The perturbation expansion in the Rossby number

The system (2.17) - (2.20) can now be summarized as

(2.44) $$\frac{\partial u}{\partial t} + R_o\left(u\frac{\partial u}{\partial x} + v\frac{\partial u}{\partial y} + w\frac{\partial u}{\partial z}\right) - 2v\sin\varphi = -\frac{\partial \Phi}{\partial x} + \beta u + \frac{\gamma^{-1}}{(1+R_o f \beta)}\left\{\frac{\partial}{\partial x}\left[2\frac{\partial u}{\partial x} - \frac{2}{3}\left(\frac{\partial u}{\partial x}+\frac{\partial v}{\partial y}+\frac{H_s}{H}\frac{\partial w}{\partial z}\right)\right] + \frac{\partial}{\partial y}\left(\frac{\partial u}{\partial y}+\frac{\partial v}{\partial x}\right) + \frac{L}{H}\frac{\partial}{\partial z}\left(\frac{H_s}{L}\frac{\partial w}{\partial x} + \frac{L}{H}\frac{\partial u}{\partial z}\right)\right\}$$

(2.45) $$\frac{\partial v}{\partial t} + R_o\left(u\frac{\partial v}{\partial x} + v\frac{\partial v}{\partial y} + w\frac{\partial v}{\partial z}\right) + 2u\sin\varphi = -\frac{\partial \Phi}{\partial y} + \beta v \sin^2 I + \frac{\gamma^{-1}}{(1+R_o f \beta)}\left\{\frac{\partial}{\partial y}\left[2\frac{\partial v}{\partial y} - \frac{2}{3}\left(\frac{\partial u}{\partial x}+\frac{\partial v}{\partial y}+\frac{H_s}{H}\frac{\partial w}{\partial z}\right)\right] + \frac{L}{H}\frac{\partial}{\partial z}\left(\frac{L}{H}\frac{\partial v}{\partial z} + \frac{H_s}{L}\frac{\partial w}{\partial y}\right) + \frac{\partial}{\partial x}\left(\frac{\partial u}{\partial y}+\frac{\partial v}{\partial x}\right)\right\}$$

(2.46) $$\frac{\partial u}{\partial x} + \frac{\partial v}{\partial y} + \frac{\partial w}{\partial z} - w = 0$$

$$(2.47)\quad \frac{\partial^2 \Phi}{\partial t\,\partial Z} + R_o\left(u\frac{\partial}{\partial x} + v\frac{\partial}{\partial y}\right)\frac{\partial \Phi}{\partial Z} + WS + R_o w \frac{\partial}{\partial Z}\left(\frac{\partial \Phi}{\partial Z} + \varkappa \Phi\right)$$
$$= \frac{\varkappa \bar{K}}{\Omega^2 U L \rho R}\left(\frac{1}{H}\frac{d}{dZ}\frac{1}{H}\frac{d}{dZ}\right)\frac{d\Phi_s}{dZ} +$$
$$+ \frac{\epsilon_1}{(1+R_o f \rho)}\left\{\left(\frac{\partial^2}{\partial x^2} + \frac{\partial^2}{\partial y^2}\right)\frac{\partial \Phi}{\partial Z} + \left(\frac{L}{H}\frac{\partial}{\partial Z}\frac{L}{H}\frac{\partial}{\partial Z}\right)\frac{\partial \Phi}{\partial Z}\right\} + \dot{q}_R$$

Now for problems which deal with large scale wave disturbances or small amplitude tidal motion in the thermosphere, the following relations hold for the parameter defined above (cf. section 2.2.5).

$$(2.48)\quad R_o \ll 1\,,\quad \gamma^{-1} \ll 1\,,\quad \delta \ll 1\,,\quad \pi \ll 1$$
$$\epsilon_1 \ll 1\,,\quad \epsilon_2 = O(1)\,,\quad f = O(1)\,,\quad \frac{H}{H_s} = O(1)$$
$$\beta = O(1)\,,\quad S = O(1)\,,\quad P = \gamma^{-1}\delta^{-2} = O(1)$$

All other symbols are at most of order of unity.

Under these conditions it is possible to expand the dependent variables in the following manner.

Let ξ be anyone of the variables u, v, w, Φ or $\dot{q}_R$ and write

$$(2.49)\quad \xi = \sum_{n=0}^{\infty} \xi_n R_o^n$$

Introduce this expansion into the system (2.44)-(2.47) and require that the equation be satisfied separately for each power of R_o.

2.2.4 The nonhomogeneous zero order system

Entering the formal expansion, we obtain a sequence of ordered equations.

The zero order equation is

$$(2.50)\quad \frac{\partial u_o}{\partial t} - 2 v_o \sin\varphi = -\frac{\partial \Phi_o}{\partial x} + \beta u_o + P\frac{\partial^2 u_o}{\partial Z^2}$$

$$\frac{\partial v_0}{\partial t} + 2u_0 \sin\varphi = -\frac{\partial \Phi_0}{\partial y} + \beta v_0 \sin^2 I + P \frac{\partial^2 v_0}{\partial z^2} \tag{2.51}$$

$$\frac{\partial u_0}{\partial x} + \frac{\partial v_0}{\partial y} + \frac{\partial w_0}{\partial z} - w_0 = 0 \tag{2.52}$$

$$\frac{\partial^2 \Phi_0}{\partial t \partial z} + w_0 S = \epsilon_2 \frac{\partial^2}{\partial z^2} \frac{\partial \Phi_0}{\partial z} + \dot{q}_{R,0} \tag{2.53}$$

Although higher order systems are easily written down, we shall only consider the above system here. For many of the problems in the region of interest the higher order system will be of little interest.

The equations (2.50)-(2.53) together with appropriate boundary conditions form a complete system. The essential feature of the system is contained in equation (2.53), where the vertical velocity term is seen to be of the same order as the other terms in the equation and cannot therefore be neglected. The vertical motion appearing in the equation (2.53) is the adiabatic component associated with the positive and negative divergence of the horizontal motion field. The vertical mass flow due to the nonadiabatic heating and cooling is implicitly taken into account in the system which of course is the advantage of using the log of pressure as the vertical coordinate.

Several other properties of this set of equations should be noted:

1) The system (2.50)-(2.53) is considerably simpler than the general equations (2.1)-(2.4). Indeed, many problems in the dynamics of the upper atmosphere would be analytically intractable without the use of some such approximation.

2) The method of simplification which was employed in this section lead to sets of ordered equations. The system we have selected for our

purpose occurs to the zero order in R_o, the Rossby number. Since the system occurs uniformly to the order of R_o, we have obtained a dynamically consistent set of simplified equations applicable to all large scale thermospheric motions.

3) The system (2.50)-(2.53) has the dependent variables u, v, w and Φ. The four equations together with appropriate boundary conditions form a mathematically closed system.

4) When we consider the momentum equations, the present analysis allows us to see clearly which terms are important. Previous investigations of the momentum balance in the thermosphere have omitted the coriolis force (Lindzen, 1966, 1967), the ion drag (Lindzen 1966) or the inertial force (Geisler 1966).

5) In the equation of momentum the geopotential gradient is the driving force for the thermospheric wave disturbance. The geopotential gradient is the result of the diurnal oscillation of temperature. Balance between the forcing term and viscocity, ion drag, inertia and coriolis force must occur at all levels. At lower altitudes the balance takes place between the forcing, inertia and coriolis term. This region may be called the inviscid domain. In the altitude range between about 150 km. to 300 km. all terms have the same order of magnitude. Above about 300 km. the dissipative effect of the viscocity and the ion drag becomes dominant. Still further up in the thermosphere the only term balancing the geopotential gradient is the viscocity. (cf. table 2.)

6) The important role played by the vertical velocity and the static

stability in the thermodynamic equation should be emphasized here. The fact that horizontal advective terms are not present is consistent with the momentum equation. The nonlinear advective terms are of higher order and are therefore smaller in magnitude than the terms that we have retained in our system. The fact that vertical velocity is important is a significant result. Without some such analysis it might appear that horizontal advection would be more important in the energy balance of the upper atmosphere and indeed it has been thought that the only process which could account for the second heat source (other than corpuscular radiation) postulated by Harris and Priester (1962, 1965) was the energy transport by horizontal advection. It now appears more naturally that the second heat source may be due to the vertical velocity with the corresponding adiabatic heating and cooling of the thermosphere. This will be seen to be the case for a simple numerical model to be described below.

Further information about the relative importance of each term in the momentum and thermodynamic equations can be obtained from table 2. and equations (2. 50)-(2. 53). For example, if we wish to examine the role played by the heating due to the vertical velocity and heating due to conduction, we only need to compare the magnitude of S and ϵ_2 in table 2. In this way we find that below about 250 km. adiabatic heating is larger than the heating by conduction, whereas above this level, the latter are much larger than the former.

2.2.5 Numerical values for the parameters

From our physical assumptions stated above we may summarize the characteristic length and time scale for the system.

L = horizontal scale $\sim 10^7$ meters

H_s = vertical scale $\sim$ 60 km.

U = horizontal velocity $\sim 100\ m\ sec^{-1}$

Ω^{-1} = time scale $\sim$ 1 day

R_o = Rossby numer $\sim$ 0.1

$\bar{\mu}$ = characteristic dynamic viscocity $\sim 5.5 \times 10^{-4} g(m^{-1} sec^{-1})$

$\bar{\nu}$ = characteristic kinematic viscocity $\sim 10^6\ m^2\ sec^{-1}$

$\bar{K}$ = characteristic thermal conductivity $\sim 10^4 erg\ cm^{-1} sec^{-1} deg^{-1}$

γ = Taylor numer $\sim 1.4 \times 10^4$

δ^2 = $(H_s / L)^2$ $\sim 3.6 \times 10^{-5}$

ϵ_1 = thermal diffusivity $\sim 2.5 \times 10^{-4}$

S = static stability $\sim$ 0.5

π = ratio defined by equation (2.41) $\sim 2 \times 10^{-3}$

β = ion drag $\sim$ 1.5 night
$\sim$ 7.0 day

The values presented above are taken to be characteristic and therefore constant for the purpose of the scale analysis; however, most of them have a large variability with altitude and temperature. The magnitude of these parameters at a given height is a measure of the relative importance of each term in the equation for that particular altitude. Hence, it is convenient to know the range of variability of these nondimensional parameters.

Tables 1 and 2 indicate the variation of the parameters with altitude and with speed. The values of the dynamic and kinematic viscocity, the Taylor number, the thermal conductivity, thermal diffusivity, π, and the static stability have been obtained from the model result described in chapter 4. The quantities such as ion concentration, collision frequency needed for the calculation of the ion drag coefficient have been obtained from the calculation of Hanson (1961) and interpolated to the mean of the sunspot cycle.

Table 1.

Rossby number as α function of speed

$U(m\ sec^{-1})$	10	50	100	200	400
R_o	0.014	0.069	0.137	0.274	0.550

The values of β presented in table 2. represent an upper limit and depend largely on the ionization profile.

2.3 Boundary Conditions

In order to uniquely define solutions to (2.50)-(2.53) boundary conditions must be specified. The treatment of the lower boundary condition should be given special attention since this boundary is not rigid but open. Any mathematical model should be able to take into account the interaction between the lower atmosphere and the thermosphere. In particular, sources of energy in the lower atmosphere that might force the thermosphere into motion must be carefully considered. This includes, for example, transmission of energy

Table 2:

Nondimensional Parameter as a Function of Altitude

Height (Km)	β Night	β Day	γ^{-1}	δ^{-1}	ρ	S	ϵ_1	ϵ_2
100	0.006	0.38	3.24×10^{-9}	1.67×10^{3}	0.009	0.177	5.70×10^{-9}	0.016
200	0.025	2.60	7.35×10^{-6}	2.30×10^{2}	0.39	0.820	1.22×10^{-5}	0.650
300	1.70	7.60	9.0×10^{-5}	1.70×10^{2}	2.60	0.940	1.44×10^{-4}	4.200
400	2.10	7.30	8.26×10^{-4}	1.40×10^{2}	16.00	1.080	1.27×10^{-3}	24.800
500	1.50	5.20	2.34×10^{-3}	1.20×10^{2}	34.00	1.120	1.43×10^{-3}	50.000

through the lower boundary by vertically propagating gravity and Rossby waves and tides.

To a first approximation, these possible effects might be included in the lower boundary condition. At present, however, their inclusion is somewhat involved, mainly because the parameters describing these processes are not accurately known.

The selection of our boundary conditions is therefore somewhat arbitrary, many possibilities being present. We might specify values of the horizontal wind, the vertical velocity, the temperature or the temperature gradient at the lower or upper boundary or we might assume a rigid horizontal boundary at the bottom or the top. We might also assume an open boundary or try a free surface upon which the pressure is zero.

If we fix the lower boundary (the reference level) at 80 km. which is about the height of the mesopause, and the upper boundary at infinity, it seems most reasonable to apply a radiation condition at the lower boundary and require the condition of no flux of heat, momentum and mass at infinity. The radiation condition require that upward propagation of energy through the open boundary must be taken to be zero.

Since we are using a cartesian coordinate system, certain artificial boundary conditions must arise at those values of Y where we choose to limit the system. We could express the absence of an interaction between the regions outside and inside the boundary by having no energy flux across the boundaries, or we could erect vertical walls at $Y = \pm L$ to form a horizontal bounded system. In the latter case the lateral boundary condition is $\phi_{zY} = 0$ at $Y = \pm L$.

Since we are considering the behaviour of the disturbance right around the earth, it will suffice to assume that all variables are periodic in x. Finally, an initial condition must be specfied. This condition may be specified on Φ_z, or may set Φ_z equal to zero at the initial time.

3. ANALYTICAL SOLUTION TO THE TIME DEPENDENT HEAT CONDUCTION EQUATION

3.1 Derivation of the One Dimensional System

This section examines the possibility of obtaining expressions for the temperature in closed form. For many practical purposes the physical properties of the thermosphere can be described by the equation of thermal energy together with the ideal gas law and the hydrostatic equation. When no horizontal variability is allowed, the equation of thermal energy reduces to a simple heat conduction equation with sources and sinks. To obtain an analytic solution to this equation, some assumption regarding the thermal conductivity is required. If the ratio of the thermal conductivity to the scale height is assumed to be constant or to depend only on height, then the heat conduction equation has analytic solutions. The expression so obtained describes the diurnal temperature variation due to solar heating, radiational cooling and conduction.

Analytic solutions are obtained in terms of a Green's function for various boundary conditions and for several cases of the ratio of the thermal conductivity to the scale height. From these solutions one can ascertain more clearly the physical processes involved in the problem and in particular understand the effects of the boundary condition on the general solutions. Furthermore, the method presented here for the simple cases allows us to generalize to more complex situations where a different type of thermal conductivity change has to be considered.

When no horizontal variability is allowed, the system (2.50)-(2.53) reduces to (in dimensional units)

$$\frac{\partial \dot{z}}{\partial z} - \dot{z} = 0 \tag{3.1}$$

(3.2) $$c_p \frac{\partial T}{\partial t} + \dot{Z} c_p \left(\frac{\partial T}{\partial Z} + \frac{RT}{c_p} \right) = \frac{1}{\rho H} \frac{\partial}{\partial Z} \left(\frac{K}{H} \frac{\partial T}{\partial Z} \right) + q$$

where $$Z = - \ln p/p_0 \quad ; \quad \dot{Z} = \frac{dZ}{dt}$$

$$q = \dot{q}_{SR} + \dot{q}_{IR}$$

and all other terms have been defined in section (2.2).

Equation (3.1) has the solution $\dot{Z}$ proportional to e^{Z}, but the constant of proportionality must be zero since we require no mass flow at infinity. Therefore, the equations (3.1) and (3.2) reduce to the heat conduction equation, namely

(3.3) $$c_p \frac{\partial T}{\partial t} = \frac{1}{\rho H} \frac{\partial}{\partial Z} \left(\frac{K}{H} \frac{\partial T}{\partial Z} \right) + q$$

since $\rho H = \frac{p}{g}$ and $p = p_0 e^{-Z}$, (3.3) may be written as

(3.4) $$b^2 \frac{\partial T}{\partial t} = e^{Z} \frac{\partial}{\partial Z} \left(\frac{K}{H} \frac{\partial T}{\partial Z} \right) + Q$$

where $$b^2 = \frac{c_p p_0}{g} \quad ; \quad Q = \frac{p_0}{g} q$$

Equations (3.4) can be further simplified by making the following formation

(3.5) $$\varsigma = e^{-Z} = p/p_0$$

with the result

(3.6) $$b^2 \frac{\partial T}{\partial t} = \frac{\partial}{\partial \varsigma} \left(\frac{K}{H} \varsigma \frac{\partial T}{\partial \varsigma} \right) + Q$$

3.2 Green's Function for Finite Domain

3.2.1 Case 1.

$$\frac{K}{H} = \frac{\Gamma_0}{\rho} \quad , \quad \Gamma_0 = \text{constant}$$

Under this condition equation (3.6) simply becomes

$$\frac{\partial^2 T}{\partial \rho^2} - a^2 \frac{\partial T}{\partial t} = -\rho(\rho, t) \tag{3.7}$$

where

$$a^2 = b^2/\Gamma_0 \quad ; \quad \rho(\rho, t) = Q/\Gamma_0$$

It is possible to solve this inhomogeneous and initial-value problem in terms of a Green's function which satisfies homogeneous boundary conditions and a causality condition:

$$G(\rho, \rho'; t, t') = 0 \quad \text{if} \quad t < t' \tag{3.8}$$

We take G to satisfy the equation:

$$\left(\frac{\partial^2}{\partial \rho^2} - a^2 \frac{\partial}{\partial t}\right) G(\rho, \rho'; t, t') = -\delta(\rho - \rho')\delta(t - t') \tag{3.9}$$

The point-source forcing may be interpreted as a unit heat impulse introduced at the time t', and G is considered to represent the resulting transient temperature. The function G gives the temperature at a future time for any other point of the domain, thus describing the manner in which heat is conducted away from its initial position. The Green's function satisfying (3.9) depends only on the difference in coordinates ($\rho - \rho'$) and time ($t - t'$).

To find the solution of (3.7), we proceed as follows:

write (3.7) and (3.9) in the form

$$(3.7) \qquad \left(\frac{\partial^2}{\partial \mathcal{Y}'^2} - a^2 \frac{\partial}{\partial t'}\right) T(\mathcal{Y}', t') = - \rho(\mathcal{Y}', t')$$

$$(3.9) \qquad \left(\frac{\partial^2}{\partial \mathcal{Y}'^2} - a^2 \frac{\partial}{\partial t'}\right) G(\mathcal{Y}, \mathcal{Y}'; t, t') = - \delta(\mathcal{Y}-\mathcal{Y}')\delta(t-t')$$

where the sign of the term involving the time derivative in (3.9) has been changed, since the function G satisfies the reciprocity condition

$$(3.10) \qquad G(\mathcal{Y}, \mathcal{Y}'; t, t') = G(\mathcal{Y}', \mathcal{Y}; -t', -t)$$

Multiplying (3.7) by G and (3.9) by T, subtracting the two equations and integrating over space and time from 0 to t^+ , we obtain:

$$(3.11) \qquad \int_0^{t^+} dt' \int d\mathcal{Y}' \; T \frac{\partial}{\partial \mathcal{Y}'^2} G - G \frac{\partial}{\partial \mathcal{Y}'^2} T$$
$$+ a^2 \int d\mathcal{Y}' \int_0^{t^+} dt' \; T \frac{\partial G}{\partial t'} + G \frac{\partial T}{\partial t'} = \int_0^{t^+} dt' \int d\mathcal{Y}' \rho G - T(\mathcal{Y}, t)$$

Applying Green's theorem to the first integral and performing the integration of the second integral, we obtain,

$$(3.12) \qquad T(\mathcal{Y}, t) = \int_0^{t^+} dt' \int d\mathcal{Y}' \rho(\mathcal{Y}', t') \, G(\mathcal{Y}, \mathcal{Y}'; t, t')$$
$$+ \int_0^{t^+} dt' \left[G \frac{\partial T}{\partial \mathcal{Y}'} - T \frac{\partial G}{\partial \mathcal{Y}'} \right]_{\mathcal{Y}_0'}^{\mathcal{Y}_1'} + a^2 \int d\mathcal{Y}' [TG]_{t'=0}$$

The first integral in R. H. S. of (3.12) represents the effect of the forcing function (heating and cooling rates). The second integral represents the effect of the boundary conditions, and the last integral takes into account the initial distribution of temperature.

The Green's function for our bounded domain may be obtained by using eigenfunction expansion.

For simplicity we require here that the temperature gradient vanishes at the boundaries; that is, we impose the condition of vanishing heat flux at in-

finity and at the mesopause. These conditions can be expressed in our coordinate system as

$$\lim_{\varsigma \to 0} \quad \varsigma \frac{\partial T}{\partial \varsigma} = 0 \tag{3.13}$$

$$\lim_{\varsigma \to 1} \quad \varsigma \frac{\partial T}{\partial \varsigma} = 0$$

We take as an initial condition

$$T(\varsigma, 0) = T_0(\varsigma) \tag{3.14}$$

The solution of the scalar Helmhotz equation

$$\frac{d^2}{d\varsigma^2} \Upsilon_n + \lambda_n^2 \Upsilon_n = 0 \tag{3.15}$$

in the interval (0, 1), in which Υ_n satisfies a homogeneous boundary condition, namely

$$\lim_{\varsigma \to 0} \quad \frac{d\Upsilon_n}{d\varsigma} = 0 \quad ; \quad \lim_{\varsigma \to 1} \quad \frac{d\Upsilon_n}{d\varsigma} = 0 \tag{3.16}$$

is given by

$$\Upsilon_n = A_n \cos n\pi\varsigma \tag{3.17}$$

with

$$\lambda_n = n\pi \quad , \quad n = 1, 2, \cdots$$

Since the functions Υ_n form a complete set

$$\int \Upsilon_n \Upsilon_m \, d\varsigma = \delta_{nm} \tag{3.18}$$

we may expand the Green's function in terms of them.

Let then

$$G(\varsigma, \varsigma'; t, t') = \sum_n A_n(t, t') \Upsilon_n(\varsigma) \Upsilon_n(\varsigma') \tag{3.19}$$

Introducing this expansion into (3.9), we obtain the first order differential

equation for An:

$$a^2 \frac{dA_n}{dt} + \lambda_n^2 A_n = \delta(t-t') \tag{3.20}$$

with solution

$$A_n = \left(\frac{1}{a^2}\right) e^{-\frac{\lambda_n^2}{a^2}(t-t')} u(t-t') \tag{3.21}$$

where u (t-t') is the step function defined by

$$u(t-t') = \begin{cases} 0 & t < t' \\ 1 & t \geq t' \end{cases} \tag{3.22}$$

Hence

$$G(\gamma,\gamma';t,t') = \left(\frac{1}{a^2}\right) u(t-t') \sum_n e^{-\frac{\lambda_n^2}{a^2}(t-t')} \cos n\pi\gamma \cos n\pi\gamma' \tag{3.23}$$

and the solution of the one dimensional heat conduction equation (3.7) with boundary condition (3.13) and initial condition (3.14) is given by

$$T(\gamma,t) = \sum_n \int_0^{t^+} dt' \frac{u(t-t')}{a^2} e^{-\frac{\lambda_n^2}{a^2}(t-t')} \int_0^1 d\gamma' f(\gamma',t') \cos n\pi\gamma \cos n\pi\gamma' + \sum_n e^{-\frac{\lambda_n^2}{a^2}t} \int_0^1 d\gamma' T_0(\gamma') \cos n\pi\gamma \cos n\pi\gamma' \tag{3.24}$$

3.2.2 Case 2.

$\frac{K}{H} = \Gamma_0$ = constant

Under this assumption equation (3.6) reduces to

$$\left(\frac{\partial}{\partial\gamma}\gamma\frac{\partial}{\partial\gamma} - a^2\frac{\partial}{\partial t}\right)T(\gamma,t) = -f(\gamma,t) \tag{3.25}$$

The equation satisfied by the Green's function now becomes

$$\left(\frac{\partial}{\partial\gamma}\gamma\frac{\partial}{\partial\gamma} - a^2\frac{\partial}{\partial t}\right)G(\gamma,\gamma';t,t') = -\delta(\gamma-\gamma')\delta(t-t') \tag{3.26}$$

Let us consider the same boundary and initial conditions as (3.13) and (3.14). Note that we could use any type of boundary condition since the general expression for the temperature given by (3.12) allows us to specify this condition easily.

We require the solution of the scalar equation

(3.27) $$\frac{d}{d\rho}\left(\rho \frac{d}{d\rho} Y_n\right) + \lambda_n^2 Y_n = 0$$

with homogeneous boundary conditions. Equation (3.27) can be identified as Bessel's equation with general solution.

(3.28) $$Y_n = Z_0 (2 \lambda_n \rho^{1/2})$$

where

(3.29) $$Z_0(x) = c_1 J_0(x) + c_2 Y_0(x)$$

To satisfy our boundary condition at $\rho = 0$, we require $c_2 = 0$, hence

(3.30) $$Y_n = c_n J_0 (2 \lambda_n \rho^{1/2})$$

where the characteristic values of λ_n are determined as the roots of the equation

(3.31) $$J_0'(2\lambda_n) = J_1(2\lambda_n) = 0$$

Since the function (3.30) forms a complete set, we may expand the Green's function in terms of them

(3.32) $$G(\rho,\rho';t,t') = \sum_n c_n (t-t') J_0 (2\lambda_n \rho^{1/2}) J_0 (2\lambda_n \rho'^{1/2})$$

Following the same procedure as in section (3.2.1) we obtain the expression for the Green's function

(3.33) $$G(\rho,\rho';t,t') = \left(\frac{1}{a^2}\right) u(t-t') \sum_n e^{-\frac{\lambda_n^2}{a^2}(t-t')} J_0(2\lambda_n \rho^{1/2}) J_0(2\lambda_n \rho'^{1/2})$$

and the solution of the heat conduction equation (3.25) with boundary condition (3.13) and initial condition (3.14) is

$$(3.34)\quad T(\zeta,t) = \sum_n \int dt' \frac{u(t-t')}{a^2} e^{-\frac{\lambda_n^2}{a^2}(t-t')} \int_0^{\prime} d\zeta' \rho(\zeta',t') J_0(2\lambda_n \zeta'^{1/2}) J_0(2\lambda_n \zeta'^{1/2}) + \sum_n e^{-\frac{\lambda_n^2}{a^2} t} \int_0^{\prime} d\zeta' T_0(\zeta') J_0(2\lambda_n \zeta'^{1/2}) J_0(2\lambda_n \zeta'^{1/2})$$

3.2.3 Case 3.

$$\frac{K}{H} = \frac{K_0}{H_0} \left(\frac{H(P_0)}{H(P)} \right)^{1/2}$$

This condition assumes that t the ratio of the thermal conductivity to the scale height can be expressed in terms of its value at some reference level times the square root of the ratio of the scale height at the reference level to the scale height at any other position.

Let

$$(3.35)\quad \frac{K_0}{H_0} = \Gamma_0 \quad ; \quad \left(\frac{H(P_0)}{H(P)} \right)^{1/2} = \gamma$$

Then equation (3.6) reduces to

$$(3.36)\quad \left[\frac{\partial}{\partial \zeta} \left(\gamma \zeta \frac{\partial}{\partial \zeta} \right) - a^2 \frac{\partial}{\partial t} \right] T(\zeta,t) = -\rho(\zeta,t)$$

Now the variability of γ in the thermosphere is negligible, above about 150 km. $\gamma \approx 1$. Hence equation (3.36) becomes identical to the case 2. discussed above.

3.2.4 Case 4.

$$\frac{K}{H} = \Gamma_0 \rho^{m-1} \quad , \quad \Gamma_0 = \text{constant}$$

In this case we can write equation (3.6) in the form

$$\left[\frac{\partial}{\partial \rho}\left(\rho^m \frac{\partial}{\partial \rho}\right) - a^2 \frac{\partial}{\partial t}\right] T(\rho,t) = -\rho(\rho,t) \tag{3.37}$$

To solve (3.37) we need to find the Green's function for the equation, just as we did above. The Green's function will satisfy the equation

$$\left[\frac{\partial}{\partial \rho}\left(\rho^m \frac{\partial}{\partial \rho}\right) - a^2 \frac{\partial}{\partial t}\right] G(\rho,\rho';t,t') = -\delta(\rho-\rho')\delta(t-t') \tag{3.38}$$

Consider again the same boundary condition (3.13) and initial condition (3.14). The solution of the scalar equation

$$\frac{\partial}{\partial \rho}\left(\rho^m \frac{\partial}{\partial \rho} Y_n\right) + \lambda_n^2 Y_n = 0 \tag{3.39}$$

with homogeneous boundary conditions is obtained in terms of the Bessel's function

$$Y_n = \rho^{\frac{1-m}{2}} Z_p\left(\frac{\lambda_n}{s}\rho^s\right) \tag{3.40}$$

where

$$s = -\frac{m-2}{2} \quad , \quad p = \frac{1-m}{2s}$$

and the characteristic values λ_n are determined as the roots of the equation

$$J_p'\left(\frac{\lambda_n}{s}\rho^s\right) - \frac{m-1}{2}\rho^{-1} J_p\left(\frac{\lambda_n}{s}\rho^s\right) = 0 \tag{3.41}$$

To obtain the Green's function, we again expand G in terms of (3.40), substituting this expansion in (3.38). We obtain

$$G(\rho,\rho';t,t') = \frac{1}{a^2} u(t-t') \sum_n e^{-\frac{\lambda_n^2}{a^2}(t-t')} \rho^{\frac{1-m}{2}} \rho'^{\frac{1-m}{2}} J_p\left(\frac{\lambda_n}{s}\rho^s\right) J_p\left(\frac{\lambda_n}{s}\rho'^s\right) \tag{3.42}$$

and the solution for T (ρ , t) is readily obtained as:

$$(3.43)\quad T(\varsigma,t) = \sum_n \int_0^{t^+} dt' \frac{u(t-t')}{a^2} e^{-\frac{\lambda_n^2}{a^2}(t-t')} \int_0' d\varsigma' \rho(\varsigma',t') \varsigma^{\frac{1-m}{2}} \varsigma'^{\frac{1-m}{2}} J_0\left(\frac{\lambda_n}{s}\varsigma^s\right) \times$$

$$\times J_0\left(\frac{\lambda_n}{s}\varsigma'^s\right) + \sum_n e^{-\frac{\lambda_n^2}{a^2}t} \int_0' d\varsigma' T_0(\varsigma') \varsigma^{\frac{1-m}{2}} \varsigma'^{\frac{1-m}{2}} J_0\left(\frac{\lambda_n}{s}\varsigma^s\right) J_0\left(\frac{\lambda_n}{s}\varsigma'^s\right)$$

3.3 Green's Function for an Infinite Domain

Case $\frac{K}{H} = \frac{\Gamma_0}{\varsigma}$; Γ_0 = constant

Next we shall consider the case in which the domain is extended from $+\infty$ to $-\infty$. We may assume again the same boundary conditions as in section (3.2), that is, the heat flux vanishes far away from the region of interest. In our transformed coordinate system these conditions imply

$$(3.44)\quad \lim_{\varsigma \to 0} \varsigma \frac{\partial T}{\partial \varsigma} = 0$$

$$\lim_{\varsigma \to \infty} \varsigma \frac{\partial T}{\partial \varsigma} = 0$$

The initial condition may be expressed as $T(\varsigma, 0) = T_0(\varsigma)$

In similar manner to case 1, section (3.2), the heat conduction equation (3.6) reduces to

$$(3.45)\quad \left(\frac{\partial^2}{\partial \varsigma^2} - a^2 \frac{\partial}{\partial t}\right) T(\varsigma,t) = -\rho(\varsigma,t)$$

Likewise, the Green's function satisfies the equation

$$(3.46)\quad \left(\frac{\partial^2}{\partial \varsigma^2} - a^2 \frac{\partial}{\partial t}\right) G(\varsigma,\varsigma';t,t') = -\delta(\varsigma-\varsigma')\delta(t-t')$$

In this case the Green's function, the temperature at ς at the time t due to the instantaneous point source at ς' at time t', is provided by the method of images and is given by (cf. Morse and Feshbach, 1953)

$$(3.47)\quad G(\varsigma,\varsigma';t,t') = \frac{1}{2a\sqrt{\pi(t-t')}} e^{-\frac{a^2(\varsigma-\varsigma')}{4(t-t')}}$$

Hence the temperature at ζ at time t is given by

$$(3.48)\quad T(\zeta,t) = \frac{1}{2a}\int_0^{t^+} \frac{dt'}{\sqrt{\pi(t-t')}} \int_0^{\infty} d\zeta' \rho(\zeta',t')\, e^{-\frac{a^2(\zeta-\zeta')}{4(t-t')}} + \frac{a}{2\sqrt{\pi t}} \int_0^{\infty} d\zeta' T_0(\zeta')\, e^{-\frac{a^2(\zeta-\zeta')}{4(t-t')}}$$

This method may be extended easily to obtain solutions to the heat conduction equation for a variety of conditions on $\frac{K}{H}$, as well as to any type of boundary conditions as was stated above. The nature and physical interpretation of the solution can be obtained when the sources of heat are specified.

So far it has been assumed that the source function is known. Actually the heating and cooling rates depend on the thermospheric structure and therefore they must be calculated simultaneously. However, the results of the numerical computation indicate that the change in the cooling rates are negligible and therefore easily expressed in closed form. Likewise, the heating rates could be modeled by some simple smooth function which fits the observational data or the numerically computed values.

Without loss of generality a simpler physical interpretation of the gross features of the solution might be obtained by assuming a source of the form $Q(\zeta, t) = \delta(\zeta)\,\delta(t)$, the temperature distribution is then evaluated from G and the appropriate initial and boundary conditions.

An immediate extension of the method described above to the dynamical system would be, for example, to make a decoupling approximation of the

dynamic and heat energy equations. Several simple analytical solutions could be then discussed. The horizontal momentum equations are completely analogous to the heat conduction equation (except for one or two linear terms which may be included with no difficulty), and therefore the technique described above can similarly be applied. These possibilities will be discussed to some extent in chapter 6.

The approximate analytical solutions presented above greatly facilitate the physical understanding and are easy to manipulate.

4. NUMERICAL SOLUTION TO THE TIME DEPENDENT HEAT CONDUCTION EQUATION WITH SOURCES AND SINKS.

4.1 General Remarks

The preceeding section has raised the following questions which require the analysis of radiative heating and cooling in the thermosphere:

What is the variability and distribution of the solar heating and infrared cooling over the globe throughout the day and seasons?

How do these changes in the heating and cooling rates influence the temperature and density distribution over the globe?

The amplitude of heating sources depends on the atmospheric density which in turn depend on the sources. Therefore, any study of the heating rates should be made simultaneously with study of the distribution and changes in the atmospheric density.

To answer the above questions a simplified model for the thermosphere with only vertical variability will be considered. This approach is designated as the one dimensional model. With this simplification the hydrodynamic and thermodynamic equations reduce to the time dependent heat conduction equation. The solution to this equation together with that of the hydrostatic equation constitute the so-called "quasi-static model."

The quasi-static model allows time variability as well as vertical motion associated with nonadiabatic heating, that is, motion that arise by expanding and contracting the thermosphere when the medium is heated by solar radiation.

In order to deal with a realistic description of the interaction between the energy sources and atmospheric density, numerical techniques must replace the analytical methods. We also recall that in order to obtain an analytical solution to the heat conduction equation in chapter 3, we had to linearize the system by assuming some simple model for the dependence of the ratio of the thermal conductivity to the scale height. The use of numerical techniques to solve this problem lacks the elegance of purely analytical treatment; however, this will be compensated by the fact that the solution will correspond more closely to reality.

A summary of various modeling studies describing energy sources and structural changes in the thermosphere is presented in the next section; a discussion of the results of the model calculation regarding the amplitude and phase of the temperature and density appears next; and in section (4.2.4) we investigate the horizontal variability of the properties of the thermosphere when changes in season are also included.

4.2 A Modeling Study of the Structure of the Thermosphere

4.2.1 Description of various models

The original idea postulated by Spitzer (1949) regarding the importance of molecular conduction of heat in the energy balance of the thermosphere was developed both qualitatively and quantitatively by Bates (1951) and Nicolet (1960, 1961). Nicolet's calculation for example predicted the existence of a thermopause above which the atmosphere is isothermal. Based

on the Bates' estimates, Johnson (1956, 1958) computed the vertical temperature distribution for steady-state conditions. Further calculations were also performed by Hunt and Van Zandt (1961).

The first numerical model describing the time dependence of the structure of the thermosphere was carried out by Harris and Priester (1962, 1965), in the region between 120 and 2000 km., and more recently Mahoney (1966) has developed another numerical model which uses more extensive data for the calculation of the heating rates.

Both Harris and Priester's and Mahoney's models allow variability in altitude and time only, and are representative of equinox conditions. Both models compute the total heating rates and the subsequent structural changes at each time step. The model of Harris and Priester employs geometrical altitude as the vertical coordinate. Boundary conditions are specified at 120 km. A time interval of 15 minutes and a vertical resolution of 1 km. were used.

Mahoney's calculations are referred to surfaces of constant pressure which allows a larger grid spacing. Time steps of two hours are used. Boundary conditions are specified at 80 km. The model extends from 80 to 500 km. A more detailed description of the latter model will be given after a discussion of the main results of these two models.

The results of Harris and Priester's calculations when the energy sources are due solely to ultraviolet solar radiation, do not agree with the results of satellite observations in two ways: First the calculations yield a

diurnal maximum of temperature and density at 17 hours local time, not at 14 hours local time as is observed. Second, if the incident flux is adjusted to give the observed average temperature, the calculations predict a diurnal variability which is large compared to the observed amplitude. Harris and Priester have proposed a "second heat sources" with the proper characteristics to reconcile the results of their computations with observations. They attribute this second heat source to solar corpuscular radiation or its "steady" component, the solar wind. They give no explanation, however, for the assumed time dependence of the second heat source, nor do they specify the space dependence.

The results of Mahoney's calculation indicate that the amplitude of the computed diurnal temperature and density variation is related to the choice of latitude and of the absorption cross section. His model can yield reasonable thermospheric structure only for a limited range of the various atmospheric parameters. However, the phase of the computed temperature variation is not sensitive to changes in the model parameters, and he finds that the maximum temperature occurs around 18 hours local time. He has also suggested that horizontal energy transport must be included in order to improve the model calculation so as to achieve the phase relationship deduced from satellite data.

Harris and Priester

It should be pointed out here that both Priester and Harris, and Mahoney have included in their models the effect of the vertical motion associated with nonadiabatic heating, however, the subsidence heating and the effect of the

vertical velocity associated with the positive and negative divergence of the horizontal wind field have been neglected. These effects will be discussed in section 5. 2.

It should be worth while to mention here that when the time dependence of the heat conduction equation is neglected the model reduces to the description of an equilibrium state. The solution of these equations is commonly referred to as "The Mean Atmosphere." The model characterizing the properties of the thermospheric structure is then called a "static model," or a "steady-state" model. However, at high altitudes--i. e. above the thermopause--the densities have a large diurnal variability and therefore, a mean reference atmosphere has little meaning. Nevertheless, the static models have provided much useful information concerning the properties of the upper atmosphere. The construction of the static models have been undertaken by many investigators and the results are widely used. The major contributors to this important task are Nicolet (1960, 1961), Chapman (1961), Bates (1951), Mange (1955, 1957, 1961), Johnson (1956, 1958), and Jacchia (1960, 1961) among others.

Radiative sources and sinks of energy and heat conduction are important mechanisms in the thermosphere and only by the consideration of these processes can the structure of the upper atmosphere be adequately described.

Absorption of solar ultraviolet radiation is the main energy source; it is present only in the daytime and, although energy loss by radiation is smaller and less important in the upper thermosphere, it is significant in the lower

thermosphere throughout the day and night. Vertical conduction of heat is also important in the heat balance of the thermosphere. During the night when the sun is absent the vertical heat flux is mainly controlled by conduction.

4.2.2 Calculations of the energy sources and the structure of the thermosphere

The basic model and the computational scheme used to calculate the energy sources and the structural changes of the thermosphere is described in full by Harris and Priester (1962, 1965) and Mahoney (1966), so it is unnecessary to repeat it here.

In the present work the numerical model of Mahoney will be adopted and only a brief summary of the basic principles will be presented here. The governing equation describes heat conduction with energy sources in an atmosphere composed of O, O_2 and N_2, and extending from 80 to about 500 km. All calculations are referred to 15 surfaces of constant pressure and no explicit horizontal variability is permitted in the model. The pressure changes by a factor of e, 2.718, between adjoining standard surfaces, and the height of the lowest surface labelled surface 1 is fixed at 80 km. O_2 and N_2 are assumed to be perfectly mixed between 80 and approximately 105 km., and the vertical distribution of 0 in that region is specified in a manner so that the effects of the photo-dissociative production and the subsequent vertical diffusion of 0 are taken into account. Diffusive equilibrium is specified for all three constituents above 105 km.

When no horizontal variability is permitted in the model we saw, in

section (3.1) that the hydrodynamic and thermodynamic equations reduce to the simple form (cf. equation (3.2)).

$$(4.1) \qquad c_p \frac{\partial T}{\partial t} = \dot{q}_{TOT} = \dot{q}_{SR} + \dot{q}_{IR} + \dot{q}_{COND}$$

where $T = T(Z, t)$ = temperature, (deg. K).

c_p = specific heat at constant pressure (ergs gm^{-1} deg^{-1})

$\dot{q}_{TOT}$, $\dot{q}_{SR}$, $\dot{q}_{IR}$, $\dot{q}_{COND}$ = total and individual heating rates per unit mass (ergs $gm^{-1}sec^{-1}$).

It is assumed that the heating due to the absorption of solar radiation ($\dot{q}_{SR}$) is accomplished by the portion of the solar spectrum for which $1775\ A^{\circ} > \lambda > 30\ A^{\circ}$; this part of the spectrum is divided into 32 wavelength bands, and absorption coefficients for N_2, O and O_2 for each of the bands are specified. The solar heating at level k due to the flux in wavelength interval ℓ is calculated as

$$(4.2) \qquad \dot{q}^{k}_{SR}(\ell) = \sum_{i=1}^{3} F_{\infty}(\ell) \in \frac{n_i^k \mu_i(\ell) m_i}{n^k \bar{m}^k} \exp - \left(\sum_{i=1}^{3} \mu_i(\ell) \Gamma_i^k \right)$$

where $F_{\infty}(\ell)$ = solar flux in interval ℓ outside the atmosphere (ergs cm^{-2} sec^{-1}),

$\in$ = efficiency factor for solar heating,

n_i^k = number density of i^{th} constituent ; (O, O_2 and N_2) at level K(cm^{-3}),

n^k = total number density at level K,

$\mu_i(\ell)$ = absorption cross-section in interval for i^{th} constituent ($cm^2 gm^{-1}$),

m_i = gram-molecular weight for i^{th} constituent (gm),

$\bar{m}^k$ = mean molecular weight at level K (gm)

Γ_i^k = absorption path length for i^{th} constituent above level K.

The total solar heating at level k is computed as the sum of the contributions from all 32 wavelength bands. Solar energy flux data corresponding to average values of solar activity were used (Hinteregger et al., 1965) and the heating efficiency ϵ was set equal to 0.60 for $\lambda \leq 1200A^{o}$ and 0.10 for $\lambda > 1200A^{o}$.

The heat loss ($\dot{q}_{IR}$) is due primarily to the radiation of atomic oxygen at 63μ . Its magnitude is quite small compared to the heat gain by EUV radiation in the region above 150 km. However, below this altitude, it has an important role in determining the temperature distribution.

The radiational cooling rate at level k is calculated according to the form suggested by Bates (1951) and used by Harris and Priester (1962):

$$\dot{q}^{K}_{IR} = \frac{n^{K}(O) \times 10^{-18}}{\rho^{K}} \left(\frac{1.68 \exp(-228/T^{K})}{1 + 0.6 \exp(-228/T^{K}) + 0.2 \exp(-325.3/T^{K})} \right) \quad (4.3)$$

ergs $gm^{-1} sec^{-1}$

where ρ^{K} = total mass density at level k (gm cm^{-3}).

The conduction heating at level k is calculated as

$$\dot{q}^{K}_{COND} = \frac{1}{\rho^{K} \bar{H}^{K}} \frac{\partial}{\partial Z} \left(\frac{\bar{K}}{\bar{H}} \frac{\partial T}{\partial Z} \right)^{K} \quad (4.4)$$

where $\bar{H}^{K}$ = mean scale height at level k (cm)

$\bar{K}$ = coefficient of heat conduction averaged according to concentration of the constituents (erg cm^{-1} deg^{-1} sec^{-1}).

Equations (4.2)-(4.4) for the individual heating rates are substituted into equation (4.1); the resulting equation is a parabolic equation for T = T(Z, t). This equation is integrated numerically with the aid of an implicit

scheme (which is required for computational stability), and the new temperature at each of the standard pressure levels is calculated every time step because these changes influence the calculation of the heating rates. Thus the data available at the end of each time step include the temperatures and heights of the 15 constant pressure surfaces, the individual and total mass and number densities, the individual and mean scale heights, the mixing ratios for the constituents, and the individual and net heating rates.

4.3 Seasonal and Latitudinal Variation of the Temperature and Density in the Thermosphere.

4.3.1 Description of experiments

In this section the horizontal variability of the thermospheric structure is investigated when changes in season and latitude are permitted in the model. Mahoney's calculation for the equinox case is extended and a new set of calculations representing solstice condition in both hemispheres are obtained.

During the first solstice calculations the initial temperature profiles from the equinox cases were used; however, several model days elapsed before the solutions converged. Subsequently, initial temperature values which could converge rapidly toward diurnally repeating solutions were chosen. (Convergence toward a diurnal cyclical state is taken as the criterion for true solutions). Two hour time steps were used throughout the experiments until nearly cyclical solutions were achieved; then final data were obtained using one hour time steps. Because of the larger number of model days

Table 3
Results of Numerical Experiments According to Model Calculation.
See Text for Identification of Terms

Equinox

LAT (deg)	T_I^{15}(0600) (^oK)	N (days)	T_F^{15} (0600) (^oK)	Conv (%)	R
60N	967.9	9	640.7	1.5	1.59
45N	749.0	5	799.5	0	1.54
30N	1420.0	12	968.8	0.1	1.49
15N	1066.6	3	1069.6	0.1	1.46
0	967.9	9	1097.1	0.4	1.45
15S					
30S					
45S	(same as in northern hemisphere)				
60S					

June Solstice

LAT (deg)	T_I^{15}(0600) (^oK)	N (days)	T_F^{15}(0600) (^oK)	Conv (%)	R
60N	985.8	9	1533.9	1.8	1.27
45N	1370.0	5	1514.4	0.7	1.32
30N	1042.9	10	1370.0	0.7	1.37
15N	1092.1	6	1153.9	0.5	1.44
0	1090.2	3	1064.3	0.8	1.46
15S	969.3	6	855.6	1.0	1.52
30S	754.8	8	607.7	1.5	1.65
45S	467.0	5	381.0	2.2	1.77
60S	664.4	9	211.6	4.3	1.63

needed to obtain true solutions at 60^{o} latitude, no experiments were carried out for latitudes larger than 60^{0}.

A survey of the numerical experiments is shown in Table 3. T_I^{15} (0600)and T_F^{15}(0600) represent the temperature of level 15 at 0600 hours during the initial and final model day of each calculation. As discussed below T^{15} represents the temperature above the thermopause. N is the number of model days needed in the experiment to obtain cyclical solutions. "Conv" is a measure of the convergence toward a cyclical state for the model defined as

$$Conv = \frac{T^{15}_{LAST\ DAY}(0600) - T^{15}_{PREVIOUS\ DAY}(0600)}{T^{15}_{LAST\ DAY}(0600)} \times 100$$

The last column in table 3 indicates the calculated ratio of the maximum to the minimum temperature (R) for the last model day at level 15 at each latitude.

4.3.2 Model results for heating rates

This section includes the distribution and changes of the energy gain and loss according to the model calculation. Only a small sample is presented here.

Once the structure of the thermosphere is known, the heating and cooling rates are computed for each level in the model every time step. The investigation of seasonal and latitudinal variation of the heating rates is accomplished by allowing seasonal and latitudinal dependence in the absorption path length for each constituent. The absorption path length is a function of the integrated density above a given altitude as well as of the solar zenith angle (ψ). The solar zenith angle dependence takes into account the unequal solar radia-

tion distribution in the earth's atmosphere and is related to the solar declination (δ), latitude (φ), and the hour angle (h) by the equation

(4.5) $$\cos\psi = \sin\delta \sin\varphi + \cos\delta \cos\varphi \cos h$$

Thus the response of the model thermosphere to lengthened (long summer days) and shortened (long winter nights) periods of solar radiation and the subsequent heating rate changes are studied.

Figures 1 and 2 illustrate the vertical profile of the heating and cooling rates for several latitudes for equinox and solstice conditions. Very little seasonal change occurs in low latitudes, however, in middle and higher latitudes the seasonal variability is important. The seasonal changes in general occur in the region between 100 and 300 km. Figure 1 shows also that the heating and cooling rates in the winter season have larger values than in the equinox and summer season. These differences generally take place in the altitude range of 150 and 250 km.

This paradoxical behavior is understood if we consider the variability of the heating rate with density and absorption path length (see equation 4.2). When seasonal changes are examined, the density at a certain height is greater in summer than in winter. Similarly the absorption path length is larger in the summer than in winter. These differences increase with latitude. Consequently the heating rate at a constant altitude becomes smaller in summer than in winter. We could also say that the heating rate remains approximately constant along a surface of constant density. Hence, it becomes evident from figure 12 why the heating rates have the nature described above. A similar argument applies to cooling rates.

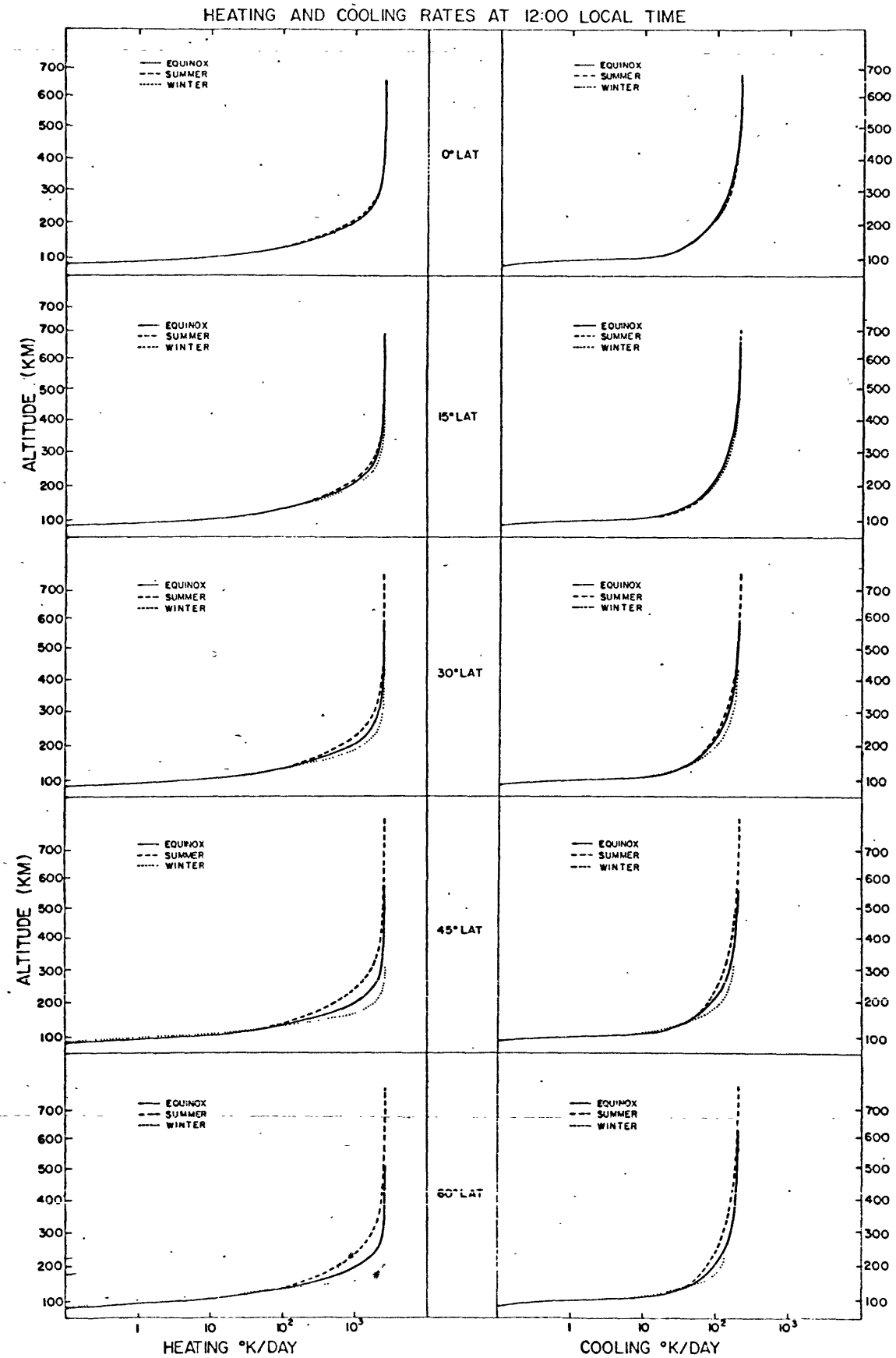

Figure 1: Vertical distribution of heating rates by absorption of EUV Solar radiation for several latitudes and seasons; and cooling rates by long wave radiation emitted by O at 1200 local time.

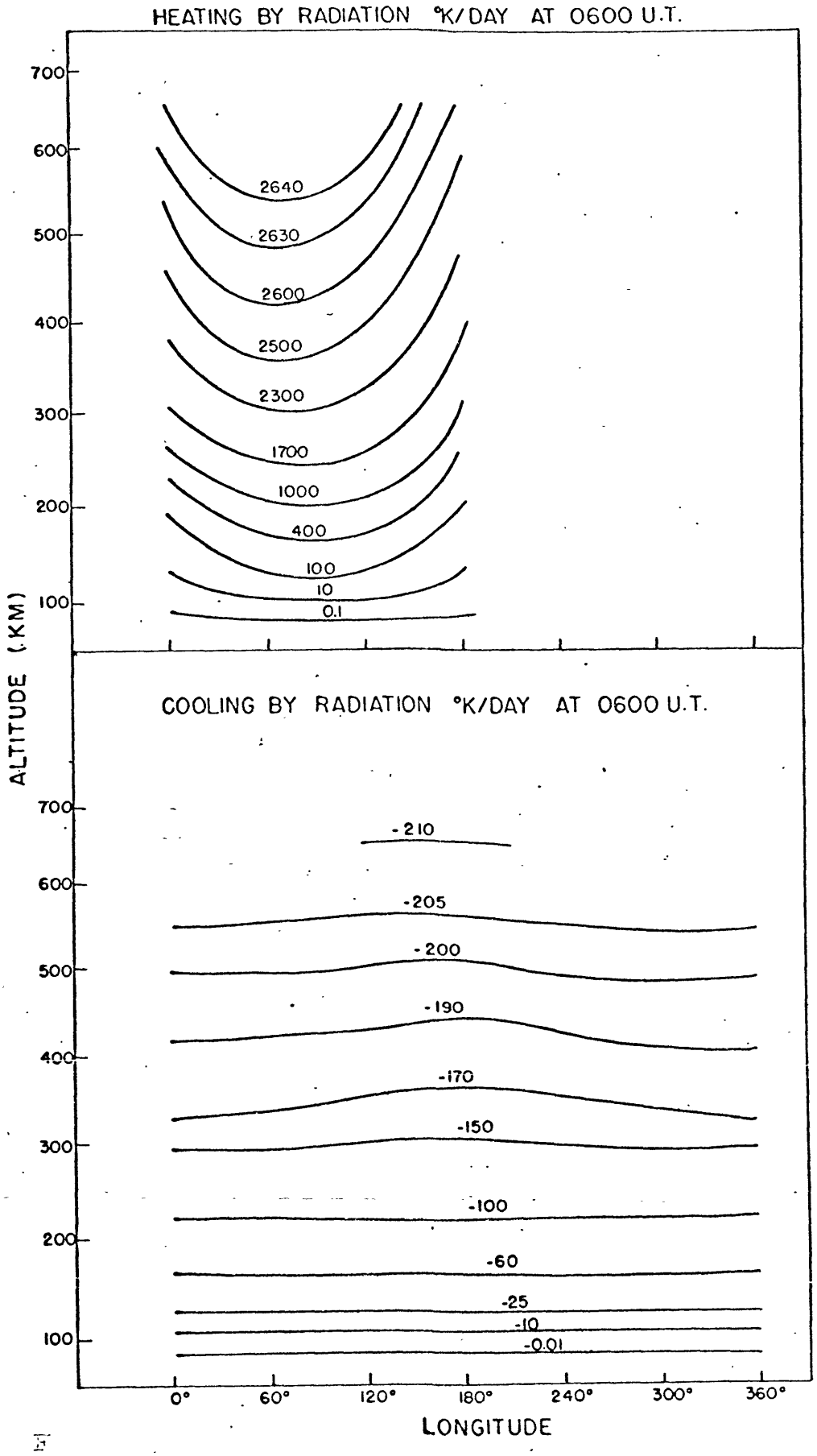

Figure 2: Longitudinal cross-section of heating and cooling rates at 0600 universal time.

We must keep in mind that the results discussed above are somewhat unrealistic since no horizontal transport of mass has been allowed in the model calculations. When horizontal motion takes place and the mass transport is not sufficient to over come the seasonal effect, the discussion above might be expected to apply with reduced differences. This is supported by density measurements, including variations with latitude and season. May (1963) and Anderson (1966a, 1966b) have reported the existence of large density variability with latitude. This will be discussed in section (4.3.4).

Figure 2 shows the variability of heating and cooling rates with longitude or with local time. As pointed out by Mahoney (1966) there is very little variation of cooling rates with local time.

In the region above 150 km. the magnitude of the cooling rate is about ten per cent of the magnitude of the heating rate; however, below this altitude both are equally important.

4.3.3 Model results of temperature variation

This section contains a survey of the computed variability of temperature in the thermosphere as a function of altitude, local time, latitude and season.

We have stressed above that the temperature distribution in the thermosphere is governed mainly by heat conduction and by absorption of the incident EUV solar radiation. Any change in the source input leads to changes in the temperature field and therefore it is important to know the kind of variations we would expect in the atmospheric properties when the sources undergo sea-

Figure 3: Diurnal and seasonal temperature variability with altitude at 15 and 45 deg. latitude according to the model calculations.

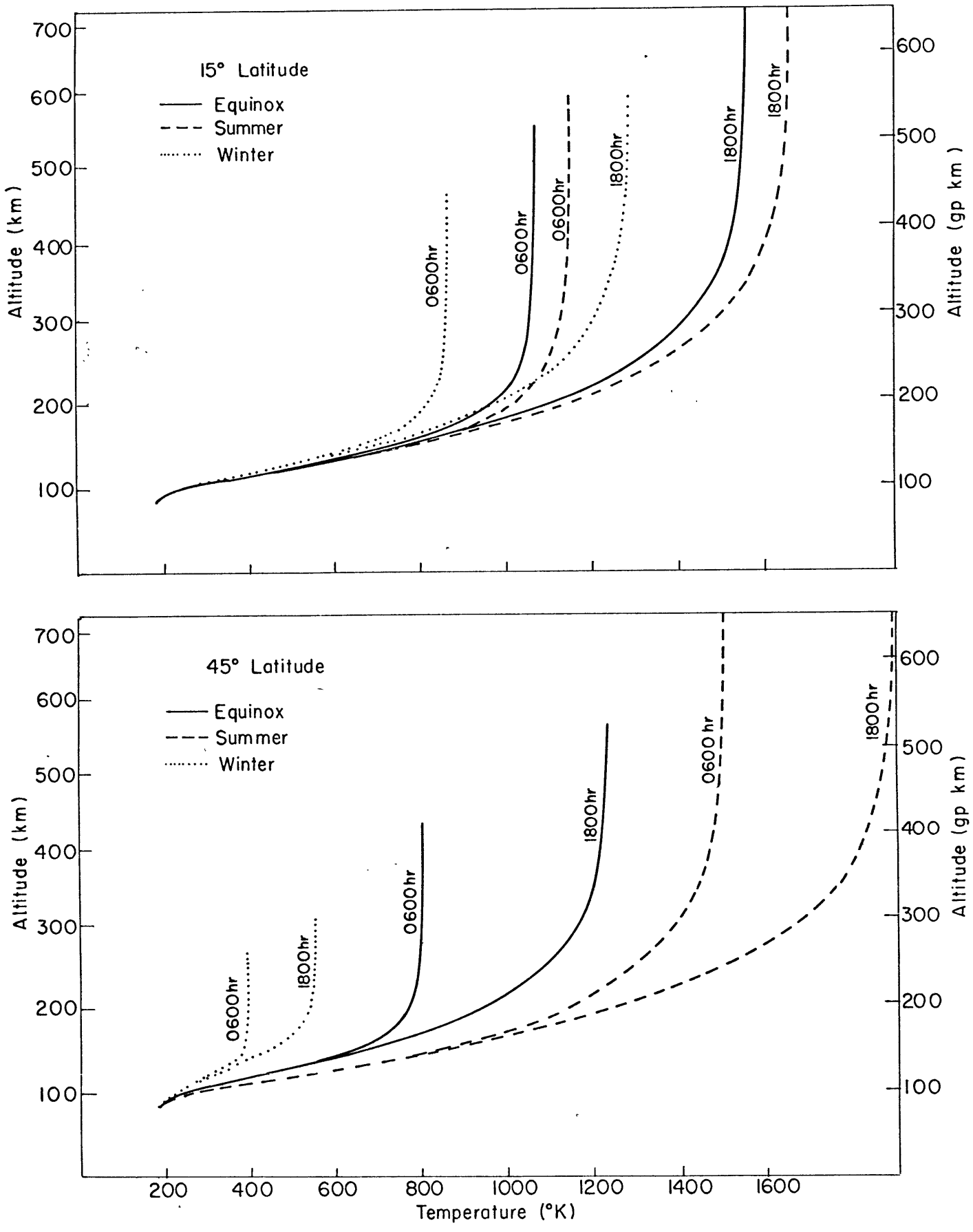
15° Latitude
Equinox
Summer
Winter
0600hr
0600hr
0600hr
1800hr
1800hr
1800hr
Altitude (km)
Altitude (gp km)
700
600
500
400
300
200
100
45° Latitude
Equinox
Summer
Winter
0600hr
1800hr
0600hr
1800hr
0600 hr
1800hr
Altitude (km)
Altitude (gp km)
200
400
600
800
1000
1200
1400
1600
Temperature (°K)

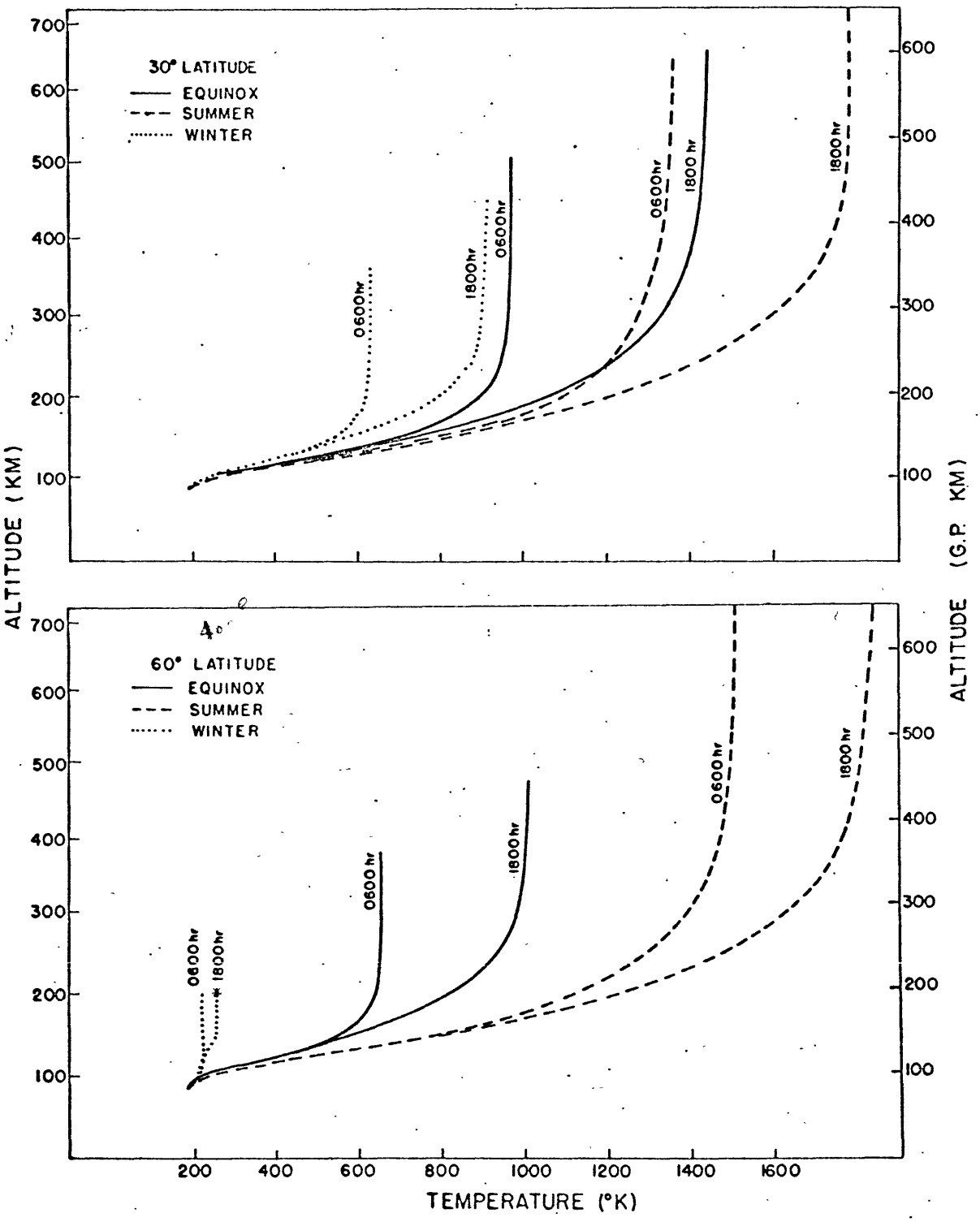

Figure 4: Same as figure 3, but at 30 and 60 deg. latitude.

sonal and latitudinal changes.

Figures 3 and 4 illustrate the computed vertical temperature profiles for low, mid and high-latitude cases. The altitude scales in these figures, as well as in figures 8, 10, and 11 are presented in both geometric and geopotential height units. Geopotential heights, based upon a reference level of 80 km., are used in the model calculations. Temperature profiles in figures 3 and 4 correspond to 0600 and 1800 hours local time; these are approximately the time of minimum and maximum temperatures for all calculations except those corresponding to the high latitude winter and summer cases.

Figures 3 and 4 illustrate that there is a region of rapidly increasing temperature between approximately 100 and 200 km. in all cases. The thermopause (i. e. the base of the isothermal region) is directly related to the temperature in that region, low temperature structure corresponding to low thermopause heights, and vice versa. The magnitude of diurnal temperature variability as measured by the difference between the 1800 and 0600 temperature profiles, decreases as latitude increases. At the lower latitudes the amplitude of diurnal temperature variability is significantly larger than the amplitude of seasonal variability; however seasonal variability dominates diurnal variability at middle and higher latitudes.

The temperature difference between the summer and equinox cases for the highest level of the model is 20°K at the equator and about 700°K at 45° latitude at 0600 hours. The corresponding values for the difference be-

Figure 5: Latitudinal variability of temperature for four of the constant pressure surfaces used in the model calculations, for the equinox case. Profiles are presented for 0600 and 1800 hours local time.

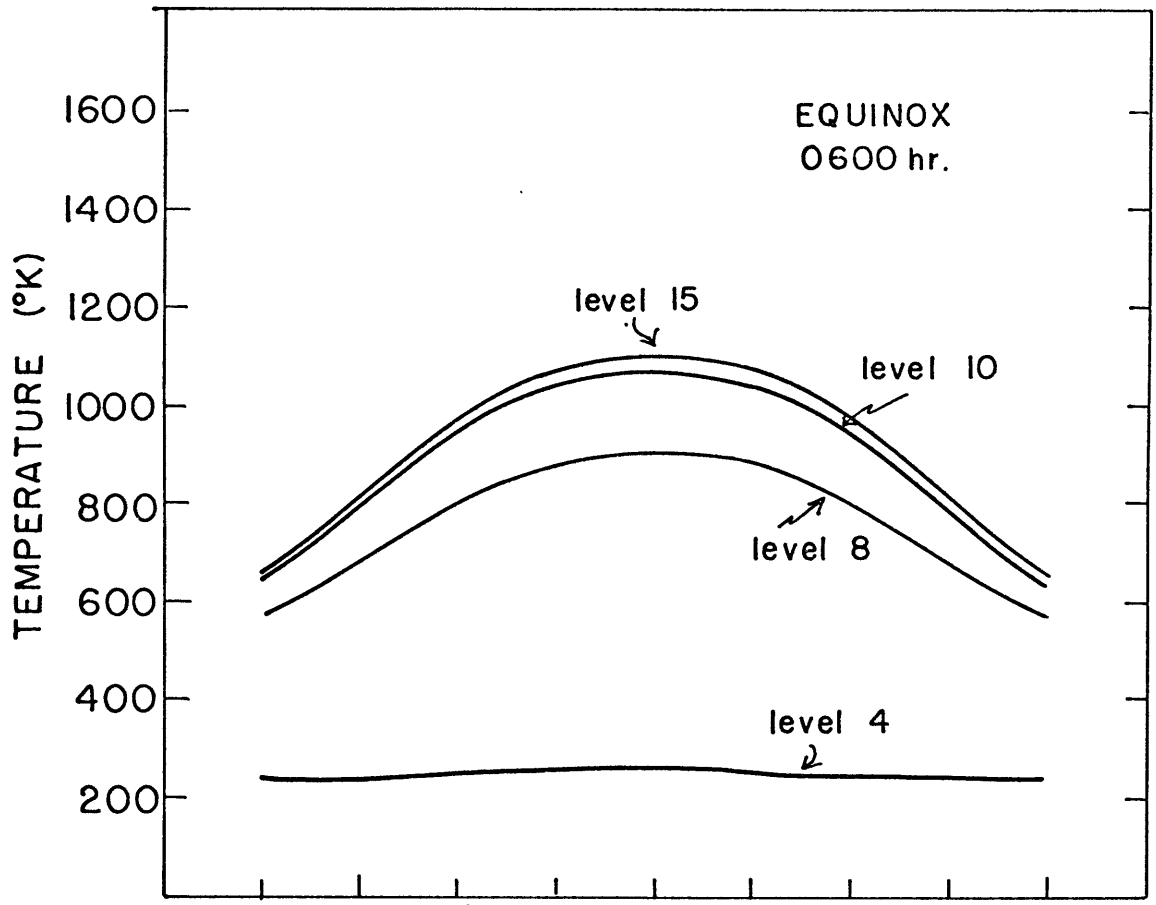
EQUINOX
0600 hr.
level 15
level 10
level 8
level 4
TEMPERATURE (°K)
1600
1400
1200
1000
800
600
400
200

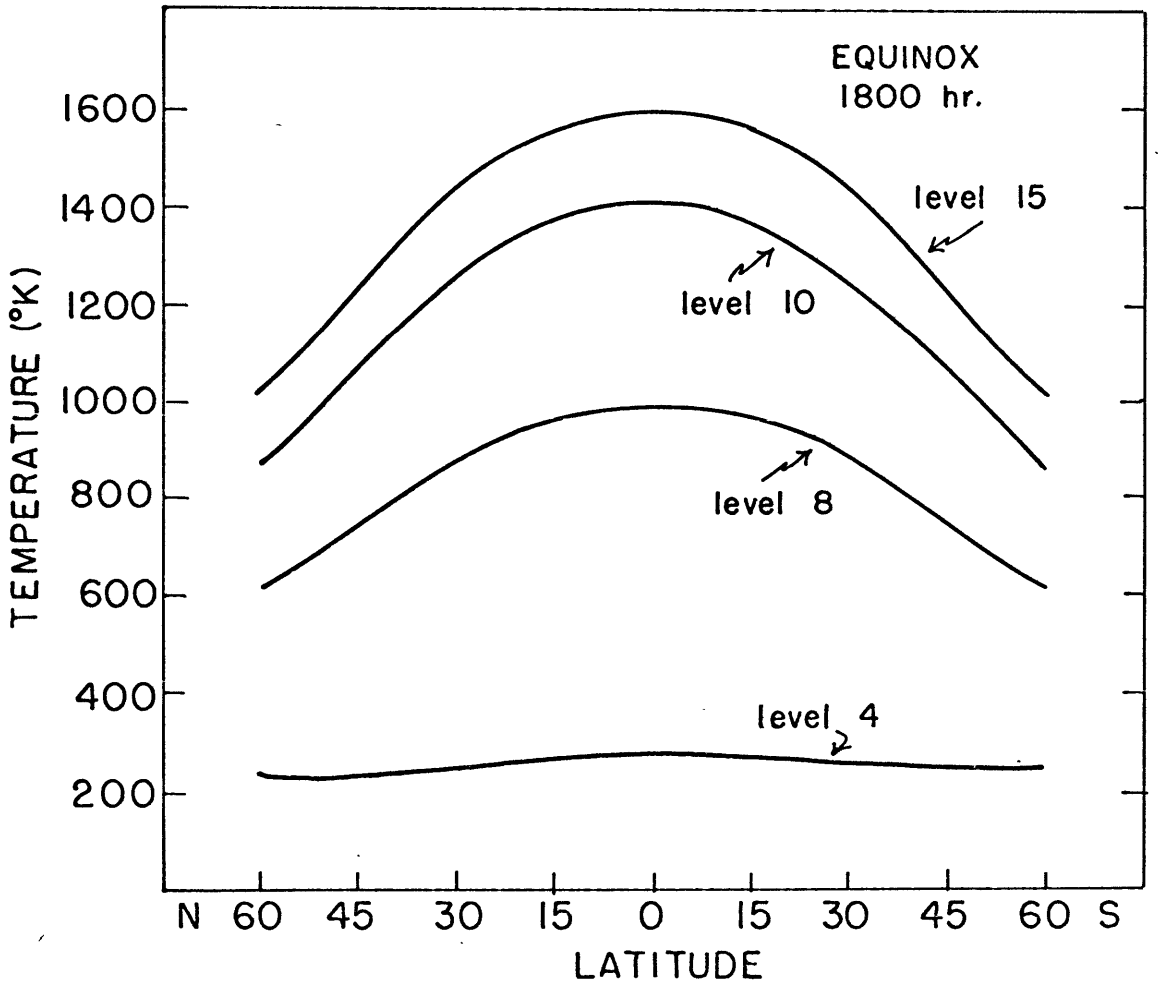
EQUINOX
1800 hr.
level 15
level 10
level 8
level 4
TEMPERATURE (°K)
1600
1400
1200
1000
800
600
400
200
N 60 45 30 15 0 15 30 45 60 S
LATITUDE

Figure 6: Same as Figure 5, but for the June solstice case.

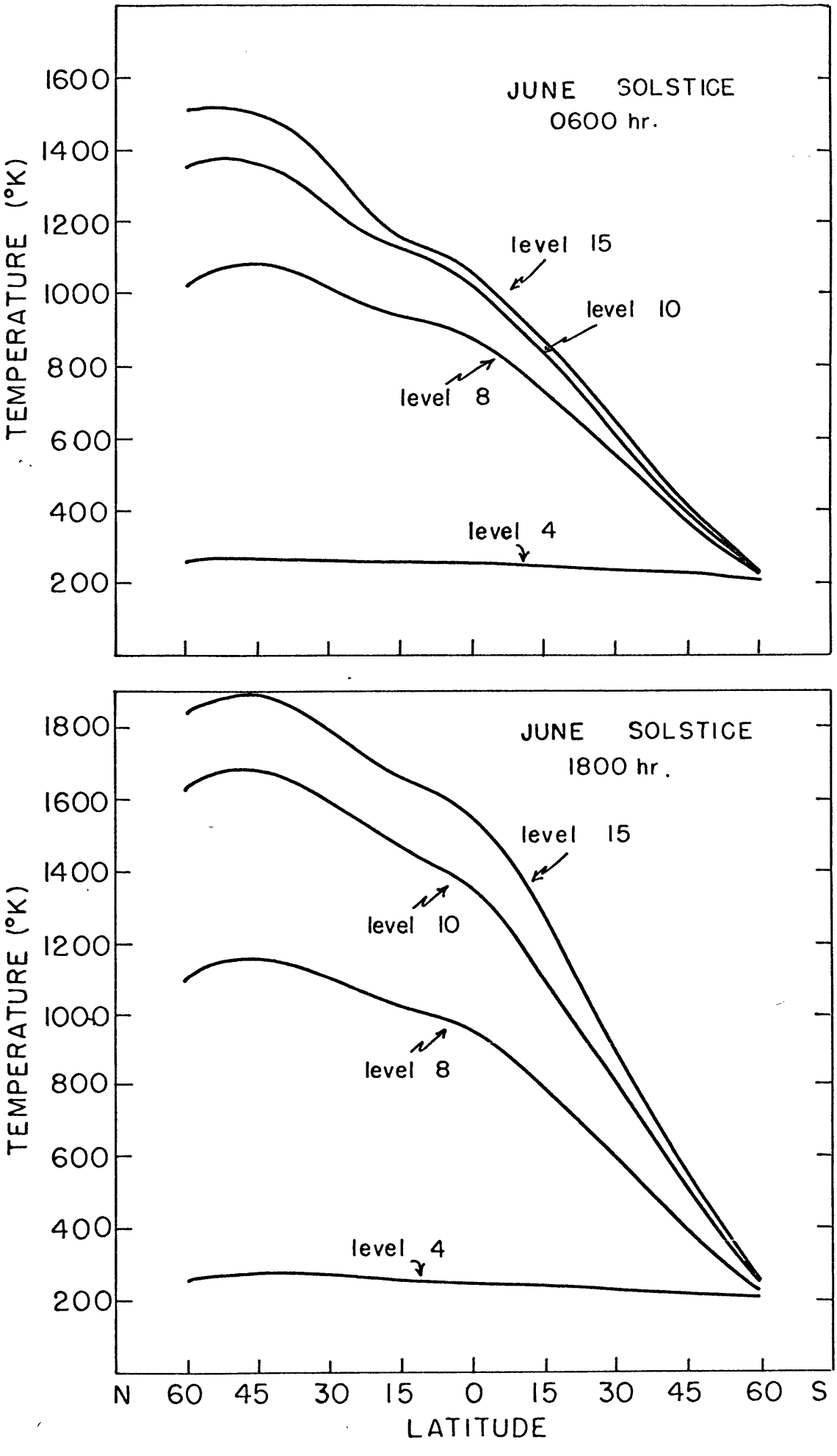
JUNE SOLSTICE
0600 hr.
level 15
level 10
level 8
level 4
TEMPERATURE (°K)
1600
1400
1200
1000
800
600
400
200
JUNE SOLSTICE
1800 hr.
level 15
level 10
level 8
level 4
TEMPERATURE (°K)
1800
1600
1400
1200
1000
800
600
400
200
N 60 45 30 15 0 15 30 45 60 S
LATITUDE

tween the winter and equinox cases are 20°K at the equator and about 410°K at 45° latitude.

Figure 5 shows the temperature distribution with latitude at the equinoxes for 0600 hours and 1800 hours local time. The distribution has been plotted only for model levels 4, 8, 10 and 15. Below level 5 the temperature distribution has very small variation with latitude. Above level 5 the tendency for the latitudinal variability increases with increasing altitude.

The temperature gradient along the meridional circles is negative and its magnitude increases as the latitude increases. This result suggests that the transport of energy across the latitude circles between 0° and 30° latitude is small, but at higher latitudes the meridional transport of energy is increasingly important.

The distribution of temperature with latitude for the same four model levels at the June solstice time is shown in figure 6. In the summer hemisphere temperature increases poleward; the meridional temperature gradient is positive and its magnitude remains almost constant from the equator up to 45° latitude where the gradient changes sign slowly. In the winter hemisphere temperature decreases monotonically from the equator to the pole. The meridional temperature gradient is steeper at solstice than at the equinoxes throughout the winter hemisphere.

The calculated temperatures at high latitudes in the winter hemisphere are much lower than those observed for this region (jacchia, 1965). This result suggests that energy transport toward the winter pole, caused by

Figure 7: Latitudinal cross-section of temperature for local midnight and noon, according to the model calculations.

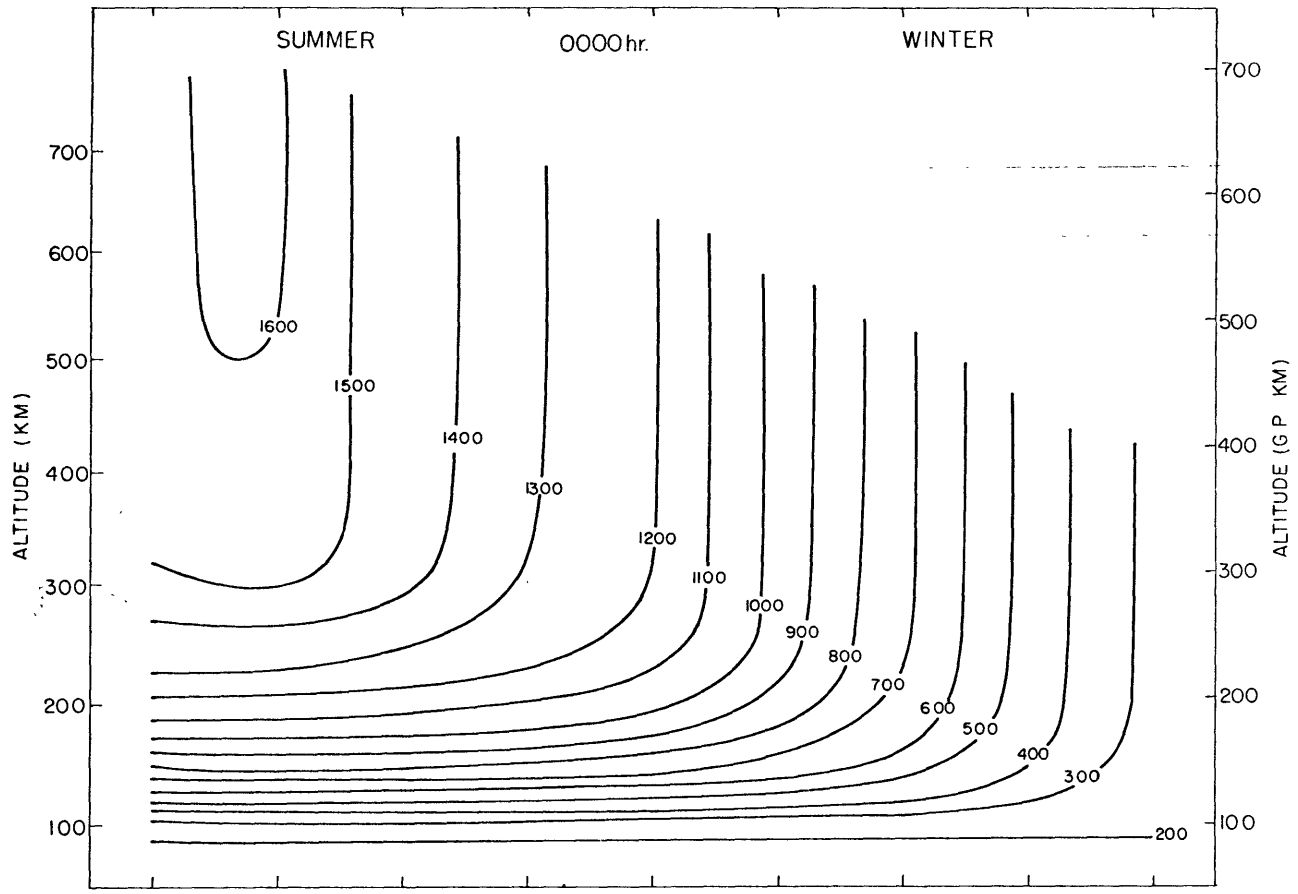
SUMMER
0000hr.
WINTER
ALTITUDE (KM)
ALTITUDE (G P KM)
100
200
300
400
500
600
700
1600
1500
1400
1300
1200
1100
1000
900
800
700
600
500
400
300
200

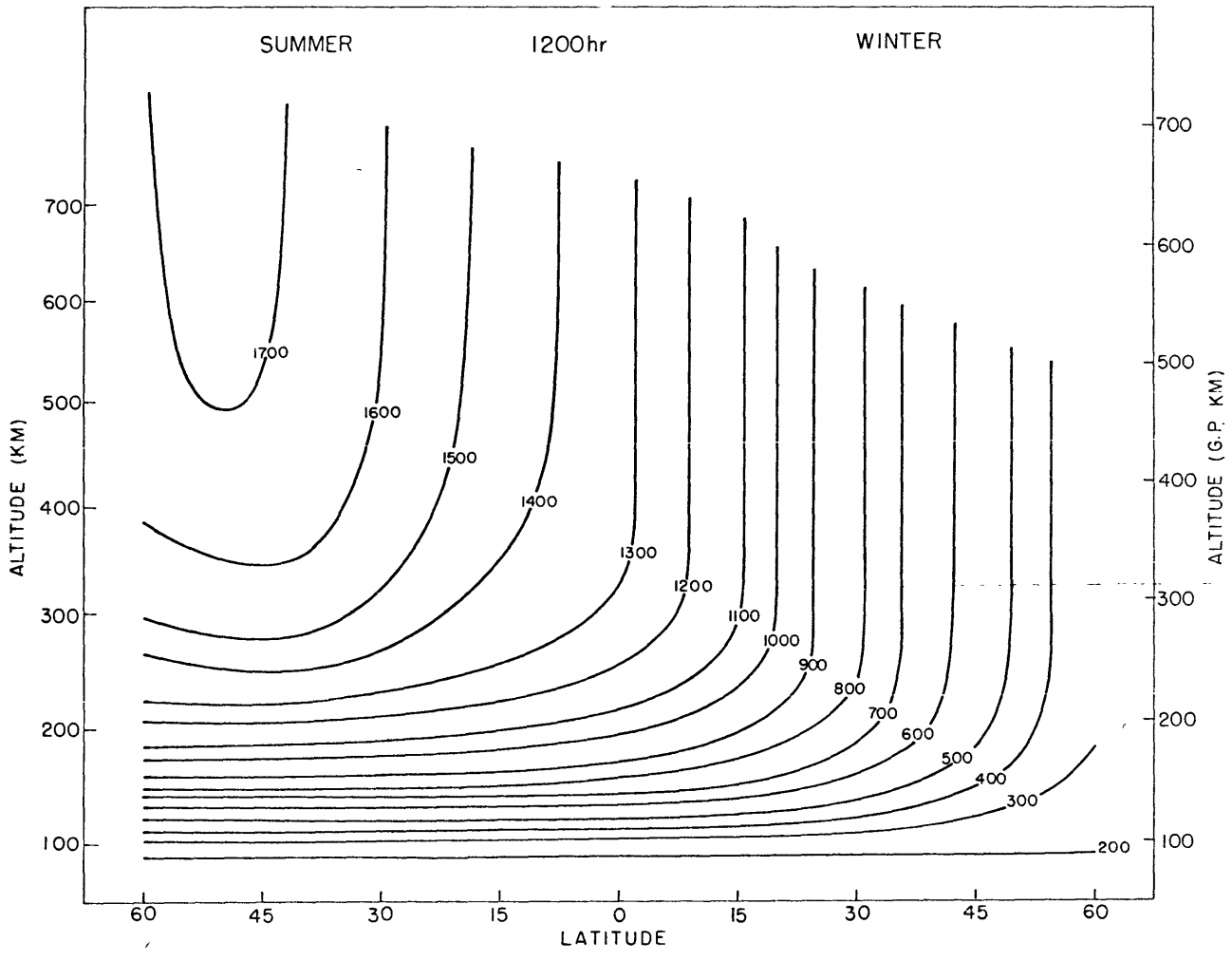
SUMMER
1200hr
WINTER
ALTITUDE (KM)
ALTITUDE (G.P. KM)
100
200
300
400
500
600
700
1700
1600
1500
1400
1300
1200
1100
1000
900
800
700
600
500
400
300
200
60
45
30
15
0
15
30
45
60
LATITUDE

Figure 8: Same as figure 7, but for 0600 and 1800 hours local time.

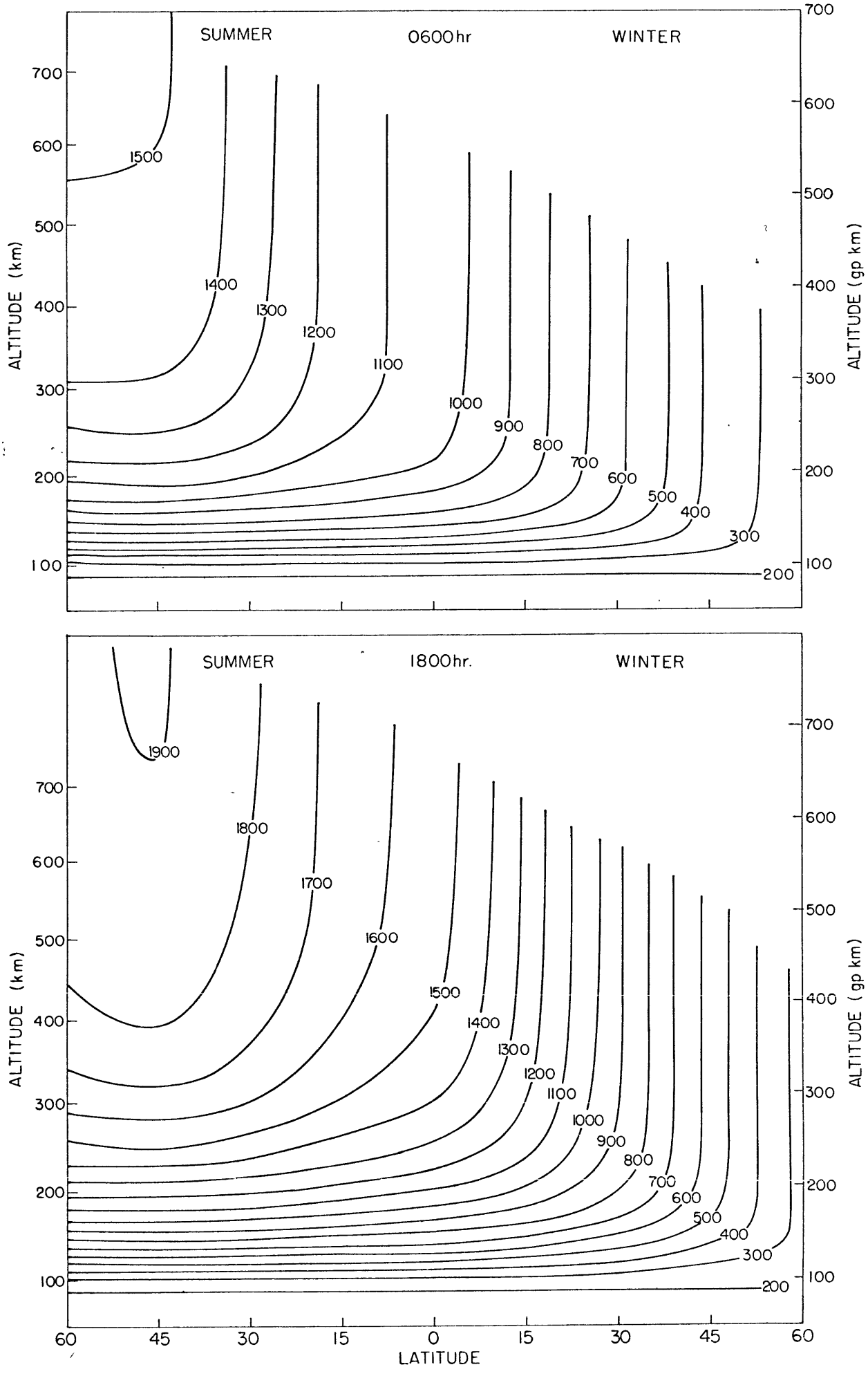
SUMMER
0600hr
WINTER
1500
1400
1300
1200
1100
1000
900
800
700
600
500
400
300
200
ALTITUDE (km)
ALTITUDE (gp km)
100
200
300
400
500
600
700
SUMMER
1800hr.
WINTER
1900
1800
1700
1600
1500
1400
1300
1200
1100
1000
900
800
700
600
500
400
300
200
ALTITUDE (km)
ALTITUDE (gp km)
60
45
30
15
0
15
30
45
60
LATITUDE

horizontal conduction and ~~horizontal~~ and mean meridional, ~~vertical advection~~, is the dominant energy source for the entire region poleward of 45° latitude.

Figures 5 and 6 imply that at equinox the dependence of the temperature distribution on the solar zenith angle is small in low latitudes, but significant at middle and higher latitudes. In the winter the solar zenith angle dependence is reinforced by the effect of shorter days, leading to a very low temperature structure. In the summer the effect of continuous heating of the atmosphere by the sun due to longer days is predominant in low and middle latitudes, but in higher latitudes the effect of large zenith angle reduces the net heating rates. The turning point at 45° latitude during the summer is a consequence of these two effects. Thus in higher latitudes even when the solar heating persists for longer periods the calculated temperatures do not increase poleward of 45° latitude.

A more detailed illustration of the latitude dependence of the calculated model temperatures at the June solstice appears in figures 7 and 8. Figure 7 contains an analysis of the temperature field at local noon and midnight for the entire range of latitude and altitude employed in the study, and figure 8 contains a similar analysis for 0600 and 1800 hours local time.

The calculated temperature profiles at noon and midnight are generally similar. The temperature maximum at approximately 45° latitude in the summer hemisphere is indicated, and the low thermopause heights in the winter hemisphere are also shown.

The temperature profiles for 0600 and 1800 hours, shown in figure

8 differ significantly from one another; the difference between the two profiles is an approximate measure of the amplitude of diurnal temperature variation. This amplitude is approximately 400°K above 300 kilometers everywhere in the summer hemisphere; in the winter hemisphere the amplitude decreases with increasing latitude, reaching approximately 100°K at 45°latitude.

Because molecular heat conductivity is inversely proportional to mass density, the vertical temperature gradient in the model atmosphere (and in the real atmosphere) decreases as altitude increases. The model calculations indicate that the vertical temperature gradient is always negligible between model levels 13 and 15; therefore the horizontal temperature distribution at any of these levels is representative of the temperature distribution above the thermopause in the real atmosphere.

The global temperature distributions calculated for level 15 at equinox and at solstice are shown in figure 9. These model results can be compared to similar data deduced from satellite drag observations by Jacchia (1965). At equinox the calculated temperature distribution is necessarily symmetric around the equator, and the maximum temperature at each latitude occurs about one half hour before sunset. As noted previously by Harris and Priester (1962, 1965), some other energy source or energy transfer process must act to bring the time of maximum temperature back to approximately 1400 hours local time, as indicated by the satellite observations (Jacchia, 1965).

The lower diagram in figure 9 again indicates that the maximum cal-

Figure 9: Horizontal mapping of the temperature field for the highest constant pressure level in the model calculations. Profiles correspond to the equinox and June solstice cases.

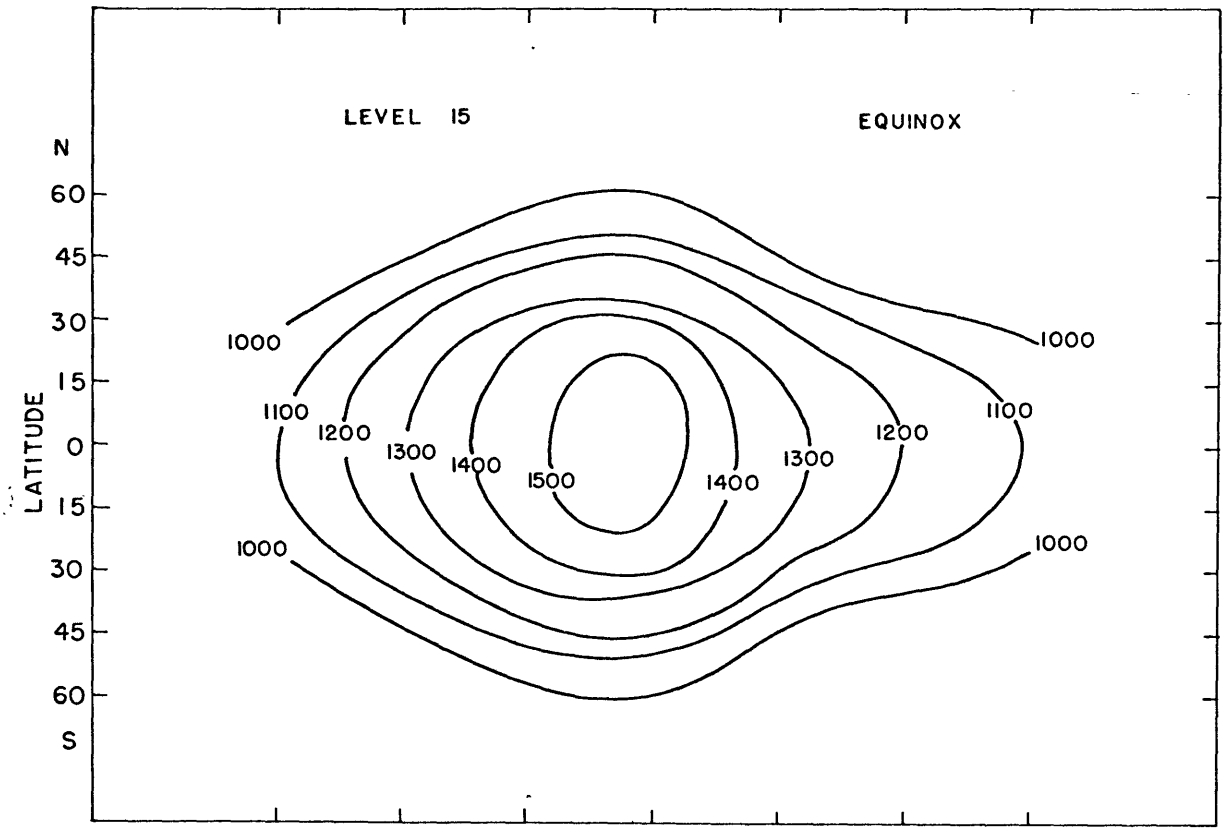
LEVEL 15
EQUINOX
N
60
45
30
15
0
15
30
45
60
S
LATITUDE
1000
1100
1200
1300
1400
1500

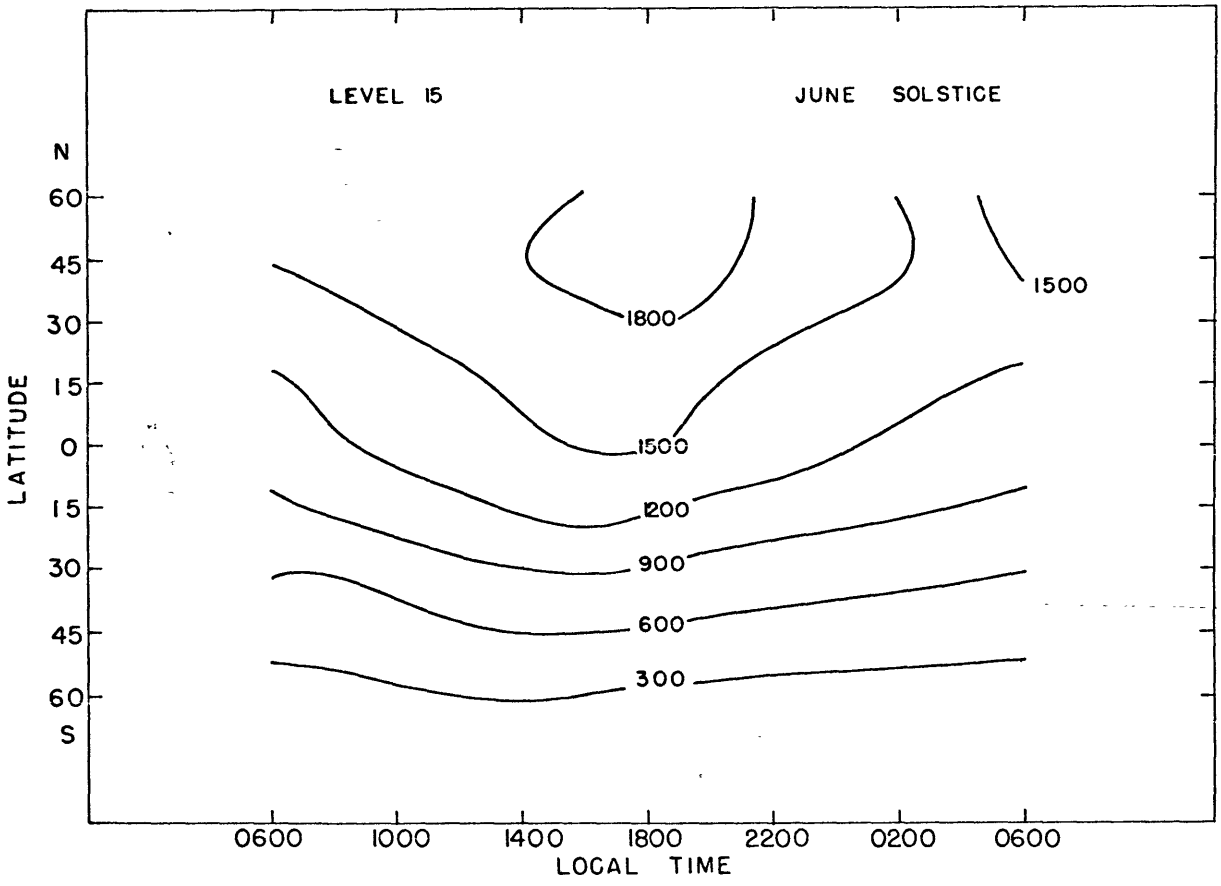
LEVEL 15
JUNE SOLSTICE
N
60
45
30
15
0
15
30
45
60
S
LATITUDE
1800
1500
1200
900
600
300
0600
1000
1400
1800
2200
0200
0600
LOCAL TIME

culated temperature in the summer hemisphere occurs at about 45° latitude, instead of the latitude of the sub-solar point. Recently Jacchia and Slowey (1966) have reported a better fit for the satellite density data when the diurnal bulge, the region of higher temperature, is centered on the equator, rather than at the latitude of the sub-solar point. In the winter hemisphere the daily maximum temperatures occur at successively earlier times as latitude increases; this change follows the change in the local time of sunset.

Jacchia (1965) has also investigated the amplitude of diurnal temperature variability in the region of above the thermopause, and he has found that the ratio of daily maximum to minimum temperature remains very near 1.3 independent of latitude and season. Similar data from the model calculations appear in table 3, which is discussed in section (4.3.1). The calculated ratios are generally larger; the values range from 1.45 to 1.59 at equinox and 1.27 to 1.77 at solstice.

Newell (1966) has suggested that horizontal energy transport due to tidal motions would reduce the range of temperature variability produced by the EUV heating. From scale analysis it would seem that ~~most of the northward heat transport must be due to~~ mean ~~meridional vertical motions~~ rather than tides. The difference between the calculated and observed ratios is a measure of the magnitude of horizontal transport needed to bring the calculated and observed temperature structure into agreement. Where the calculated temperature ratios are significantly larger than 1.3, larger energy

transports are required (e. g., transport from equator-to-pole at equinoxes and south of 30^{o}N latitude at the June solstice). Where the calculated maximum to minimum temperature ratio is about 1.3, little horizontal energy transport is required (e. g., near 45^{o}N latitude at the June solstice). The pressure and mean heights corresponding to the model levels 1 to 15 are presented in table 4. The numbers have been printed in exponential notation; for example E04 following a number indicates that the number should be multiplied by 10^{4}.

4.3.4 Model results of density variation

Most of the properties of the thermospheric structure known up to this date have been inferred from theoretical considerations and direct measurement of density. Determination and further analysis of vertical density profiles and their variations are presently the basic material for the understanding of the physics of the upper atmosphere.

Available information of the atmospheric structure in the region between 80 and 200 km. comes from rocket measurements and for heights greater than 150 km. the observational material consists of densities determined from atmospheric drag on artificial satellites. Thus calculations of density variability from theoretical models are suitable for comparison with observational data. In this section a small sample of computed density variability is presented.

Because of the relationship between density and temperature, all that we have said about the temperature changes also applies to density variations.

Figure 10: Diurnal and seasonal density variability at 15 and 45 deg latitude according to the model calculations.

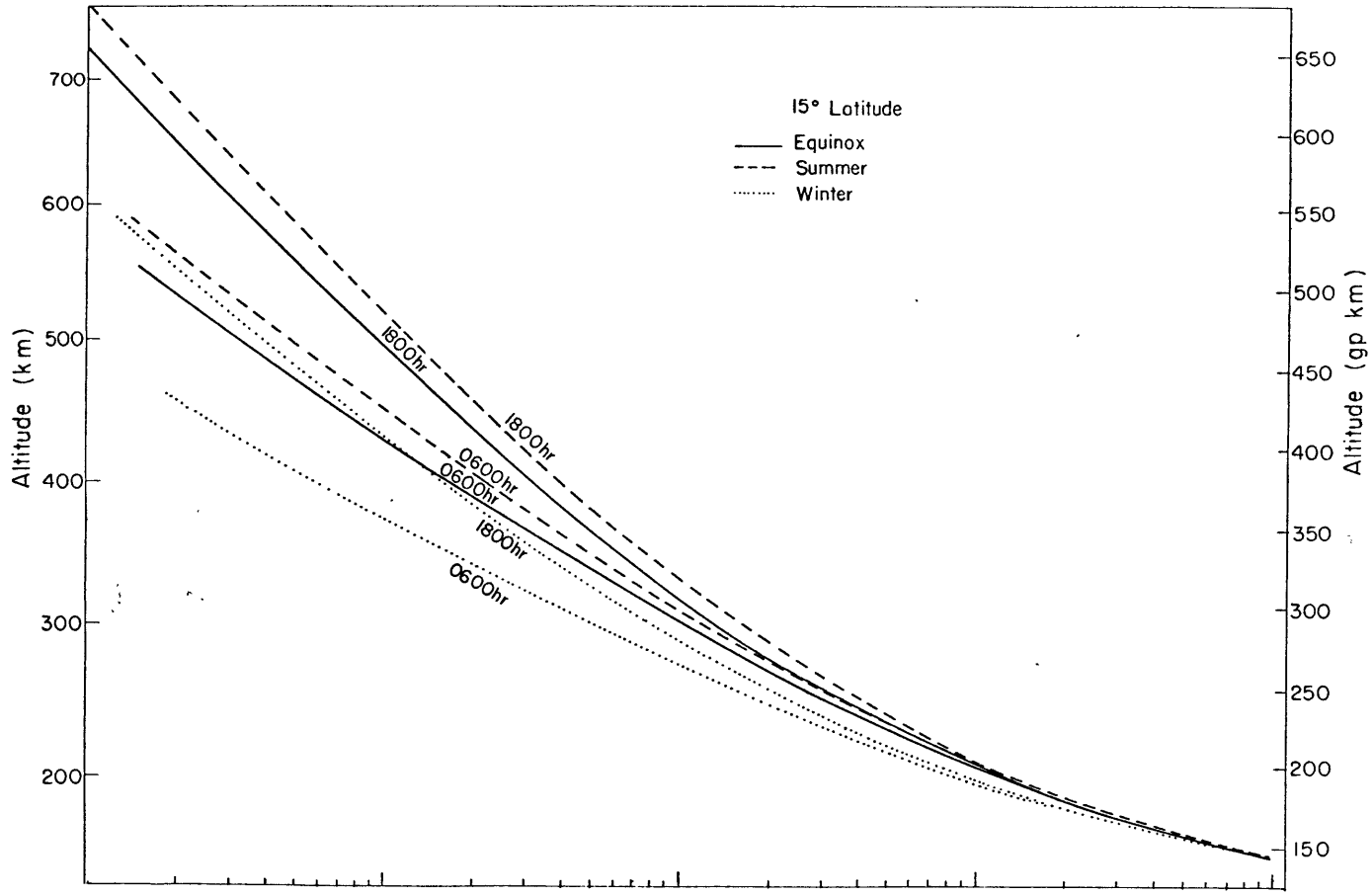
15° Latitude
Equinox
Summer
Winter
1800hr
1800hr
0600hr
0600hr
1800hr
0600hr
Altitude (km)
Altitude (gp km)
700
600
500
400
300
200
650
600
550
500
450
400
350
300
250
200
150

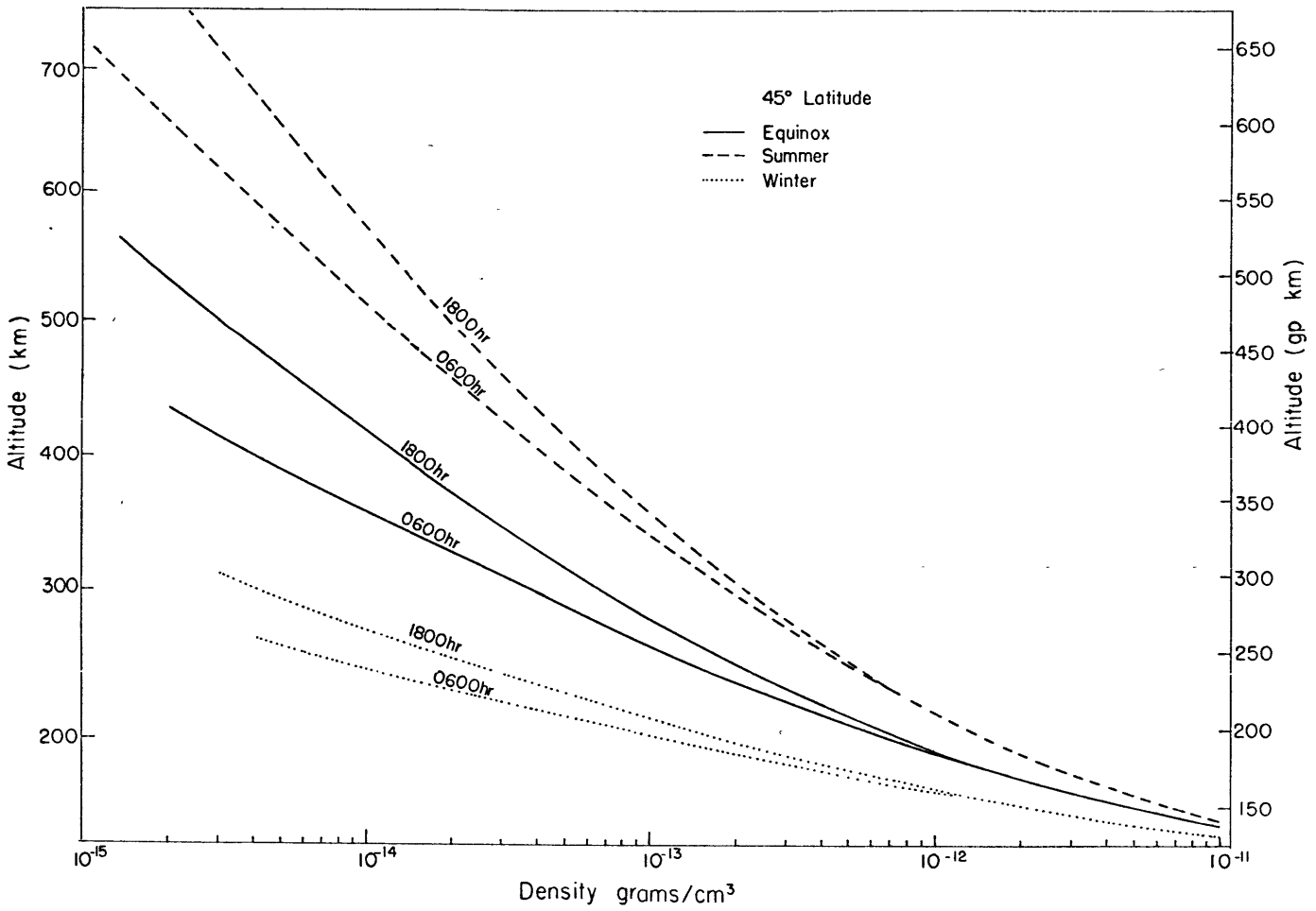
45° Latitude
Equinox
Summer
Winter
1800hr
0600hr
1800hr
0600hr
1800hr
0600hr
Altitude (km)
Altitude (gp km)
700
600
500
400
300
200
650
600
550
500
450
400
350
300
250
200
150
10-15
10-14
10-13
10-12
10-11
Density grams/cm3

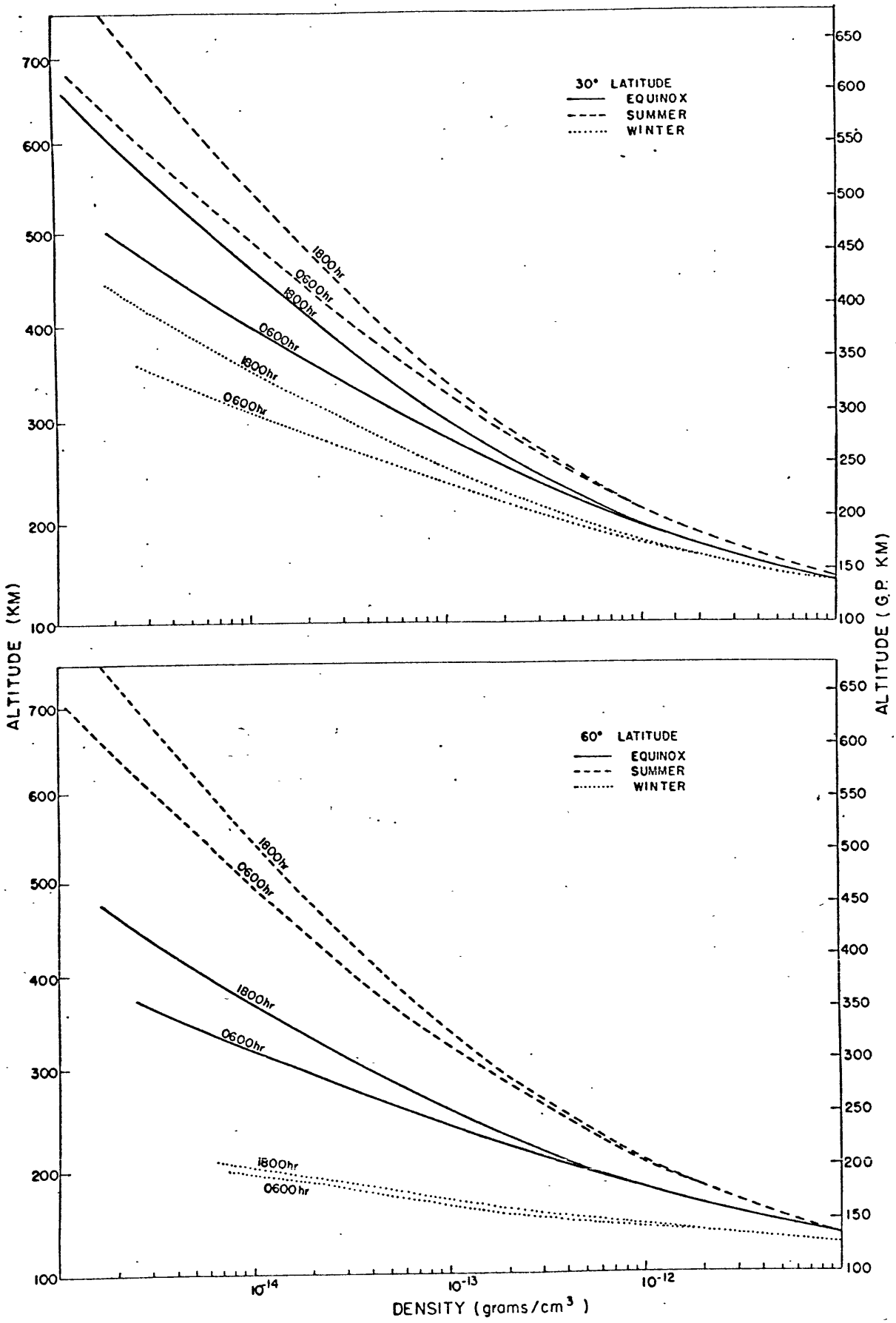

Figure 11: Same as figure 10, but at 30 and 60 deg. latitude.

Figures 10 and 11 illustrate the density variability as a function of altitude calculated by the model for various times of day, seasons and latitudes. Relatively little seasonal variability occurs in the vertical density profiles at 0^{o} and 15^{o} latitude, but seasonal variability becomes important at 30^{o} latitude and at higher latitudes the seasonal variability is much more important than the diurnal variability. Figure 12 is a sample of the meridional density cross section at 1200 hours local time for the equinox and solstice conditions. The meridional density gradient implied by the result shown in figure 12 is significant at all times for latitudes higher than 30^{o} at the equinoxes. At solstice the meridional density gradient is much too large at all times, particularly in the winter hemisphere. If horizontal and vertical motion were allowed in the model calculation, the calculated density profiles would be different, reflecting the effect of horizontal and vertical mass transfer. It is expected, however, that even when motion is included in the model the calculated density profiles would indicate a marked meridional density gradient.

May (1964), after analysing data from the Discoverer series of satellites has reported the existency of a significant latitudinal variation in density. He found that the density at a constant altitude is a function of latitude and is about 30 per cent smaller at the poles than at the equator. More recently Anderson (1966a, 1966b) has shown that this is the case and based on this fact he gives a qualitative explanation for the semi-annual effect appearing in satellite orbital decay data. Furthermore his analyses indicate that the latitudinal density variation is more important in the winter hemisphere.

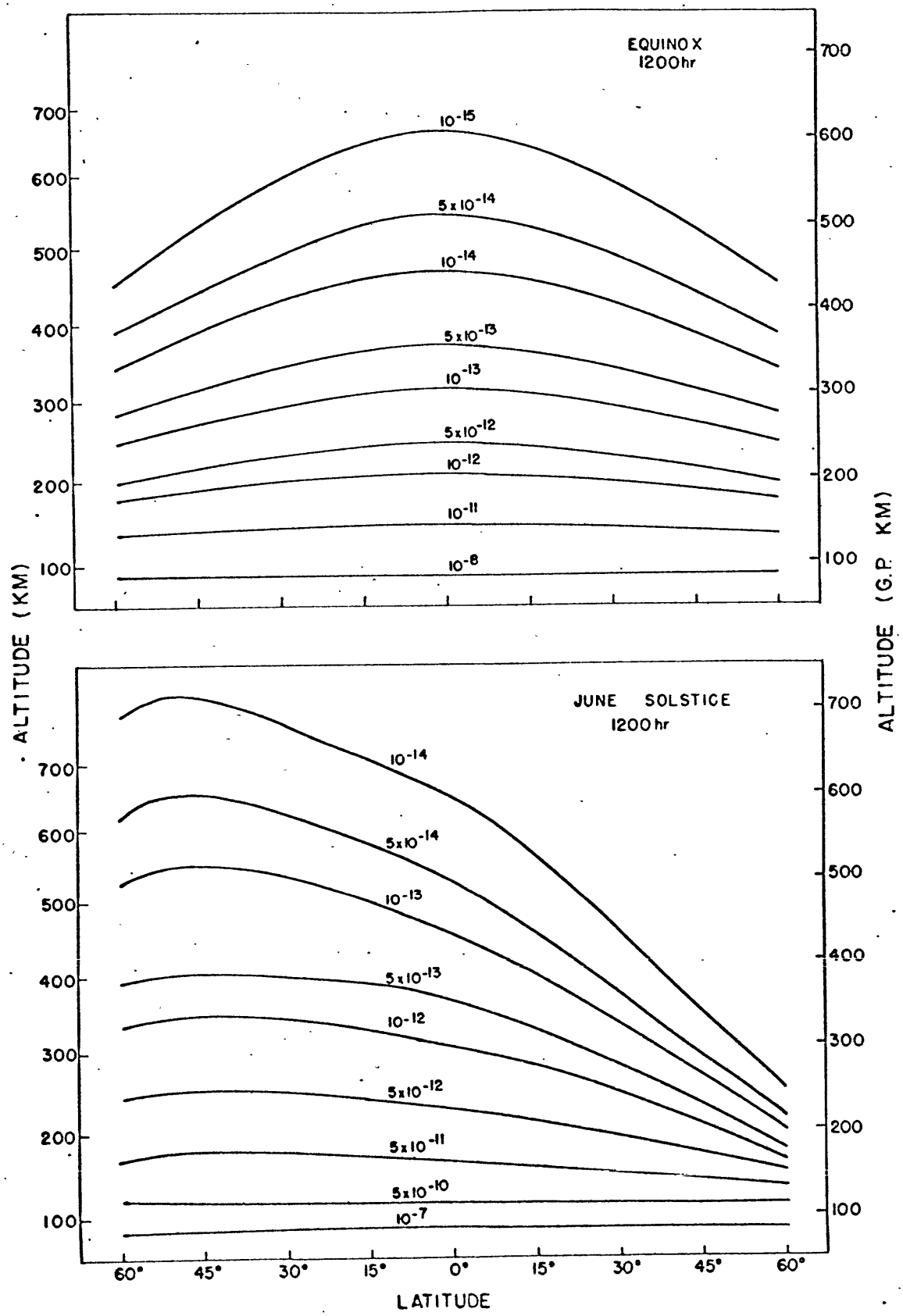

Figure 12: Latitudinal cross-section of density at 1200 hours local time for the equinox and solstice cases according to the model calculations.

5. A TWO DIMENSIONAL NUMERICAL MODEL OF THE DYNAMICS OF THE THERMOSPHERE

5.1 Construction of the Model

The results of the previous sections indicate the desirability of a complete dynamical study of the thermosphere. Large-scale transport processes are important and must be included in the study for a better understanding of the physics of the upper atmosphere. For a full study of the equations of heat energy, momentum and mass there must be an allowance for horizontal variability in the model. When the sources of energy, momentum and mass are specified or calculated, a complete investigation of the dynamics and general circulation of the thermosphere can be carried out. When the mean state and the short and long time variation of the temperature and wind fields are known, the following topics may be considered in detail:

a) The role of vertical transport of energy and angular momentum in the thermosphere.

b) Meridional transport of energy, angular momentum and mass in the thermosphere.

c) The generation and conversion of zonal and eddy kinetic and potential energy in the thermosphere.

d) Large scale eddy processes in the thermosphere.

e) The effect of the wind system on the ionized component of the upper atmosphere.

The main purpose of this chapter is to investigate the role of the vertical and horizontal motion in determining the structure of the thermosphere and its variation, and specifically to investigate whether the inclusion in the model of the subsidence of heat and vertical advection of heat can bring into agreement the calculated and observed amplitude and phase of the diurnal temperature and density variation.

To carry out this task we shall simplify the dynamical equation derived in chapter 2 and solve by numerical techniques. It is hoped that the highly simplified model will provide the basis for a more complete study of the general features of the thermospheric dynamics.

5.1.1 Simplification of the dynamical equations.

The method used in this section for the simplification of the hydrodynamic and thermodynamic equations consists of omitting certain terms which are of secondary importance according to some criteria, or terms whose omission will facilitate at first mathematical or numerical calculation. In doing so we may expect to gain some insight concerning the relative importance of the terms retained and omitted.

The criterion for determining the order of magnitude of each term in the equation is the scale analysis developed in chapter 2. By neglecting certain terms we may decouple various physical processes while retaining the desired phenomenological features.

Dependent variables are expanded in a series of orthogonal functions. A suitable set for such a spectral expansion is a Fourier Series. The set

of coefficients of these eigenfunctions becomes the new dependent variable. This set is capable of representing the features of principal interest.

The simplified two dimensional model, which is an extension of the model described in section (4. 2), is obtained with the following initial assumptions: 1) only a latitudinal plane is considered, with $v = 0$ and $\frac{\partial}{\partial y} = 0$; and 2) any interaction between the ionized and neutral constituents in the thermosphere is neglected, which amounts to the omission of the ion drag term in the horizontal momentum equation. Under these conditions the governing equations (2. 50)-(2. 53) in (x, Z, t) coordinates reduce to (in dimensional units)

(5. 1) $$\frac{\partial u}{\partial t} - \frac{1}{\rho H}\frac{\partial}{\partial Z}\left(\frac{\mu}{H}\frac{\partial u}{\partial Z}\right) = -g\frac{\partial h}{\partial x}$$

(5. 2) $$\frac{\partial u}{\partial x} + \frac{\partial \dot{Z}}{\partial Z} - \dot{Z} = 0$$

(5. 3) $$c_p\frac{\partial T}{\partial t} + \underline{c_p u\frac{\partial T}{\partial x}} + \dot{Z}S - \frac{1}{\rho H}\frac{\partial}{\partial Z}\left(\frac{K}{H}\frac{\partial T}{\partial Z}\right) = Q$$

where $$S = c_p\left(\frac{R^*}{M}\frac{T}{c_p} + \frac{\partial T}{\partial Z}\right) \; ; \; Q = \dot{q}_{SR} + \dot{q}_{IR}$$

According to our scale analysis the term underlined is approximately an order of magnitude less than the rest of the terms in equation (5. 3). However, it will be included in the system to investigate to what extent its effect may have on the amplitude and phase of the diurnal temperature and density variation. Calculations have been carried out with and without this term, and these will be discussed below.

5.1.2 Equations in the domain of wave number

We next express each of the dependent variables in the latitudinal plane with horizontal scale L in terms of a Fourier expansion of the general form

$$\psi(x,Z,t) = \frac{b_0}{2} + \sum_{n=1}^{\infty} \left[a_n(Z,t) \sin n\lambda x + b_n(Z,t) \cos n\lambda x \right] \tag{5.4}$$

where a_n and b_n are the Fourier coefficients, dependent upon Z and t and $\lambda = 2\pi/L$. For a boundary condition ψ is taken to be periodic with wave length L in x.

With the use of the relations presented in appendix A, we may now transform the governing equations (5.1)-(5.3) from the space domain to the domain of wave number.

The final step in the simplification process is the truncation of the spectral expansion (5.4) such that only a finite number of coefficients a_n and b_n will be retained..

The selection of the truncated set is closely related to the physical process we want to investigate. If only low wavenumber terms are retained only large-scale features will be retained in the model.

Our main interest is the observed diurnal variation of the thermosphere, which may be considered to be a planetary scale disturbance. Therefore, we shall restrict ourselves to keeping in the system only the mean zonal component and the lowest wave number disturbance.

The simple dynamical system is therefore formed by retaining only those three terms for which n assumes the value of 0 and 1. The depen-

dent variable ψ in (5.4) then takes the simple form

(5.5) $$\psi(x,Z,t) = \psi_0(Z,t) + \psi_s(Z,t)\sin\lambda x + \psi_c(Z,t)\cos\lambda x$$

where

$$\psi_0 = b_0/2$$
$$\psi_s = a,$$
$$\psi_c = b,$$

The first term in R. H. S. of (5.5) represents the mean zonal component, the remaining terms represent disturbances superposed on the zonal component and together they depict a disturbance of a single wave number.

The basic equations obtained by substitution of (5.5) directly into (5.1)-(5.3) are presented in appendix B. Here we display only the relevant equation for the equation of heat energy,

(5.6) $$c_p\frac{\partial T_0}{\partial t} = \frac{K_0}{\rho_0 H_0^2}\frac{\partial^2 T_0}{\partial Z^2} + \frac{1}{\rho_0 H_0}\frac{\partial T_0}{\partial Z}\frac{\partial}{\partial Z}\left(\frac{K_0}{H_0}\right)$$
$$+\underline{\tfrac{1}{2}\lambda c_p u_s T_c - \tfrac{1}{2}\lambda c_p u_c T_s}$$
$$-\tfrac{1}{2}c_p\dot{Z}_s\frac{\partial T_s}{\partial Z} - \tfrac{1}{2}c_p\dot{Z}_c\frac{\partial T_c}{\partial Z}$$
$$-\tfrac{1}{2}\frac{R^*}{M}\dot{Z}_s T_s - \tfrac{1}{2}\frac{R^*}{M}\dot{Z}_c T_c + Q_0$$

(5.7) $$c_p\frac{\partial T_s}{\partial t} = \frac{K_0}{\rho_0 H_0^2}\frac{\partial^2 T_s}{\partial Z^2} + \frac{1}{\rho_0 H_0}\frac{\partial T_s}{\partial Z}\frac{\partial}{\partial Z}\left(\frac{K_0}{H_0}\right)$$
$$+\underline{\lambda c_p u_0 T_c} - c_p\dot{Z}_s\frac{\partial T_0}{\partial Z} - \frac{R^*}{M}Z_s T_0 + Q_s$$

(5.8) $$c_p\frac{\partial T_c}{\partial t} = \frac{K_0}{\rho_0 H_0}\frac{\partial^2 T_c}{\partial Z^2} + \frac{1}{\rho_0 H_0}\frac{\partial T_c}{\partial Z}\frac{\partial}{\partial Z}\left(\frac{K_0}{H_0}\right)$$
$$-\underline{\lambda c_p U_0 T_s} - c_p\dot{Z}_c\frac{\partial T_0}{\partial Z} - \frac{R^*}{M}\dot{Z}_c T_0 + Q_c$$

5.1.3 Method of numerical solution

Equations (5.6)-(5.8) together with equations (B.4)-(B.6) are a set of nonlinear differential equations and must be converted into a set of algebraic equations by replacing vertical and time derivatives by finite differences. To avoid the problem of computational instability that may arise, an implicit scheme for the finite difference approximations has been adopted (Crank and Nicholson, 1947).

Let us define the symbol $\psi^i_{n,m}$ $(i = 0, s, c)$ to indicate the value of ψ^i at level n and time step m. The time derivatives are evaluated as simple forward differences in time

$$\left(\frac{\partial \psi^i}{\partial t}\right)_{n,m} = \frac{\psi^i_{n,m+1} - \psi^i_{n,m}}{\Delta t} \tag{5.9}$$

where Δt is a measure of the time step and the superscript denotes the i^{th} component in (5.5) (i.e. $\psi^s = \psi_s$). The vertical differencing has a spacing of $\Delta Z = 1/2$ for the second derivative and $\Delta Z = 1$ for the first derivatives. Thus

$$\left(\frac{\partial \psi^i}{\partial Z}\right)_{n,m} = \frac{1}{2}\left[\left(\frac{\psi^i_{n+1,m} - \psi^i_{n-1,m}}{2}\right) + \left(\frac{\psi^i_{n+1,m+1} - \psi^i_{n-1,m+1}}{2}\right)\right] \tag{5.10}$$

$$\left(\frac{\partial^2 \psi^i}{\partial Z^2}\right)_{n,m} = \frac{1}{2}\left[\left(\psi^i_{n+1,m} - 2\psi^i_{n,m} + \psi^i_{n-1,m}\right) + \left(\psi^i_{n+1,m+1} - 2\psi^i_{n,m+1} + \psi^i_{n-1,m+1}\right)\right] \tag{5.11}$$

In order to evaluate the vertical derivatives at the top and bottom of the model, boundary conditions must be specified at the boundary surfaces. The boundary conditions should be prescribed in accordance with section 2.3. The homogeneous boundary conditions applied as $Z \to 0$ and $Z \to \infty$, are

$$(5.12)\qquad \lim_{z\to 0}\ \frac{\partial \psi}{\partial z} = 0\ , \qquad \psi = T,\ u$$

$$\lim_{z\to \infty}\ \frac{\partial \psi}{\partial z} = 0\ , \qquad \psi = T,\ u$$

which implies the fact of no flux of heat and momentum through the boundaries, and

$$(5.13)\qquad \lim_{z\to \infty}\ \rho\,\psi = 0\ , \qquad \psi = \dot{z}$$

which implies the fact of no flux of mass at infinity. Since the finite difference approximations can not be carried out to infinity, the above boundary conditions have been applied at level zero and level 16 of the model calculation. Similar boundary conditions have been also applied for $\psi = \rho,\ H,\ K$ and μ in the finite difference scheme. These boundary conditions are weak, especially the lower boundary condition, however, we shall assume it to be sufficient for the present investigation. A more detailed specification of the boundary conditions must follow this study.

The zonal component of the horizontal momentum equation is evaluated at level n and time step m from (B. 5) for i = S

$$(5.14)\qquad \left(\frac{\partial u^S}{\partial t}\right)_{n,m} = \frac{\mu^\circ_{n,m}}{\rho^\circ_{n,m}(H^\circ)^2_{n,m}}\left(\frac{\partial^2 u^S}{\partial Z^2}\right)_{n,m} + \frac{1}{\rho^\circ_{n,m}H^\circ_{n,m}}\left(\frac{\partial u^S}{\partial Z}\right)_{n,m}\left[\frac{\partial(\mu^\circ/H^\circ)}{\partial Z}\right]_{n,m} + \rho\,\lambda\, h^c_{n,m}$$

with similar expressions for i = 0 and C .

The heat equation is evaluated at level n and time step m from (5. 7) for i = S

$$(5.15)\qquad (C_p)_n\left(\frac{\partial T^S}{\partial t}\right)_{n,m} = \frac{K^\circ_{n,m}}{\rho^\circ_{n,m}(H^\circ)^2_{n,m}}\left(\frac{\partial^2 T^S}{\partial Z^2}\right)_{n,m} + \frac{1}{\rho^\circ_{n,m}H^\circ_{n,m}}\left(\frac{\partial T^S}{\partial Z}\right)_{n,m}\left[\frac{\partial(K^\circ/H^\circ)}{\partial Z}\right]_{n,m} +$$

$$+\lambda (c_p)_n u^{\circ}_{n,m} T^{c}_{n,m} - (c_p)_n \dot{z}^{s}_{n,m} \left(\frac{\partial T^{\circ}}{\partial z}\right)_{n,m} - \frac{R^*}{M} \dot{z}^{s}_{n,m} T^{\circ}_{n,m} + \varphi^{s}_{n,m}$$

with similar expressions for i = 0 and c .

Through mathematical manipulations, each equation (i.e. eq. (5.14) and the corresponding for i = 0 and c) is transformed to a system of simultaneous equations which must be solved for $u^{i}_{n,m+1}$. The system of equations may be written as the matrix equation

(5.16) $$A_{jk}(UN^{i})_{k} = B_{j} \quad , \quad \begin{cases} 1 \le j \le 15 \\ 1 \le k \le 15 \end{cases}$$

where the dummy subscripts j and k both refer to level number, and $(UN^{i})_{k} = u^{i}_{n,m+1}$, $(UI^{i})_{k} = u^{i}_{n,m}$. All quantities except the new zonal wind $(UN^{i})_{k}$ are evaluated at the initial time m. $(UN^{i})_{k}$ is obtained from

(5.17) $$(UN^{i})_{k} = A^{-1}_{jk} B_{j}$$

the elements of A_{jk} are zero except those along the main diagonal and the two adjoining inferior diagonals:

(5.18) $$A_{j,j+1} = \frac{\Delta t}{2\rho^{\circ}_{j} H^{\circ}_{j}} \left[\frac{u^{\circ}_{j}}{H^{\circ}_{j}} + \frac{1}{4}\left(\frac{u^{\circ}_{j+1}}{H^{\circ}_{j+1}} - \frac{u^{\circ}_{j-1}}{H^{\circ}_{j-1}} \right) \right]$$

$$A_{j,j} = -1.0 - \frac{\Delta t}{\rho^{\circ}_{j} (H^{\circ})^{2}_{j}} u^{\circ}_{j}$$

(5.19) $$A_{j,j-1} = \frac{\Delta t}{2\rho^{\circ}_{j} H^{\circ}_{j}} \left[\frac{u^{\circ}_{j}}{H^{\circ}_{j}} + \frac{1}{4}\left(\frac{u^{\circ}_{j+1}}{H^{\circ}_{j+1}} - \frac{u^{\circ}_{j-1}}{H^{\circ}_{j-1}} \right) \right]$$

The element of B_j are:

(5.20) $$B_{j} = -(UI)^{i}_{j} - \frac{\Delta t}{2\rho^{\circ}_{j} H^{\circ}_{j}} \left[\frac{u^{\circ}_{j}}{H_{j}} \left((UI^{i})_{j+1} - 2(UI^{i})_{j} + (UI^{i})_{j+1} \right) + \frac{1}{4}\left(\frac{u^{\circ}_{j+1}}{H^{\circ}_{j+1}} - \frac{u^{\circ}_{j-1}}{H^{\circ}_{j-1}} \right)\left((UI^{i})_{j+1} - (UI^{i})_{j-1} \right) \right] - \Delta t (\rho \lambda \tilde{h}_{j})$$

where

(5.21) $$\tilde{h} = \begin{cases} 0 & i = o \\ h^c & i = s \\ h^s & i = c \end{cases}$$

The system of simultaneous equations for the temperature T are obtained following the same procedure as described above for u^i, however, here T^o, T^s, and T^c are coupled in the system of equations and therefore they must be solved simultaneously. With the following notation: $(TN^o)_K = (TN)_K$ for $1 \le K \le 15$; $(TN^s)_K = (TN)_K$ for $16 \le K \le 30$ and $(TN^c)_K = (TN)_K$ for $31 \le K \le 45$, the system of equations may be written in matrix form,

(5.22) $$A_{JK}\,(TN)_K = B_j \quad , \quad \begin{cases} 1 \le j \le 45 \\ 1 \le K \le 45 \end{cases}$$

The matrix A_{jK} may be written as

(5.23) $$A_{jK} = \left[\begin{array}{c|c|c} a^o_{JK} & b_{JK} & c_{JK} \\ \hline d_{JK} & a^s_{JK} & 0 \\ \hline e_{JK} & 0 & a^c_{JK} \end{array}\right]$$

where a^o_{JK}, a^s_{JK} and a^c_{JK} have the same general form, except for the superscript in the variables. The elements of a^o_{JK}, for example, are zero except those along the main diagonal and the two adjoining inferior diagonals:

(5.24) $$a_{j,j+1} = \frac{\Delta t}{2\rho^o_j (C_p)_j H^o_j}\left[\frac{K^o_j}{H^o_j} + \frac{1}{4}\left(\frac{K^o_{j+1}}{H^o_{j+1}} - \frac{K^o_{j-1}}{H^o_{j-1}}\right)\right]$$

(5.25) $$a_{j,j} = -1.0 - \frac{\Delta t\, K^o_j}{\rho^o_j (C_p)_j (H^o)^2_j}$$

(5.26) $$a_{j,j-1} = \frac{\Delta t}{2\rho_j^\circ (c_p)_j H_j^\circ}\left[\frac{K_j^\circ}{H_j^\circ} - \frac{1}{4}\left(\frac{K_{j+1}^\circ}{H_{j+1}^\circ} - \frac{K_{j-1}^\circ}{H_{j-1}^\circ}\right)\right]$$

The elements of b_{jK}, c_{jK}, d_{jK} and e_{jK} are zero except those along the adjoining inferior diagonals:

(5.27) $$b_{j,j+1} = -\frac{1}{8}(\Delta t)\,\dot{Z}_j^s$$

(5.28) $$b_{j,j-1} = \frac{1}{8}(\Delta t)\,\dot{Z}_j^s$$

(5.29) $$c_{j,j+1} = -\frac{1}{8}(\Delta t)\,\dot{Z}_j^c$$

(5.30) $$c_{j,j-1} = \frac{1}{8}(\Delta t)\,\dot{Z}_j^c$$

(5.31) $$d_{j,j+1} = -\frac{1}{4}(\Delta t)\,\dot{Z}_j^s$$

(5.32) $$d_{j,j-1} = \frac{1}{4}(\Delta t)\,\dot{Z}_j^s$$

(5.33) $$e_{j,j+1} = -\frac{1}{4}(\Delta t)\,\dot{Z}_j^c$$

(5.34) $$e_{j,j-1} = \frac{1}{4}(\Delta t)\,\dot{Z}_j^c$$

The elements of B_j are:

(5.35) $$B_j = B_j^\circ - \frac{\Delta t}{2}\left\{\lambda\, u_j^s\, TI_j^c - \lambda\, u_j^c\, TI_j^s - \frac{1}{4}\dot{Z}_j^s\left(TI_{j+1}^s - TI_{j-1}^s\right) - \frac{1}{4}\dot{Z}_j^c\left(TI_{j+1}^c - TI_{j-1}^c\right) - \frac{R^*}{M_j(c_p)_j}\dot{Z}_j^s TI_j^s - \frac{R^*}{M_j(c_p)_j}\dot{Z}_j^c TI_j^c + \frac{2}{(c_p)_j}\left(\dot{q}_{sR}^\circ - \dot{q}_{IR}^\circ\right)_j\right\}; \quad \text{for } 1 \le j \le 15$$

(5.36) $$B_j = B_j^s + \frac{\Delta t}{2}\left\{\dot{Z}_j^s\left(\frac{TI_{j+1}^\circ - TI_{j-1}^\circ}{2}\right) + \frac{2R^*}{(c_p)_j M_j}\dot{Z}_j^s TI_j^\circ - 2\lambda\, u_j^\circ\, TI_j^c - \frac{2}{(c_p)_j}\left(\dot{q}_{sR}^s - \dot{q}_{IR}^s\right)_j\right\}; \quad \text{for } 16 \le j \le 30$$

$$(5.37)\quad B_j = B_j^c + \frac{\Delta t}{2}\left\{ \dot{Z}_j^c \left(\frac{TI_{j+1}^o - TI_{j-1}^o}{2} \right) + \frac{2R}{(c_p)_j M_j} \dot{Z}_j^c TI_j^o + 2\lambda u_j^o TI_j^s - \frac{2}{(c_p)} \left(\dot{q}_{SR} - \dot{q}_{IR} \right) \right\}, \quad \text{for } 31 \le j \le 45$$

where

$$(5.38)\quad B_j^i = -TI_j^i - \frac{1}{2} \frac{\Delta t}{(c_p)_j \rho_j^o H_j^o} \left\{ \frac{K_j^o}{H_j^o} \left[TI_{j+1}^i - 2TI_j^i + TI_{j-1}^i \right] + \frac{1}{2} \left(\frac{K_{j+1}^o}{H_{j+1}^o} - \frac{K_{j-1}^o}{H_{j-1}^o} \right) \left[\frac{TI_{j+1}^i - TI_{j-1}^i}{2} \right] \right\}$$

Now the temperature at the new time is obtained from

$$(5.39)\quad \left(TN \right)_K = A_{JK}^{-1} B_j$$

Two assumptions that simplify the computational scheme have been used: 1) the quantities μ/H and K/H change slowly in time and hence the vertical derivative can be evaluated at the initial time only; and 2) μ/H and K/H depend on T^o only and consequently K^i/H^i, for example, can be replaced by K^o/H^o.

Given an initial condition for T^i and U^i, all quantities in the model are evaluated at level n and time m using equations (2.8) and (5.5). The zonal wind at time step m + 1 is calculated next. The vertical motion is obtained from the continuity equation and the temperature at the new time is calculated if the heating and cooling rates are known. The same procedure is then repeated over again.

5.1.4 Solar heating and radiational cooling rates

The heating and cooling rates are specified in the model calculation. These are obtained from a detailed study of the energy sources in the thermosphere carried out by Mahoney (1966). The one dimensional model re-

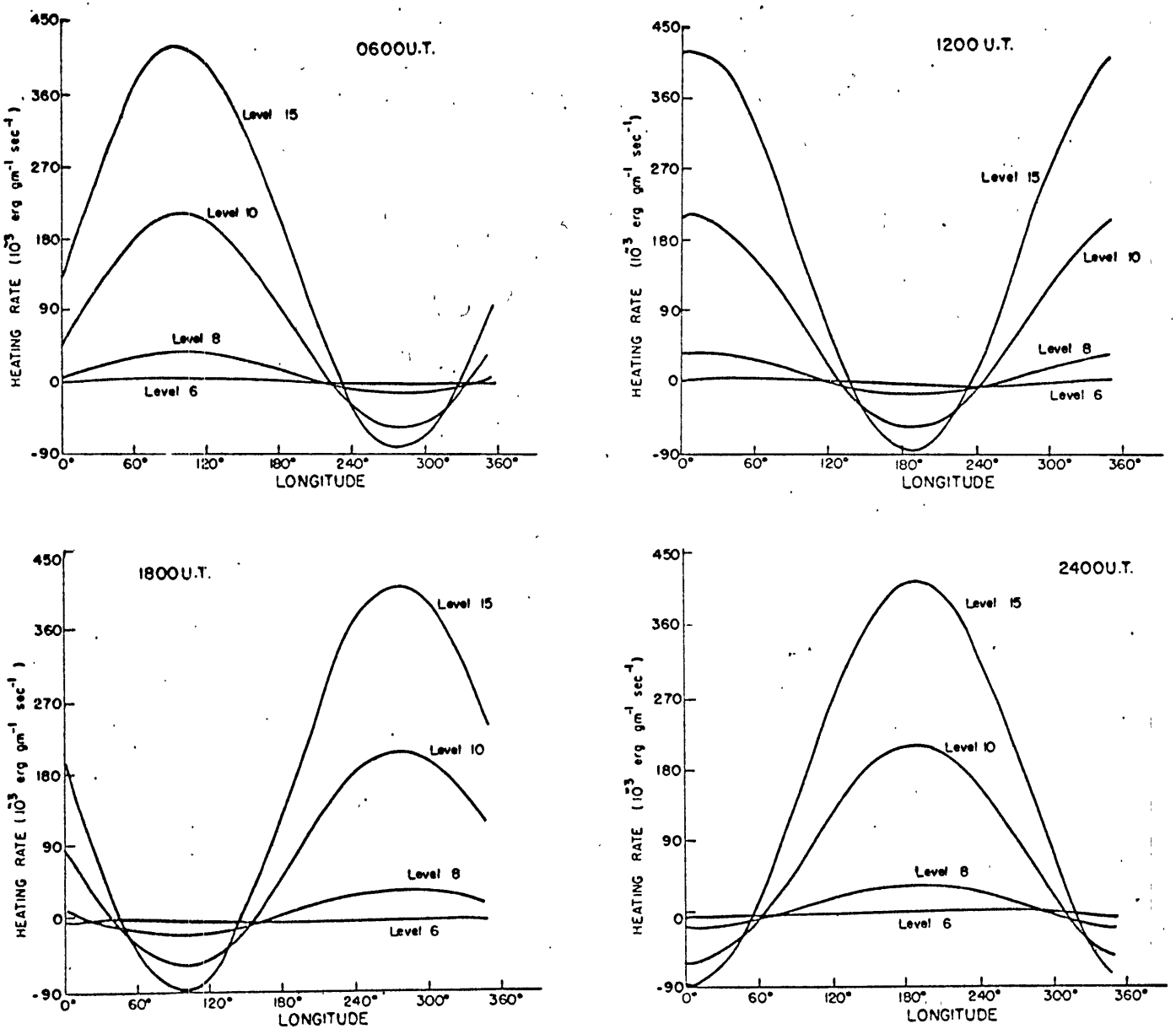

Figure 13: Longitudinal variability of heating plus cooling rates for four of the constant pressure surfaces used in the model calculations for 0600, 1200, 1800 and 0000 hours universal time.

sults for heating and cooling rates has been summarized in section 4. 3. 2. The heating and cooling rates corresponding to 30^{o} latitude for the equinox condition have been decomposed into the form of equation (5. 5) by the method of harmonic analysis, and used as input data for the two-dimensional model.

Figure 13 shows the result of this analysis. In this figure the variability of the energy source ($\dot{q}_{SR} + \dot{q}_{IR}$) with longitude and time for levels 6, 8, 10 and 15 is presented.

5. 2 Results of the Model Calculations

5. 2. 1 General description of the model calculations

The main purpose of this section is to evaluate the capability of the simple dynamical system selected for characterizing the features that were intended to be described. The questions that may be asked are: starting with a thermosphere at rest and given an externally driven thermal force, what sort of motions appear as a natural consequence of governing physical laws? What effect does this motion have on the thermal structure of the thermosphere?

By specifying the temperature field and assuming the region is at rest, the structure of the thermosphere and the motion field for future times are calculated. One would expect that eventually some sort of quasi-equilibrium would be reached, in which the heat from the sun would be balanced by some dissipational effect (c. g. molecular viscosity and airglow). All of the results presented below correspond to 30 degrees latitude at equinox.

The initial temperature field was taken from the one dimensional model result, which had about the right amplitude, but with phase lagging by about four hours. The time step was set to two hours (the finite difference scheme allows us to take any value for the time step without the problem of computational instability). The longitudinal temperature profile was selected for reference. Convergence toward a longitudinal cyclical state is taken as the criterion for physical meaningful solutions, since the observed behavior indicates that this is the case.

The result of this calculation is presented in figure 14; several comments may be given here: 1) the presence of wind system certainly can affect the temperature field; and 2) after one model day the phase of the diurnal maximum temperature has shifted to about 14 hour local time, however, the amplitude is too large. The amplitude still was increasing when the number of time steps was continued.

In the following calculations first the values of both u and $\dot{Z}$ then only u and then only $\dot{Z}$ were set consecutively equal to zero, in the thermodynamic equation. It was realized immediately that the cause of the changes in the temperature was the term involving the vertical velocity. Next, we introduced a factor ε which premultiplies the term involving the vertical velocity in the thermodynamic equation. Fig. 14 is then obtained with $\varepsilon = 1.0$. The results of the temperature field with $\varepsilon = 1.0$ imply that ε should be smaller than 1. The introduction of ε in the model is due to the fact that computation of $\dot{Z}$ from the continuity equation neglec-

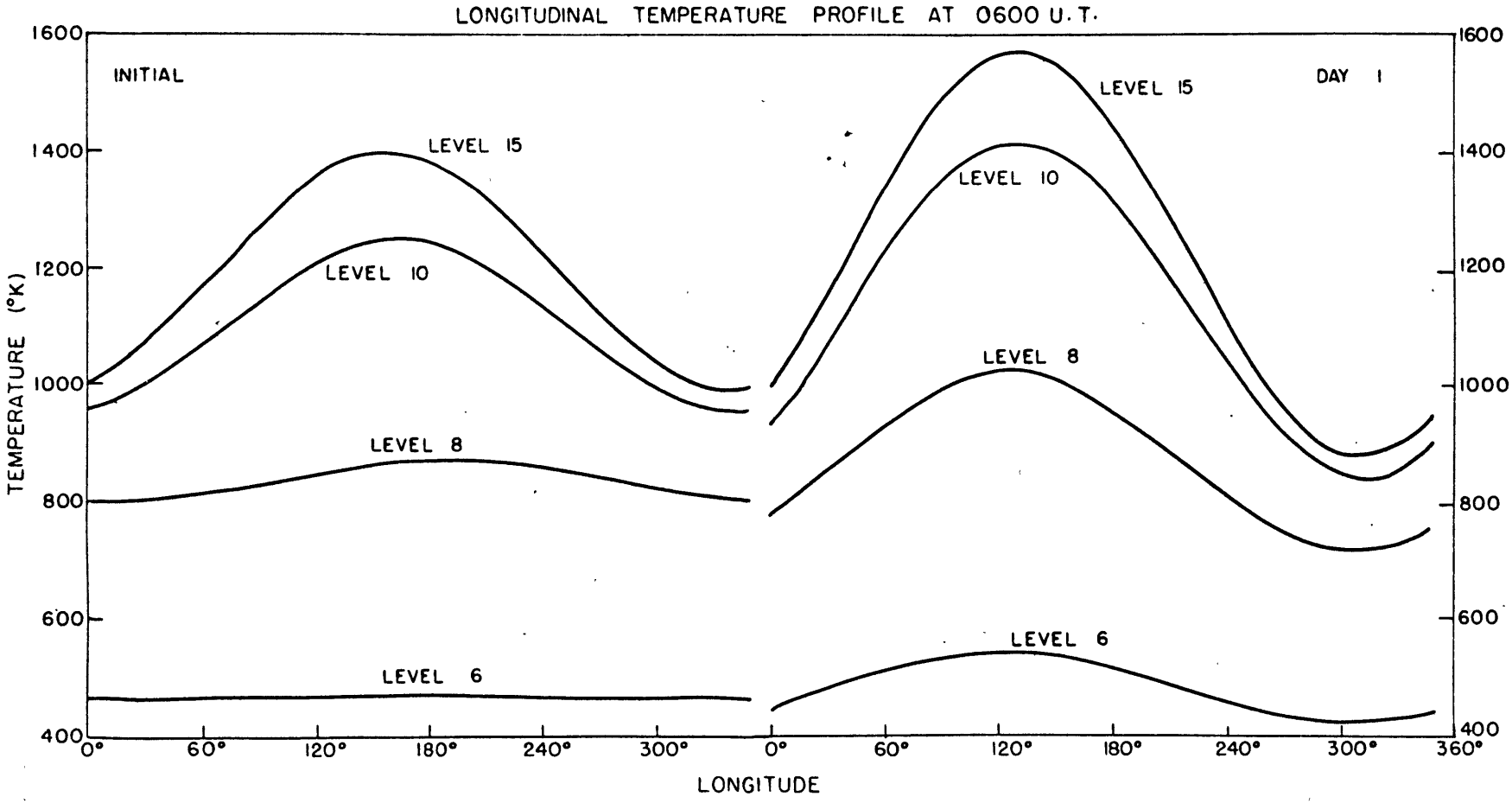

Figure 14: A comparison of initial and calculated temperature variability at 0600 hours universal time for model calculations with $\epsilon = 1$ (See text).

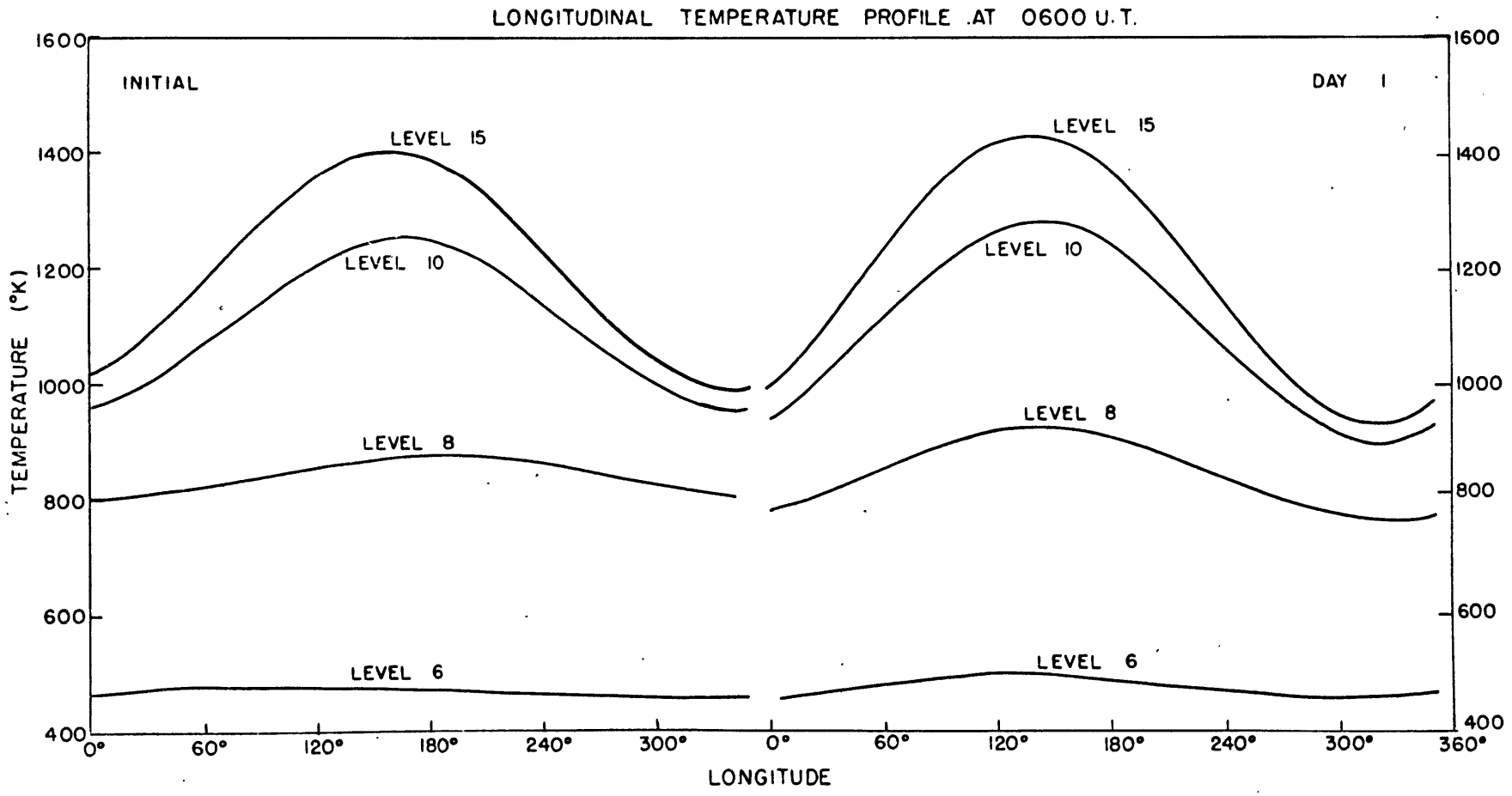

Figure 15: Same as figure 14, but for model calculations with $\varepsilon = 0.75$.

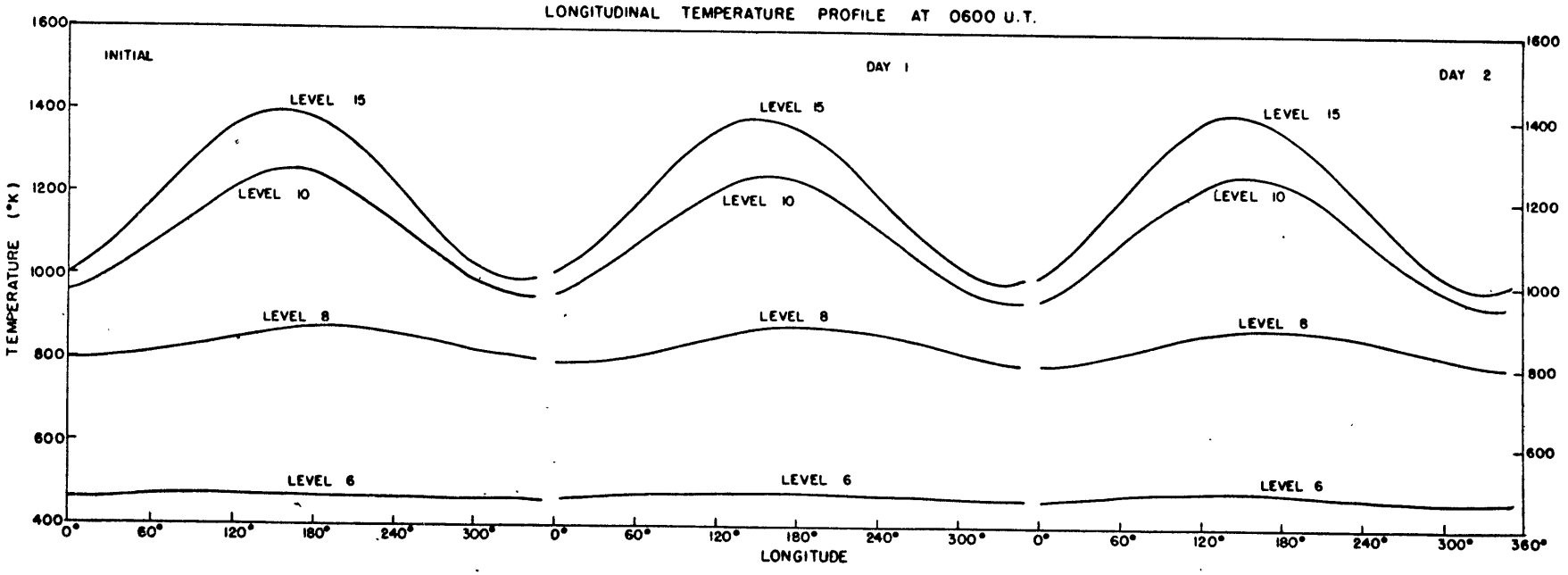

Figure 16: Same as figure 14, but for model calculations with $\varepsilon = 0.5$

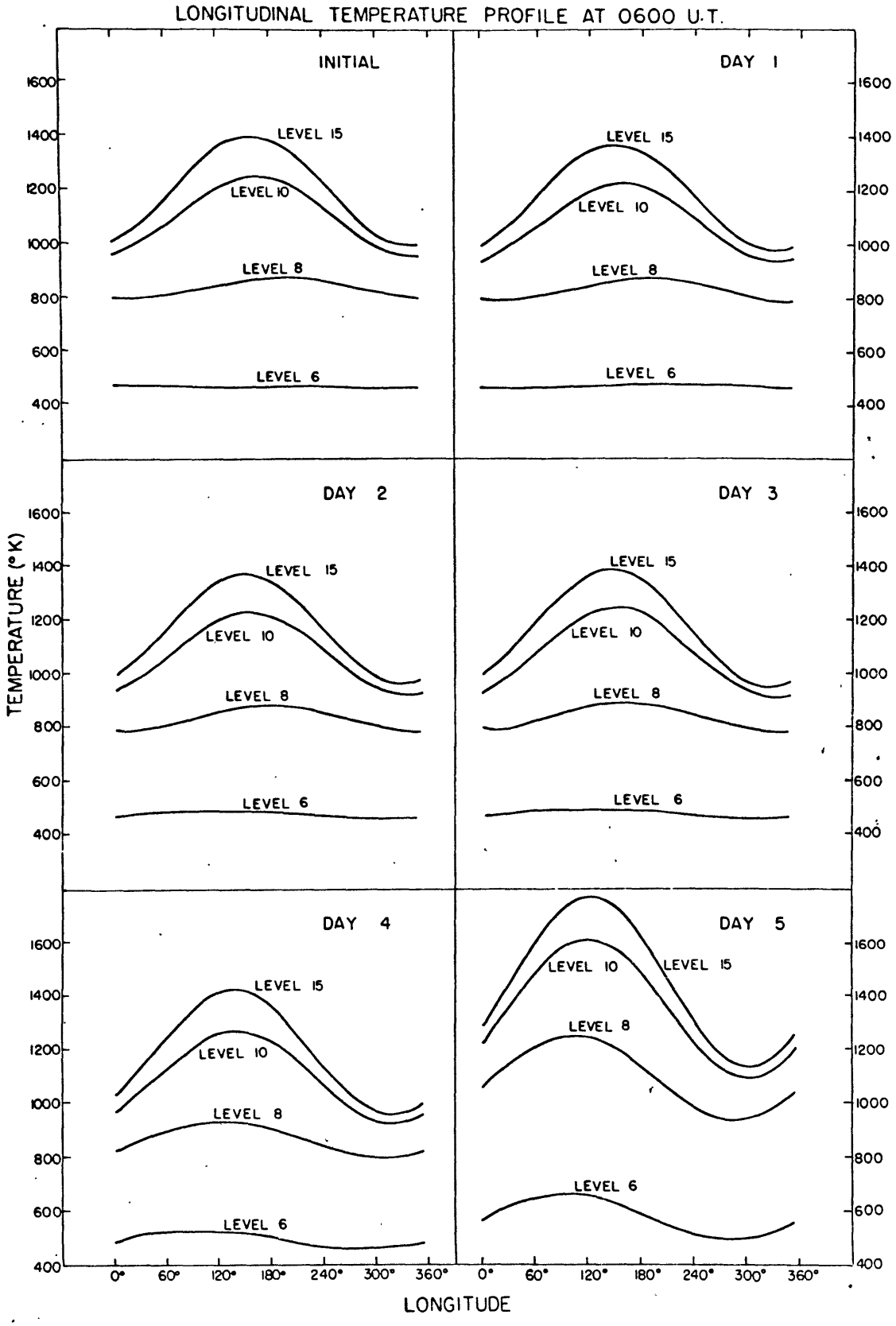

Figure 17: Same as figure 14, but for model calculations with $\varepsilon = 0.25$.

The energy transported by the horizontal advection is negligible. Results of calculations with $\varepsilon = 0$ indicate no change from the initial condition, in the temperature field. Nevertheless the calculations have been carried out including this term. The temporal variation in the model has as reference the Greenwich meridian time (U. T.).

The result of the temperature field for $\varepsilon = 0.75$ is shown in figure 15. Again the phase of the maximum temperature has shifted to about 15 hours local time after one model day. The amplitude of the temperature was still increasing after model day 2. Similar results are presented in figure 16 and 17 but for $\varepsilon = 0.5$ and $\varepsilon = 0.25$ respectively. In figure 16 the phase has shifted to about 14 hours local time, by the third model day. After several model days, the solution did not converge and the amplitude continued increasing although very slowly. Figure 17 further indicates that even when the amplitude continues to increase, the phase of the maximum temperature remains at about 14 hour local time.

Figure 18 summarizes the above results. It depicts the temperature variability for level 15 for the cases discussed above.

5.2.2 Model results for temperature variability

A sample of computed temperature variability is presented here.

Figure 19 illustrates the longitudinal temperature cross-section at 0600 U. T. In this figure the initial temperature distribution is compared with the model calculation for $\varepsilon = 0.25$ for model day 4. The influence of the initial condition on the model calculation disappears in a few

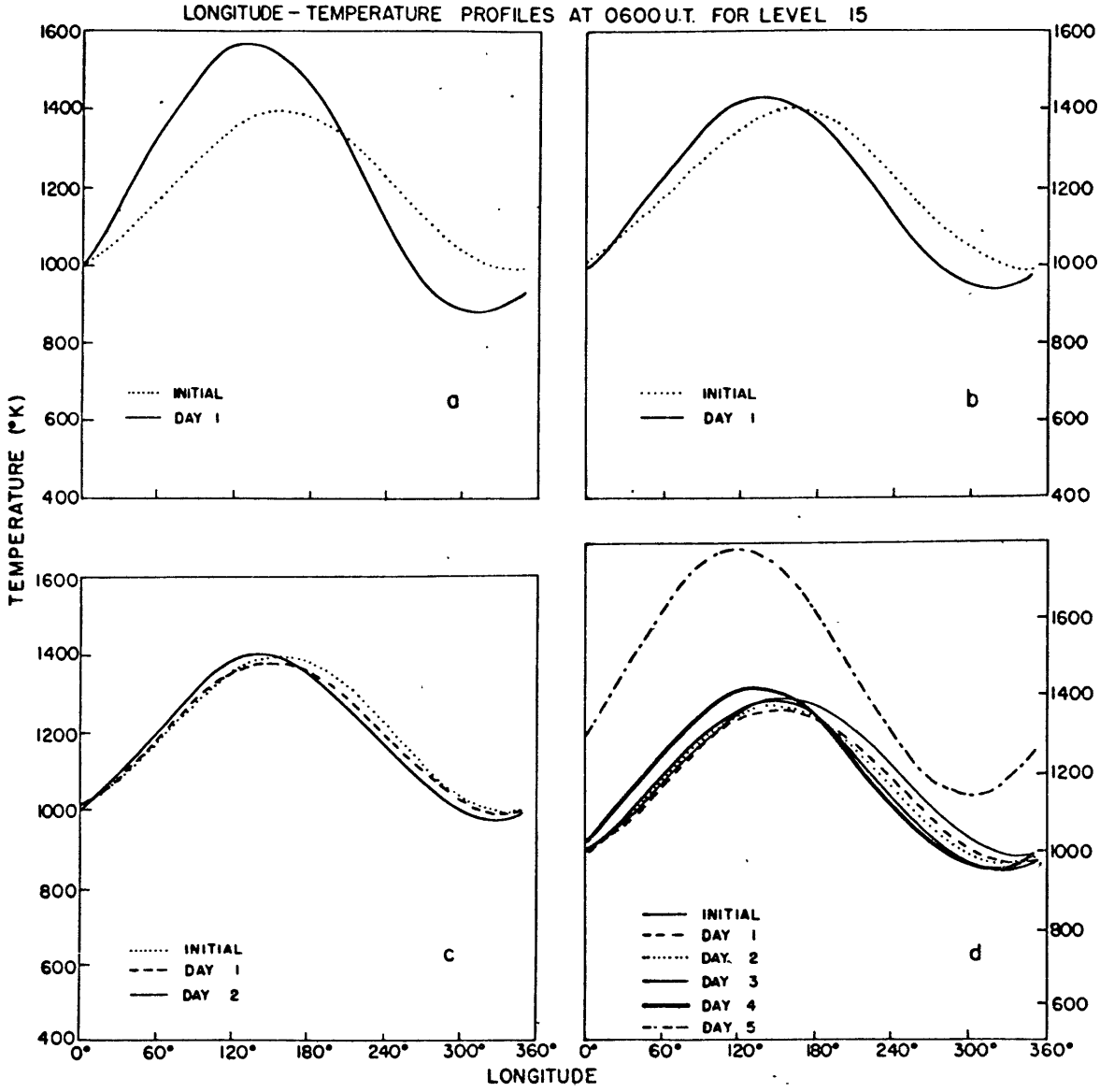

Figure 18: A comparison of initial and calculated temperature variability at 0600 hours universal time for the highest constant pressure level in the model calculations. (a) For $\varepsilon = 1$; (b) for $\varepsilon = 0.75$; (c) for $\varepsilon = 0.5$; and (d) for $\varepsilon = 0.25$.

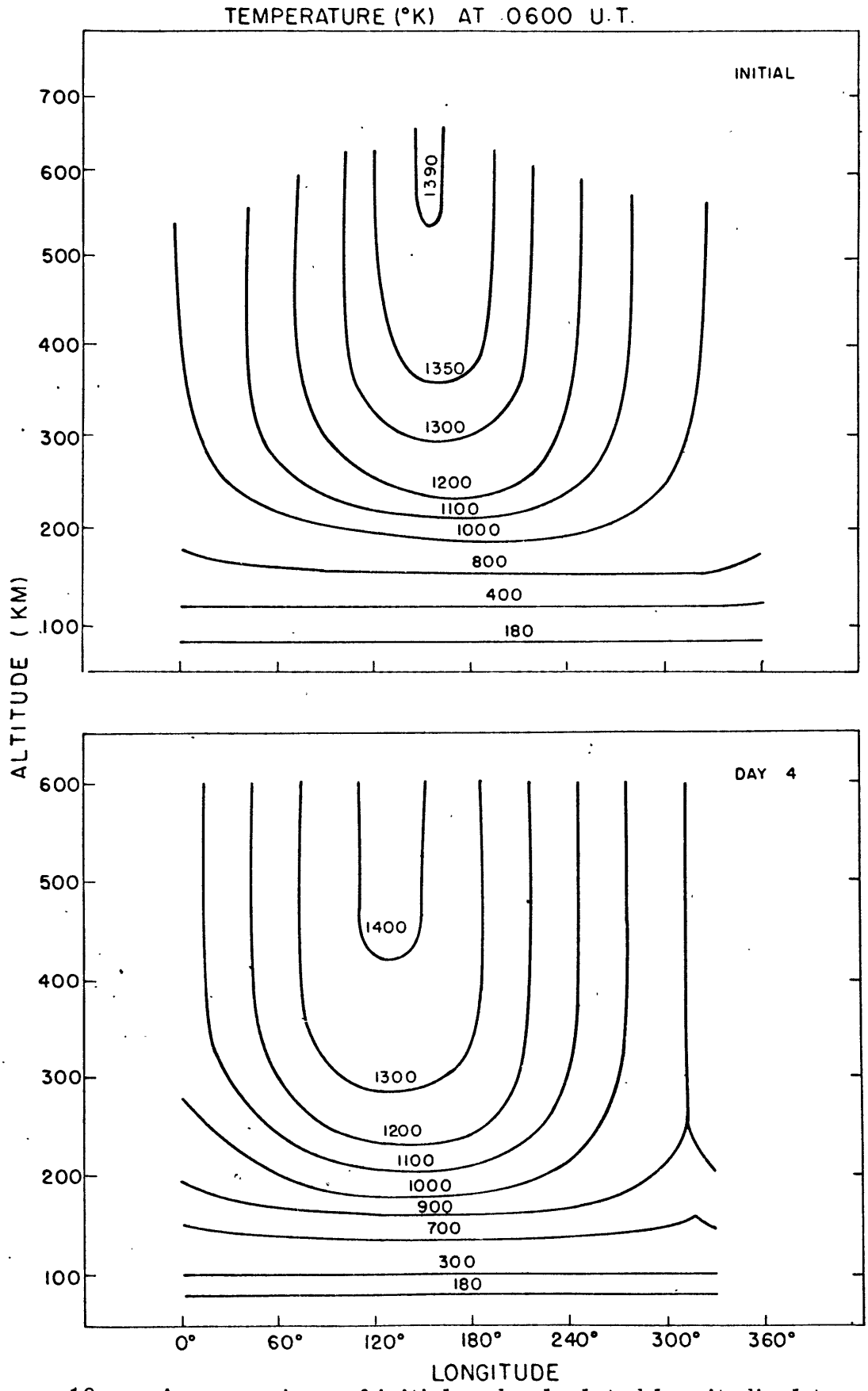

Figure 19: A comparison of initial and calculated longitudinal temperature cross-section at 0600 hours universal time for model calculations with $\varepsilon = 0.25$

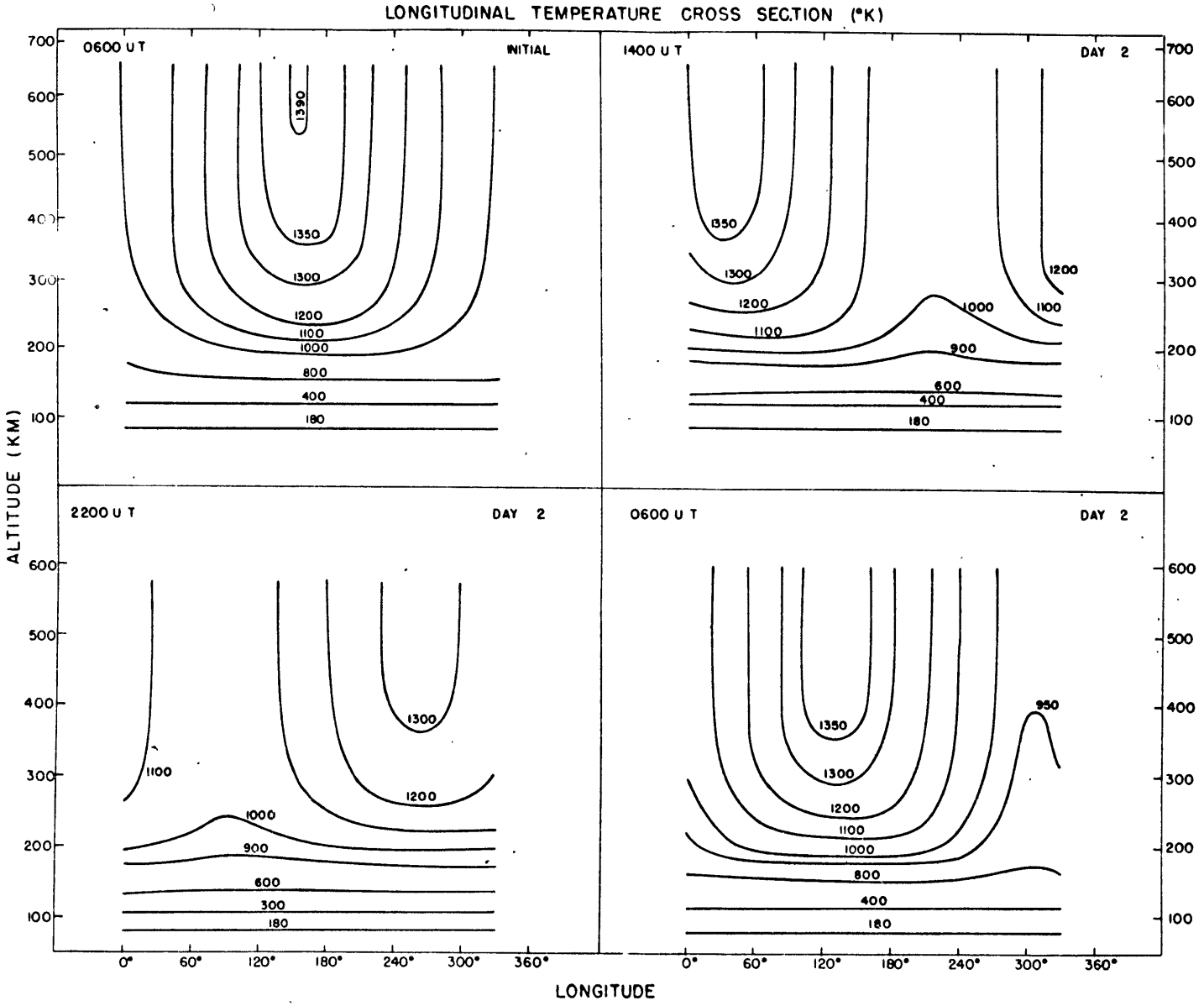

Figure 20: Same as figure 19, but at 0600, 1400 and 2200 hours universal time for model calculations with $\xi = 0.5$

time steps, the model then adjusts itself by reproducing the diurnal pattern. The large temperature gradient between about 100 km. and 200 km. is also present. Maximum temperature occurs at about 14 hours local time, thus reflecting the effect of adiabatic heating and cooling as mentioned in section 5.2.1. The amplitude of the diurnal temperature oscillation is about the same as the one dimensional model results.

Figure 19 shows that below about 180 km. the diurnal variation is very small, but above this altitude diurnal variability becomes quite large.

Figure 20 illustrate the longitudinal temperature cross-section for model calculation with $\varepsilon = 0.5$. The temperature distribution corresponds to model day 2. This figure indicates different stages of the behavior of the temperature field. The figure shows the cross-section at initial time, 1400 hours, 2200 hours and 0600 hours U. T.

In general, the model reproduces reasonable temperature distributions with altitude, longitude and time. Apart from the fact that the amplitude of the temperature oscillation increases with time, as a consequence of the intensification of the vertical velocity, the model results indicate that the adiabatic heating and cooling play an important role in the energy balance of the thermosphere. The adiabatic heating and cooling by vertical motion acts exactly as the second heat source of Harris and Priester, providing heating in the late morning and cooling in the late afternoon. The values of the vertical velocity computed from the present model are of course

a crude approximation in two respects: 1) horizontal motion in the north-south direction has not been included in the model; and 2) the effects of the coriolis force and the ion drag have been neglected in the calculation of the zonal wind component. Allowance for these factors might modulate the magnitude and the space and time variation of the vertical velocity, and thus eliminate its growth with time.

5.2.3 Model results for winds in the thermosphere

The solution of the zonal component of the momentum equation, when only inertial force, molecular viscocity and the geopotential gradient are present in the momentum balance, is given below..

At an initial time, the thermosphere is assumed to be at rest. Solutions with various other initial conditions were also obtained, but the resultant motions were found to be independent of the initial values.

The resulting wind system is made up of only two components, namely, U_1 and U_2. If U_o is set equal to zero initially, then U_o is equal to zero at all times. This is because the driving force (h_o), which is the mean zonal component of the geopotential height, has zero gradient. When initial values are specified on U_o, the molecular viscocity dissipates it within a few time steps. That is, the model can not reproduce a mean zonal wind. The results of the winds in the thermosphere in absence of mean flow are summarized in figures 21 - 24.

Figure 21 shows the longitudinal zonal wind cross-section for the model calculation with $\varepsilon = 0.25$ at 0600 Universal Time. The top dia-

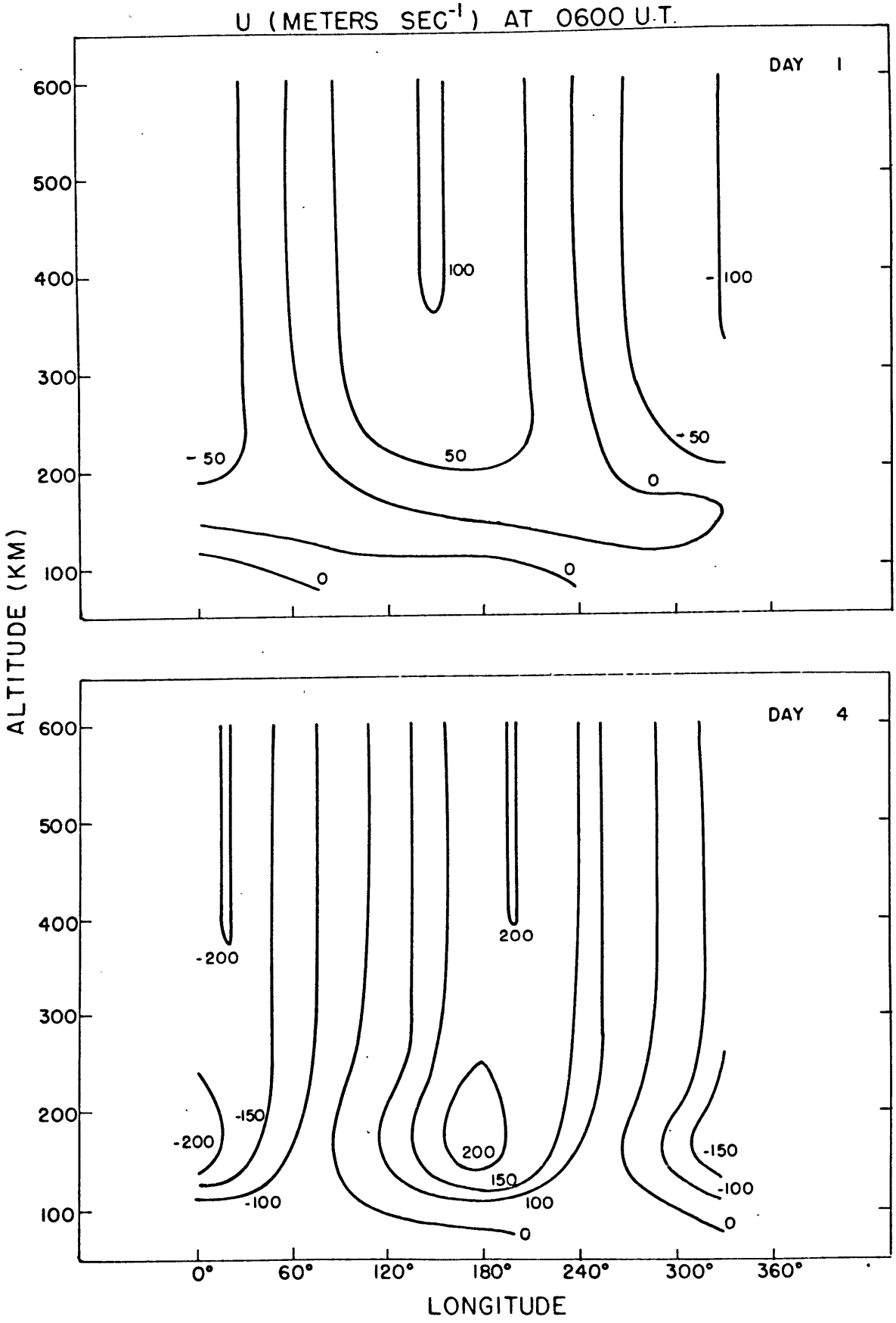

Figure 21: Longitudinal zonal wind cross-sections at 0600 hours universal time according to the model calculations for $\varepsilon = 0.25$.

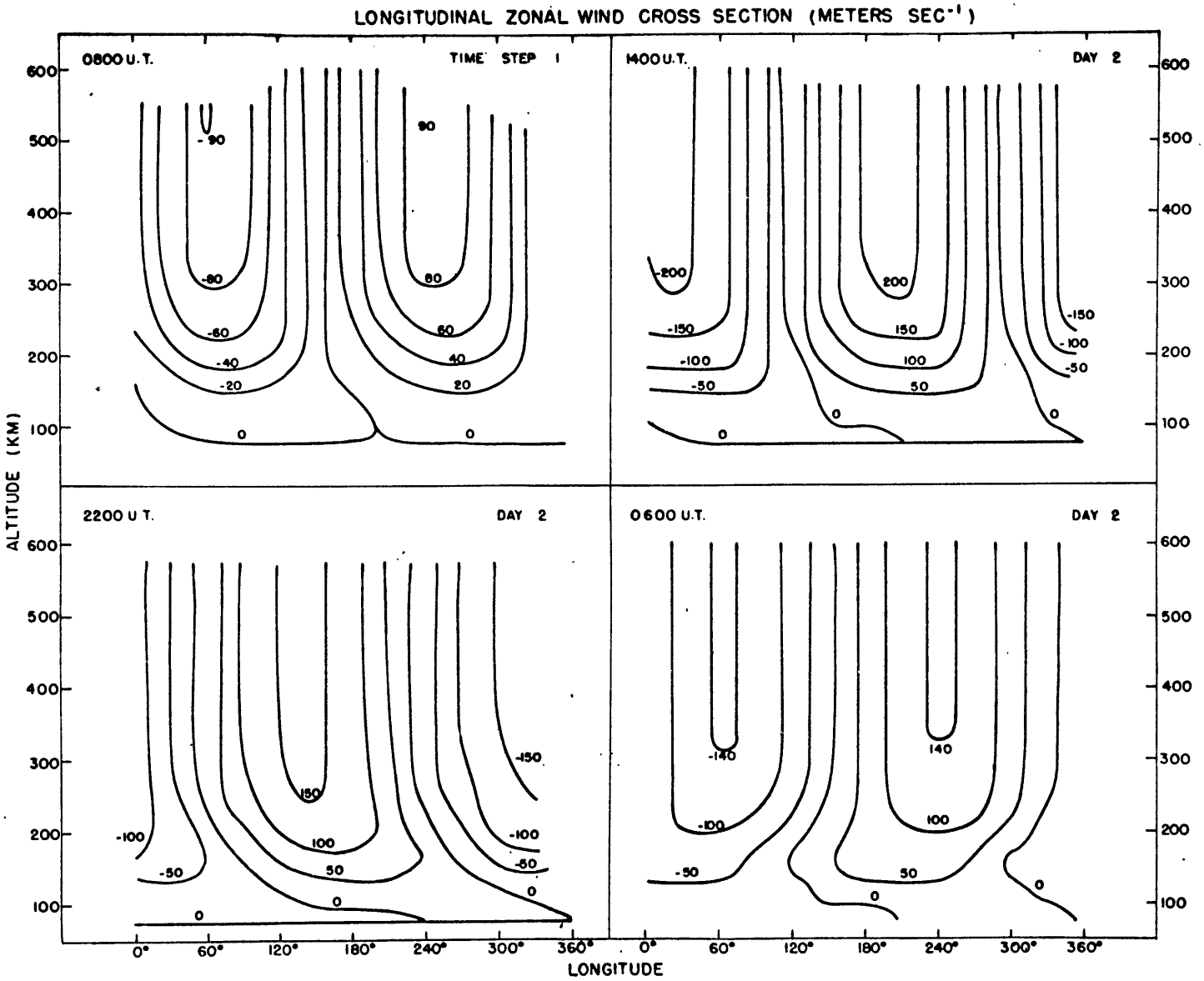

Figure 22: Same as figure 21, but at 0600, 1400, and 2200 hours universal time for model calculations with $\varepsilon = 0.5$.

gram is for model day 1 and the bottom diagram for model day 4. The intensification of the zonal wind component from the initial time to day 4 throughout the region can be seen from this figure. The largest magnitude is about 214 m sec^{-1}. The bottom diagram in figure 21 indicates the development of a west-east and east-west jet at 0600 hours and 1800 hours local time, respectively, at about 180 km. altitude.

Figure 22 is the same as figure 21, but for $\varepsilon = 0.5$ at different times of the day. The upper left diagram in figure 22 shows the result of the model calculation at time step 1 with zero initial condition. The largest magnitude of the wind is around 90 m sec^{-1} and occurs above 500 km. altitude at about 1200 hours and 24 hours local time. The remaining diagrams in figure 22 shows the development of the wind field during the model day 2.

Figure 23 illustrates the zonal wind component as a function of altitude at various times of day. The model results correspond to $\varepsilon = 0.25$. During the first three days the amplitude of the velocity oscillation did not change much; the largest value is about 100 m sec^{-1}. At the 4th day, however, the magnitude of the velocity profile has increased and the maximum value is of the order of 200 m sec^{-1}.

The results presented in figure 23 can be compared with similar wind profiles obtained by Lindzen (1967). Lindzen has included the ion drag term in the zonal component of the momentum equation. He shows that the profile of the wind amplitude largely depends on the ionization distribu-

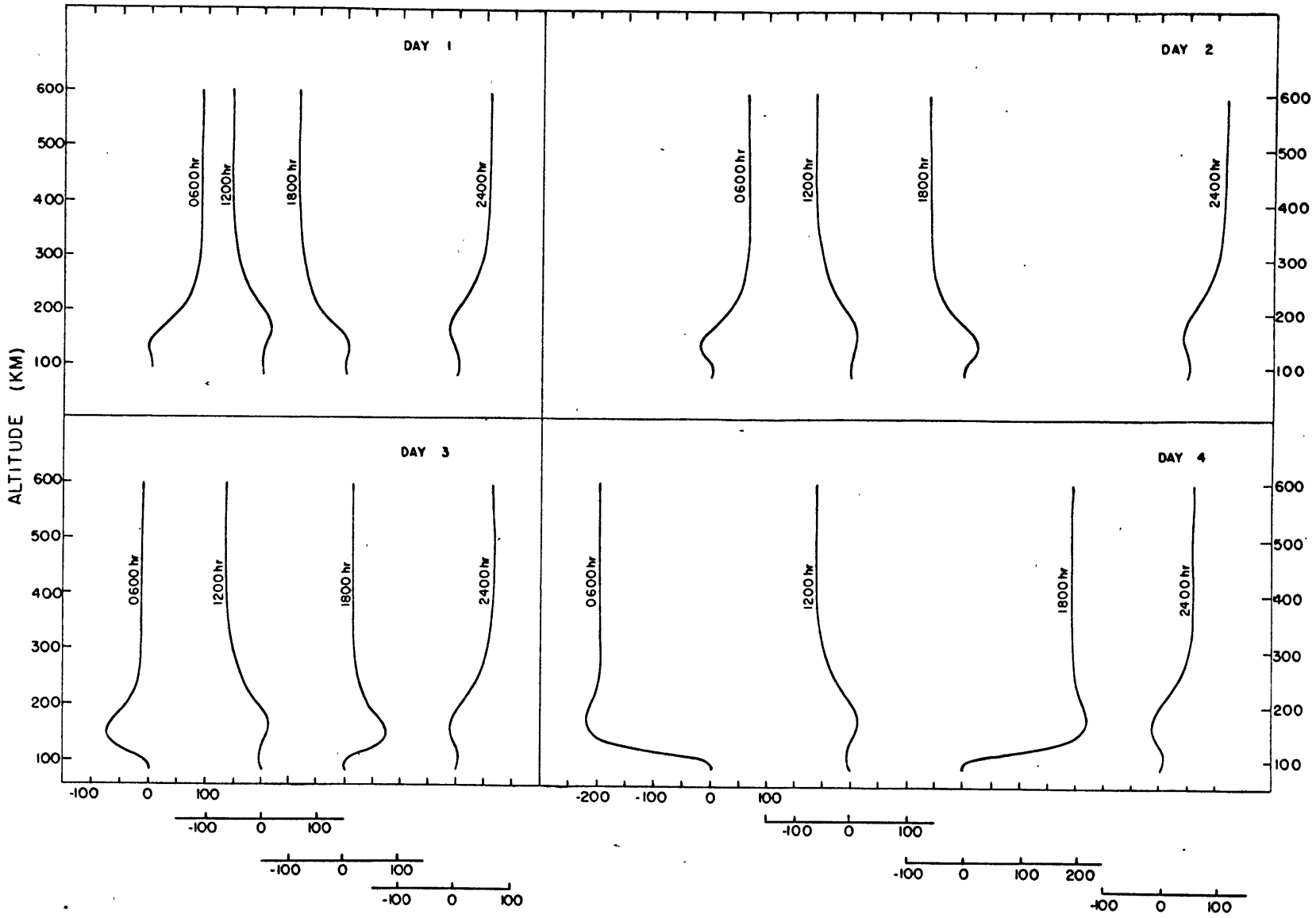

Figure 23: Zonal wind component as a function of altitude at 0600, 1200, 1800 and 2400 hours local time according to the model calculation with $\varepsilon = 0.25$.

tion. When he did not include the ion drag term, the magnitude of the zonal wind above 400 km. is around 800 m. sec.$^{-1}$. This value is four times as large as the magnitude reported here. If ion drag had been included in the present model, the speed of the zonal wind would be smaller than 200 m. sec.$^{-1}$.

The results of the model calculation for the vertical motion is displayed in figure 24. This figure depicts the distribution of vertical velocity with altitude for various times of day. Here $\omega = -pw$. The results correspond to the model calculation with $\varepsilon = 0.5$. The figure roughly indicates the regions of adiabatic heating and cooling. For example, for this day, there is adiabatic heating throughout the thermosphere in the period between 0800 hours and 1400 hours local time, adiabatic cooling throughout the region from about 2000 hours to 0200 hours local time and a combination of heating and cooling at other times at different levels.

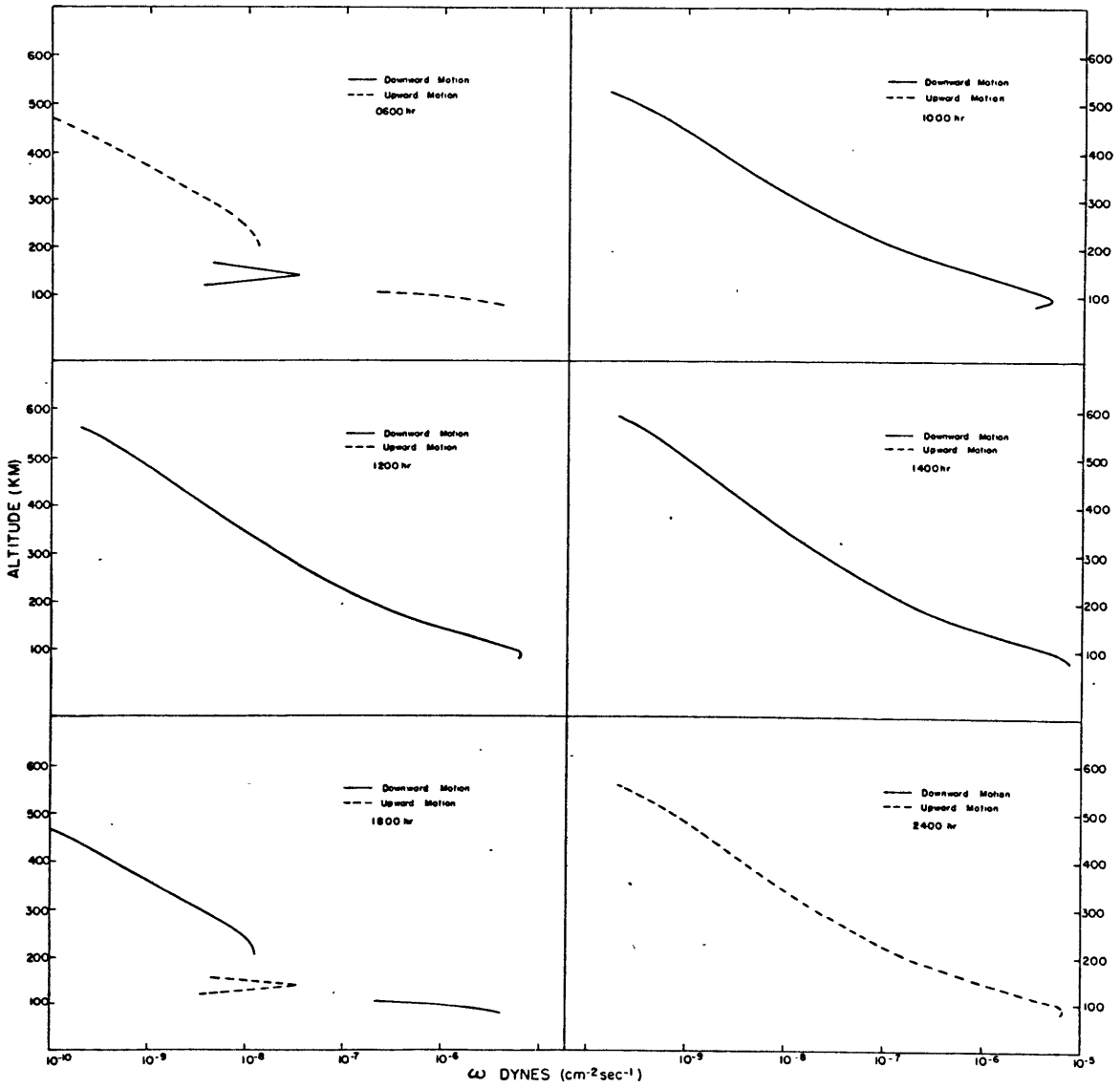

Figure 24: Vertical wind component as a function of altitude for various times of day according to the model calculations with $\varepsilon = 0.5$.

6. GENERAL DISCUSSION AND CONCLUSION

The object of this investigation has been to provide a rational basis for understanding the dynamics of the thermosphere. The study was primarily intended to describe the large-scale forced motion resulting from the diurnal heating in the thermosphere. It is to be considered as the initial step toward a more complete development of the theory of thermospheric motions by means of analytical and numerical methods.

The use of nondimensionalization has become a powerful procedure in modern meteorology and is being used extensively in many related sciences. Here the method has provided a way of simplifying the general equations which otherwise would be mathematically untractable to a set of equations capable of describing many features of interest.

If our interest were to study smaller scale thermospheric motions, the same method described in chapter 2 could be used with different characteristic scale parameters. In general, the formulation of a more elaborate tidal theory should follow along these lines.

The results presented in section (2. 2. 5) (cf. table 2) could be used to approximately obtain analytical solutions of the system of equations (5. 50) to (5. 53) in certain regions of the thermosphere. For example, in the altitude range of 80 to 150 km. the effect of viscocity and heat conduction can be neglected in the equations. Theories such as developed in dynamical meteorology might then be used to obtain the resultant temperature and wind fields. Likewise, above about 350 km., coriolis forces and inertial

forces might be neglected.

The general method used in chapter 3 to obtain solutions of the transient heat conduction equation could be extended and applied to several other similar problems. As an example, consider the problem of obtaining an approximate analytical solution to the momentum equations

$$\frac{\partial u}{\partial t} - fv = -g\frac{\partial h}{\partial x} + \frac{1}{\rho H}\frac{\partial}{\partial Z}\left(\frac{\mu}{H}\frac{\partial u}{\partial Z}\right) + \beta u \tag{6.1}$$

$$\frac{\partial v}{\partial t} + fu = -g\frac{\partial h}{\partial Y} + \frac{1}{\rho H}\frac{\partial}{\partial Z}\left(\frac{\mu}{H}\frac{\partial v}{\partial Z}\right) + \beta v \tag{6.2}$$

If $\frac{\partial h}{\partial X}$ and $\frac{\partial h}{\partial Y}$ are known and if β (coefficient of ion drag term) is assumed to be constant, then it is possible to obtain approximate analytical solutions.

With the transformation of the vertical coordinate from Z to ζ (cf. section 3.1) equations (6.1) and (6.2) reduce to

$$\frac{\partial}{\partial \zeta}\left(\frac{\mu}{H}\zeta\frac{\partial u}{\partial \zeta}\right) + cv + bu - a\frac{\partial u}{\partial t} = p_0\frac{\partial h}{\partial x} \tag{6.3}$$

$$\frac{\partial}{\partial \zeta}\left(\frac{\mu}{H}\zeta\frac{\partial u}{\partial \zeta}\right) - cu + bv - a\frac{\partial v}{\partial t} = p_0\frac{\partial h}{\partial Y} \tag{6.4}$$

where

$$\begin{aligned} a &= p_0/g \\ b &= (p_0/g)\beta \\ c &= (p_0/g)f \\ f &= 2\Omega \sin\varphi \end{aligned} \tag{6.5}$$

A single equation in the variable w = u + iv can be obtained by multiplying all terms in equation (6.4) by i and adding both equations:

$$\frac{\partial}{\partial \varsigma}\left(\frac{\mu}{H}\varsigma\frac{\partial w}{\partial \varsigma}\right) + (b - ic)w - a\frac{\partial w}{\partial t} = p_0\left(\frac{\partial h}{\partial x} + i\frac{\partial h}{\partial y}\right) \tag{6.6}$$

Equation (6. 6) is further transformed into a form similar to that of the heat conduction equation obtained in section (3. 1) (cf. equation 3. 6)

$$\frac{\partial}{\partial \varsigma}\left(\frac{\mu}{H}\varsigma\frac{\partial W}{\partial \varsigma}\right) - a\frac{\partial W}{\partial t} = \tilde{h} \tag{6.7}$$

by the substitution

$$w = e^{\frac{b-ic}{a}t} W \tag{6.8}$$

where

$$\tilde{h} = p_0 e^{-\frac{b-ic}{a}t}\left(\frac{\partial h}{\partial x} + i\frac{\partial h}{\partial y}\right) \tag{6.9}$$

Solutions of equation (6. 7) are now readily obtained in terms of Green's function for the cases discussed in section (3. 2) and (3. 3) for various assumed types of dependenc of the ratio μ/H in the vertical coordinate.

Lindzen (1967) has obtained numerical solutions of the zonal component of the momentum equation neglecting the coriolis force and using the equivalent forcing of $\partial h/\partial x$ derived from the Harris and Priester (1964) model atmosphere. An equation equivalent to (6. 7) for the zonal component when the coriolis term is neglected is

$$\frac{\partial}{\partial \varsigma}\left(\frac{\mu}{H}\varsigma\frac{\partial U}{\partial \varsigma}\right) - a\frac{\partial U}{\partial t} = \tilde{h}_x \tag{6.10}$$

where

$$u = e^{\frac{b}{a}t} U \tag{6.11}$$

and

$$\tilde{h}_x = p_0 e^{-\frac{b}{a}t} \frac{\partial h}{\partial x} \tag{6.12}$$

Solution of equation (6.10) is again easily obtained following the same procedure as outlined above. An analytical solution of (6.10) would then be of interest in order to see the accuracy of the approximations. Likewise it is important to evaluate the integrals in the analytical solution of the equations described in chapter 3. This can be carried out first by assuming a simple form of the source function (heating and cooling rates) and comparing the different approximations obtained by the assumptions of K/H with numerical results.

One obvious fault of the two dimensional model is the neglect of the coriolis force and the ion drag in the momentum equation, but even so, the model has yielded many interesting results. To obtain physically more realistic situations, these terms must be included.

It would be very important to derive the energy balance equations in the thermosphere and investigate the energy budget of the region. A first step in this direction has been made recently (Newell, 1966b). Such a study is required to establish whether sources and sinks of energy other than those employed in the present model are of importance to the dynamical behavior of the thermosphere.

The principal conclusions, which the analysis presented in the preceding chapter has made possible, may be enumerated as follows:

1) Scale analysis considerations of global scale diurnal motions indicate:

a) nonlinear advective terms in the momentum and thermodynamic equations can be neglected only if the magnitude of the zonal wind component is smaller than 200 m sec^{-1}. i.e. R_o ($u < 200$) $\lesssim 0.274$ (see table 1).

b) adiabatic heating and cooling have the same order of magnitude as other terms in the thermodynamic equation and therefore cannot be neglected.

c) as shown previously (Geisler, 1966; Volland, 1966; Lindzen, 1967), ion drag plays an important role in the momentum balance above 150 km.

2) Approximate analytical solution of the general heat conduction equation can be obtained for several assumptions about the dependence of K/H upon altitude.

3) Horizontal energy transport across latitude circles must occur at all levels above about 120 km. in the thermosphere. At or near the time of equinox, poleward energy transport must occur in middle and high latitudes in both hemispheres. At the time of solstice a marked poleward transport must occur throughout the winter hemisphere; the required horizontal transport in the summer hemisphere is much smaller.

4) The model results are reasonably representative of the variation of thermospheric temperature and density as indicated by the available

satellite and rocket data. In particular, the computed diurnal variability of temperature and density is small below 200 km., and it increases with altitude above that level.

5) Horizontal energy transport by advective processes cannot modify the phase of the diurnal temperature and density oscillation.

6) Adiabatic heating and cooling by vertical motion act as a second heat source in the thermosphere. The vertical motion responsible for this is associated with the positive and negative divergence of the horizontal wind system. When this vertical motion is included in the model calculation, the maximum temperature occurs at about 1400 hours local time. The full three-dimensional dynamical model needs to be considered to strengthen this conclusion, since the meridional component of horizontal motion would be expected to modify the field of vertical motion in some way. However, because the meridional component of motion will be of the same order as the zonal component, it is not likely to advect sufficient heat to affect the phase of the temperature oscillation.

APPENDIX A

Basic Concepts of Fourier Analysis

A summary of basic concepts of Fourier analysis is presented below (cf. Saltzman, 1957; Apostol, 1960). Let f(x) be any real, single-valued function and piecewise differentiable in the interval (a, b). Let $S = \{ \varphi_0(x), \varphi_1(x), \varphi_2(x), \cdots \}$ be an orthonormal set on (a, b). Then f(x) may be expressed as a linear combination of elements of S. Such an expansion is written in the form

$$f(x) = \sum_{n=0}^{\infty} c_n \varphi_n(x) \tag{A. 1}$$

where the numbers $c_0, c_1, c_2, \ldots$ are given by the following formulas:

$$c_n = \int_a^b f(x)\ \overline{\varphi_n(x)}\ dx \qquad (n = 0, 1, 2, \cdots) \tag{A. 2}$$

where $\overline{\varphi_n(x)}$ denotes the complex conjugate of $\varphi_n(x)$.

The series in (A. 1) is called the Fourier series of f relative to the system S and the numbers $c_0, c_1, c_2, \ldots$ are called the Fourier coefficients of f relative to S.

When S is the particular orthonormal set of trigonometric functions defined on the interval ($0, 2\pi$), the series is called simply the Fourier series generated by f . In this case we write (4. 1) in the form

$$f(x) = \frac{b_0}{2} + \sum_{n=1}^{\infty} (a_n \sin nx + b_n \cos nx) \tag{A. 3}$$

the coefficients being given by the following formulae:

$$a_n = \frac{1}{\pi}\int_0^{2\pi} f(x) \sin nx\, dx, \qquad b_n = \frac{1}{\pi}\int_0^{2\pi} f(x) \cos nx\, dx \tag{A. 4}$$

The Fourier series generated by f in (A. 3) can be also expressed in terms of complex exponentials which may be written as follows:

(A. 5) $$f(x) = \sum_{n=-\infty}^{\infty} c_n e^{inx}$$

The formulas (A. 2) for the coefficients now become

(A. 6) $$c_n = \frac{1}{2\pi} \int_0^{2\pi} f(x)\, e^{-inx}\, dx \quad , \quad (n = 0, \pm 1, \pm 2, \cdots)$$

For the purposes of the discussion in section (5. 1), we shall consider the Fourier representation of thermospheric quantities specified along a given latitude in our cartesian system. Thus, in the above, x is taken as longitude, and n is the wave number.

The quantity c_n is the representation of f(x) in the domain of wave number and is called the spectral function of f. The set of equations, (A. 1) and (A. 2) is often referred to as a Fourier Transform pair.

Consider for simplicity the set of equations (A. 5) and (A. 6); we may write the Fourier transform pairs for the derivatives of f(x, y, Z, t) as follows:

(A. 7) $$\frac{\partial f}{\partial x} = \sum_{n=-\infty}^{\infty} in\, c_n e^{inx} \quad ,$$

and

(A. 8) $$in\, c_n = \frac{1}{2\pi} \int_0^{2\pi} \frac{\partial f}{\partial x} e^{-inx}\, dx \quad ;$$

(A. 9) $$\frac{\partial f}{\partial \xi} = \sum_{n=-\infty}^{\infty} \frac{\partial c_n}{\partial \xi} e^{inx} \quad ,$$

and

(A. 10) $$\frac{\partial c_n}{\partial \xi} = \frac{1}{2\pi} \int_0^{2\pi} \frac{\partial f}{\partial \xi} e^{-inx}\, dx$$

where ξ may be y, Z or t.

Next, we consider the product of two functions, f(x) and g(x), whose spectral functions defined by (A. 6) are c_n and d_n respectively. For these functions, we may write

$$\text{(A. 11)} \qquad \frac{1}{2\pi}\int_0^{2\pi}\left[f(x)\,g(x)\right]e^{-inx}\,dx = \frac{1}{2\pi}\int_0^{2\pi} f(x)\left[\sum_{m=-\infty}^{\infty} d_m e^{imx}\right]e^{-inx}\,dx$$

$$= \sum_{m=-\infty}^{\infty} d_m \frac{1}{2\pi}\int_0^{2\pi} f(x)\, e^{-i(n-m)x}\,dx$$

or

$$\text{(A. 12)} \qquad \frac{1}{2\pi}\int_0^{2\pi}\left[f(x)\,g(x)\right]e^{-inx}\,dx = \sum_{m=-\infty}^{\infty} d_m\, c_{n-m}$$

Here we have assumed that g(x) is uniformly convergent, so that the order of integration and summation may be interchanged.

Expression (A. 12) gives the spectral function for the product of two dependent variables. As a special case, we may obtain Parseval's Formula by setting n = 0 in (A. 12)

$$\text{(A. 13)} \qquad \frac{1}{2\pi}\int_0^{2\pi} f(x)\,g(x)\,dx = \sum_{m=-\infty}^{\infty} d_m\, c_{-m}$$

and if f = g, we have

$$\text{(A. 14)} \qquad \frac{1}{2\pi}\int_0^{2\pi} f^2(x)\,dx = \sum_{m=-\infty}^{\infty} |d_m|^2$$

For the set of equations (A. 3) and (A. 4) we have,

$$\text{(A. 15)} \qquad \frac{1}{\pi}\int_0^{2\pi} f^2(x) = \frac{b_0^2}{2} + \sum_{n=1}^{\infty}\left(a_n^2 + b_n^2\right)$$

APPENDIX B

Equations in the Domain of Wave Number

The two dimensional set of dynamical equations is

(B. 1) $$\frac{\partial u}{\partial t} = -g\frac{\partial h}{\partial x} + \frac{\mu}{\rho H^2}\frac{\partial^2 u}{\partial Z^2} + \frac{1}{\rho H}\frac{\partial u}{\partial Z}\frac{\partial}{\partial Z}\left(\frac{\mu}{H}\right)$$

(B. 2) $$\frac{\partial u}{\partial x} + \frac{\partial \dot{Z}}{\partial Z} - \dot{Z} = 0$$

(B. 3) $$c_p\frac{\partial T}{\partial t} = \frac{K}{\rho H^2}\frac{\partial^2 T}{\partial Z^2} + \frac{1}{\rho H}\frac{\partial T}{\partial Z}\frac{\partial}{\partial Z}\left(\frac{K}{H}\right) - c_p u\frac{\partial T}{\partial x} - c_p\dot{Z}\left(\frac{\partial T}{\partial Z} + \frac{R^*}{M}\frac{T}{c_p}\right) + \dot{q}_{SR} + \dot{q}_{IR}$$

The dependent variables U, Z, and T are expanded in the form

(B. 4) $$\psi(x, Z, t) = \psi_0(Z, t) + \psi_s(Z, t)\sin\lambda x + \psi_c(Z, t)\cos\lambda x$$

however, the dependent variables μ/H, K/H and ρH are expressed by their zonal average. This is not an important inconsistency in the computational scheme because μ/H and K/H vary only slowly in x, and because ρH is simply equal to p/g.

Using the relation given in appendix A, the set of equations (B. 1)-(B. 3) is transformed from the space domain to the domain of wave number. By equating like coefficients the system (B. 1)- (B. 3) takes the form:

(B. 5) $$\frac{\partial u_0}{\partial t} = \frac{\mu_0}{\rho_0 H_0^2}\frac{\partial^2 u_0}{\partial Z^2} + \frac{1}{\rho_0 H_0}\frac{\partial u_0}{\partial Z}\frac{\partial}{\partial Z}\left(\frac{\mu_0}{H_0}\right)$$

(B. 6) $$\frac{\partial u_s}{\partial t} = \frac{\mu_0}{\rho_0 H_0^2}\frac{\partial^2 u_s}{\partial Z^2} + \frac{1}{\rho_0 H_0}\frac{\partial u_s}{\partial Z}\frac{\partial}{\partial Z}\left(\frac{\mu_0}{H_0}\right) + \lambda g h_c$$

(B. 7) $$\frac{\partial u_c}{\partial t} = \frac{u_o}{\rho_o H_o^2}\frac{\partial u_c}{\partial Z} + \frac{1}{\rho_o H_o}\frac{\partial u_c}{\partial Z}\frac{\partial}{\partial Z}\left(\frac{u_o}{H_o}\right) - \lambda g h_s$$

(B. 8) $$\dot{Z}_o = 0$$

(B. 9) $$-\lambda u_c + \frac{\partial \dot{Z}_s}{\partial Z} - \dot{Z}_s = 0$$

(B. 10) $$\lambda u_s + \frac{\partial \dot{Z}_c}{\partial Z} - \dot{Z}_c = 0$$

(B. 11) $$c_p \frac{\partial T_o}{\partial t} = \frac{K_o}{\rho_o H_o^2}\frac{\partial^2 T_o}{\partial Z^2} + \frac{1}{\rho_o H_o}\frac{\partial T_o}{\partial Z}\frac{\partial}{\partial Z}\left(\frac{K_o}{H_o}\right)$$
$$+ \frac{\lambda}{2} c_p u_s T_c - \frac{\lambda}{2} c_p u_c T_s - \frac{1}{2} c_p \dot{Z}_s \frac{\partial T_s}{\partial Z}$$
$$- \frac{1}{2} c_p \dot{Z}_c \frac{\partial T_c}{\partial Z} - \frac{1}{2}\frac{R^*}{M}\dot{Z}_s T_s - \frac{1}{2}\frac{R^*}{M}\dot{Z}_c T_c + \dot{q}_{o\,SR} + \dot{q}_{o\,IR}$$

(B. 12) $$c_p \frac{\partial T_s}{\partial t} = \frac{K_o}{\rho_o H_o^2}\frac{\partial^2 T}{\partial Z^2} + \frac{1}{\rho_o H_o}\frac{\partial T_o}{\partial Z}\frac{\partial}{\partial Z}\left(\frac{K_o}{H_o}\right) + \lambda c_p u_o T_c$$
$$- c_p \dot{Z}_s \frac{\partial T_o}{\partial Z} - \frac{R^*}{M}\dot{Z}_s T_o + \dot{q}_{s\,SR} + \dot{q}_{s\,IR}$$

(B. 13) $$c_p \frac{\partial T_c}{\partial t} = \frac{K_o}{\rho_o H_o^2}\frac{\partial^2 T_c}{\partial Z^2} + \frac{1}{\rho_o H_o}\frac{\partial T_c}{\partial Z}\frac{\partial}{\partial Z}\left(\frac{K_o}{H_o}\right) - \lambda c_p u_o T_s$$
$$- c_p \dot{Z}_c \frac{\partial T_o}{\partial Z} - \frac{R^*}{M}\dot{Z}_c T_o + \dot{q}_{c\,SR} + \dot{q}_{c\,IR}$$

REFERENCES

Anderson, A. D., 1966: An hypothesis for the semi-annual effect appearing in satellite orbital decay data. Plan. Space Sci. 14, 849.

Anderson, A. D. and Francis, W. E., 1966: The variation of the neutral atmospheric properties with local time and solar activity from 100 to 10,000 km. J. Atmos. Sci. 23, 110.

Apostol, T. M., 1960: Mathematical analysis. Addison-Wesley Publ. Co., Reading, Massachusetts.

Bates, D. R., 1951: The temperature of the upper atmosphere. Proc. Phys. Soc., 64B, 805.

Burger, A., 1958: Scale considerations of planetary motions of the atmosphere. Tellus, 10, 195.

Chapman, S., 1961: Scale times and scale lengths of variables with geomagnetic and ionospheric illustrations. Proc. Phys. Soc. 77, 424.

Charney, J. G., 1947: On the scale of atmospheric motions. Geofys. Publikasjoner, Norske Videnskaps. Akad, Oslo, 17 (2).

Charney, J. G. and Stern, M., 1962: On the stability of internal baroclinic jets in a rotating atmosphere. J. Atmos. Sci. 19, 1959.

COSPAR International Reference Atmosphere, 1965, North-Holland Publishing Company, Amsterdam

Crank, J. and Nicholson, P., 1947: A practical method for numerical integration of solution of partial differential equation of heat conduction type. Proc. Cambridge Philos. Soc. 43, 50.

Faire, A. C. and Champion, K. S. W., 1966: High altitude rocket density measurements at Eglin, Florida. In "Space Research VII" In press.

Geisler, J. E., 1966: Atmospheric winds in the middle latitude F-region. J. Atmos. Terr. Phys. 28, 703.

Greenspan, H. P., 1964: On the transient motion of a contained rotating fluid. J. Fluid. Mech. 20, part 4, 673-696.

Hanson, W. B., 1961: Structure of the ionosphere. In "Satellite Environmental Handbook" (Johnson, ed.) Stanford University Press, Stanford, California, 155 pp.

Harris, I., and Priester, W., 1962: Time-dependent structure of the upper atmosphere, J. Atmos. Sci., 19, 286.

Harris, I. and Priester, W., 1964: The upper atmosphere in the range from 120 to 800 km., in proposal for a new edition of the COSPAR International Reference Atmosphere, available from Institute for Space Studies, New York, N. Y. 10027.

Harris, I., and Priester, W., 1965: Of the diurnal variation of the upper atmosphere. J. Atmos. Sci., 22, 3.

Hinteregger, H. E., Hall, L. A. and Schmidtke, G., 1965: Solar XUV radiation and neutral particle distribution in July 1963 thermosphere. Space Research V, 1175-1190, North-Holland Pub. Co.

Hunt, D. C., and T. E. Van Zandt, 1961: Photoionization heating in the F-region of the atmosphere. J. Geophys. Res. 66, 1673.

Jacchia, L. G., 1960: A variable atmospheric-density model from satellite accelerations. J. Geophy. Res. 65, 2775.

Jacchia, L. G., 1961: A working model for the upper atmosphere. Nature 192, 1147.

Jacchia, L. G., 1965: The temperature above the thermopause. Space Research V, 1152-1174, North-Holland Pub. Co.

Jacchia, L. G. and Slowey, J., 1962: Accurate drag determination for eight artificial satellites; atmospheric densities and temperatures. Smithsonian Astrophys. Obs., Spec. Rept. No. 100, 117 pp.

Jacchia, L. G. and Slowey, J., 1966: The shape and location of the diurnal bulge in the upper atmosphere. Smithsonian Astrophys. Obs., Spec. Rept. No. 207, 22pp.

Jacchia, L. G., and Slowey, J. and Verniani, F., 1967: Geomagnetic perturbations and upper-atmosphere heating. J. Geophy. Res. 72, 1423.

Jacobs, R. L., 1967: Atmospheric density derived from the drag of eleven low-altitude satellites. J. Geophys. Res. 72, 1571.

Johnson, F.S., 1956: Temperature distribution of the ionosphere under control of thermal conductivity. J. Geophys. Res. 61, 71.

Johnson, F.S., 1958: Temperature in the high atmosphere. Ann. Geophys. 14, 94.

Jursa, A.S., Nakamuta, M. and Tanaka, Y., 1965: Molecular oxygen distribution in the upper atmosphere, 2. J. Geophys. Res. 70, 2699.

King-Hele, D.G., 1966a: Methods of determining air density from satellite orbits, Ann. Geophys. 22, 40.

King-Hele, D.G., 1966b: The semi-annual variation in upper atmosphere density as revealed by Samos 2. Planet. Space Sci., 14, 863.

Lindzen, R.S., 1966: Crude estimate for the zonal velocity associated with the diurnal temperature oscillation in the thermosphere. J. Geophys. Res., 71, 865.

Lindzen, R.S., 1967: Reconsideration of diurnal velocity oscillation in the thermosphere. J. Geophys. Res. 72, 1591.

Mahoney, J.R., 1966: A study of energy sources for the thermosphere. Rept. No. 17, Dept of Meteor., M.I.T., 218 pp.

Mange, P., 1955: Diffusion processes in the thermosphere. Ann. Geophys. 11, 153.

Mange, P., 1957: The theory of molecular diffusion in the atmosphere. J. Geophys. Res. 62, 279.

Mange, P., 1961: Diffusion in the thermosphere. Ann Geophys. 17, 277.

May, R.R., 1964: Upper air density derived from the orbits of discoverer satellites and its variation with latitude. Plan. Space Sci. 12, 1179.

Morse, P.M., and Feshbach, H., 1953: Methods of theoretical physics. McGraw-Hill Book Co., New York.

Newell, R.E., 1966a: The energy and momentum budget of the atmosphere above the tropopause, in "Problems of Atmospheric Circulation," ed. by R.V. Garcia and T.F. Malone, Spartan Books, Washington, 106.

Newell, R.E., 1966b: Thermospheric energetics and a possible explanation of some observations of geomagnetic disturbances and radio aurorae, Nature, 211, 700.

Nicolet, M., 1960: The properties and constitution of the upper atmosphere, in "Physics of the Upper Atmosphere," (Ratcliff, ed.), Academic Press.

Nicolet, M., 1961: Structure of the thermosphere. Plan. Space Sci. 5, 1.

Paetzold, H.K. and Zschorner, H., 1961: The structure of the upper atmosphere and its variations after satellites observations. In "Space Research II" (Van de Hulst, Jager and Moore, eds.) p. 958. North-Holland Publ. Co., Amsterdam.

Pedlosky, J., 1964: The stability of currents in the atmosphere and the ocean: Part I. J. Atmos. Sci. 21, 201.

Phillips, N.A., 1963: Geostrophic Motion. Rev. Geophys. 1, 123.

Pokhunkov, A.A., 1963a: Gravitational separation, composition and structural parameters of the night atmosphere at altitudes between 100 and 210 km. Plan. Space Sci. 11, 441.

Pokhunkov, A.A., 1963b: Gravitational separation, composition and the structural parameters of the atmosphere at altitudes above 100 km. In "Space Research III" (W. Priester, ed.), p. 132, North-Holland Publ. Co., Amsterdam.

Pokhunkov, A.A., 1963c: On the variation in the mean molecular weight of air in the night atmosphere at altitudes of 100 to 210 km. from mass spectrometer measurements. Plan. Space Sci. 11, 297.

Reber, C.A., 1967: Thermosphere conditions deduced from satellite observations. J. Geophys. Res. 72, 295.

Saltzman, B., 1957: Equations governing the energetics of the larger scales of atmospheric turbulence in the domain of wave number. J. Meteor. 14, 513.

Schaefer, E.J., 1963: The dissociation of oxygen measured by a rocket-borne mass spectrometer. J. Geophys. Res. 68, 1175.

Schlichting, H., 1962: "Boundary layer theory." McGraw-Hill Book Co., New York, 647.

Spitzer, L., Jr., 1949: The terrestrial atmosphere above 300 km. In "The Atmospheres of the Earth and Planets" (Kuiper, ed.) p. 211 Univ. of Chicago Press, Chiacago, Illinois.

Volland, H., 1966: A two-dimensional dynamic model of the diurnal variation of the thermosphere, Part 1. Theory, J. Atmos. Sci., 23, 799.